PHILOSOPHICAL TRANSACTIONS OF THE ROYAL SOCIETY A MATHEMATICAL, PHYSICAL & ENGINEERING SCIENCES

On the Large-Deflexion Vibrations of Elastic Plates

G. Z. Harris and E. H. Mansfield

Phil. Trans. R. Soc. Lond. A 1967 **261**, 289-343
doi: 10.1098/rsta.1967.0005

ON THE LARGE-DEFLEXION VIBRATIONS OF ELASTIC PLATES

By G. Z. HARRIS and E. H. MANSFIELD
Royal Aircraft Establishment, Farnborough, Hants

CONTENTS

An exact large-deflexion analysis is given of the free vibrations of unsupported elliptical plates of lenticular section, whose middle surfaces may be flat or uniformly curved. The solution is confined to the three 'fundamental modal components', two bending and one twisting, for these are the most susceptible to large-deflexion effects. Particular attention is paid to the determination of modes, and their stability, in the large-deflexion régime. Many of the results are of importance in the general field of nonlinear plate vibrations.

1. Introduction

The theoretical analysis of the vibration of plates is of importance in many branches of engineering, and it has received considerable attention in the scientific literature. One of the first investigators to consider the vibrations of rectangular and circular plates was Lord Rayleigh (1877) in his classic treatise on the Theory of Sound. This, and virtually all subsequent work, is restricted to the small-deflexion vibrations of plates of constant thickness. There is now, however, an interest in the vibrational behaviour of plates of variable thickness, particularly in the field of high-speed aerodynamics where they may form the lifting and control surfaces of missiles. For such problems approximate techniques are possible, based on a discrete element representation, but the resulting accuracy would be in doubt because of the lack of exact solutions with which comparisons may be made. Furthermore, if the plate is curved the influence of membrane action is important, even if the curvature is slight and the deflexions small; indeed, the analysis must now take account of equilibrium and compatibility in the plane of the plate. There is, in addition, an increasing interest in the large-deflexion behaviour of plates, whether flat or curved, because it is known that the effective stiffness of plates is altered in the large-deflexion régime owing to the introduction of membrane action, and there is a consequent change in

Vol. 261. A. 1122. (Price £1. 1s.; U.S. $3.15) 36 [Published 9 June 1967

the natural frequencies and, in general, in the mode shapes. The equations governing the large-deflexion vibration of plates of constant thickness were considered in great detail by Hermann (1956) who showed that inertia effects in the plane of the plate may be neglected, thus yielding the von Kármán (static) equations in which the normal loading is replaced by an inertia loading of reversed sign. Using a perturbation procedure based on these equations, Chu & Herrmann (1956) have considered the free large-deflexion vibration of a rectangular plate with hinged, immovable edges. They show that membrane action introduces a coupling effect between the fundamental (small-deflexion) mode and higher modes; by ignoring this coupling they obtain approximate solutions for the timewise variation of the amplitude of the fundamental mode. There are, needless to say, no large-deflexion plate vibrations which vary purely sinusoidally with time, but the main difficulty in obtaining exact solutions stems from the fact—highlighted by Chu & Herrmann—that large-deflexion plate vibrations are seldom 'in unison', so that the transition from a small-deflexion mode to a large-deflexion mode does not simply involve a new amplitude-time variation. Information of a quantitative nature on nonlinear vibrations in structures with more than one degree of freedom can, of course, be determined by the analysis of simple, idealized systems. Thus the nonlinear vibrations of certain mass-spring systems have been considered by a number of writers including, in particular, Rosenberg who gives numerous references in one of his own papers (1964) in which he discusses the existence and significance of nonlinear modes. Such studies are valuable, but there is no technique available for relating mass-spring characteristics to a plate undergoing large-deflexion vibrations.

In this paper we consider the free vibrations of an unsupported elliptical plate of lenticular section whose mid-surface may be flat or uniformly curved, the directions of the principal curvatures not necessarily coinciding with the axes of the ellipse. Our primary purpose is to show how the vibrations of such a plate are influenced by large-deflexion phenomena and this has been achieved without recourse to any simplifying or restrictive assumptions, for the solutions presented are exact within the spirit of large-deflexion plate theory. At the same time the results of this nonlinear analysis are simpler to understand in terms of, or in comparison with, the linear small-deflexion behaviour, and this aspect has been comprehensively treated in § 4. It is hoped, moreover, that the results of this linear analysis will themselves be of intrinsic value, particularly in so far as they relate to a plate of variable thickness and to a plate with initial curvatures. Attention is confined to the three 'fundamental modal components', two bending and one twisting, but this limitation does not detract significantly from the practicality of our analysis because vibrations which include these components are the most susceptible to membrane action, whether due to initial curvature or large deflexions. This susceptibility has much in common with the behaviour under an axial thrust P of a laterally loaded strut of length l, whose lateral deflexions depend upon the rigidity of the strut and the parameter Pl^2; again, if the strut is subjected to a given bending moment M the resultant 'end shortening' varies as M^2l^3. In a plate the higher harmonic vibrations are characterized by shorter wavelengths and a correspondingly much reduced influence of membrane action.

The complexity of the large-deflexion analysis, whether static or dynamic, of plates of constant thickness is widely recognized, while even the small-deflexion analysis of plates of variable thickness generally presents formidable difficulties. It might therefore be construed

that the present analysis would be doubly complex, but this is not so. To understand why, it is expedient to refer first to the large-deflexion behaviour of statically loaded, constant thickness plates with free edges. In the vicinity of the edges there are severe variations in the stress pattern—variations which become more abrupt as the load is increased—and it is these 'boundary layers' (a concept introduced by Fung & Wittrick 1955) which add so much to the complexities of analysis. However, as shown by Fung & Wittrick (1954) and Mansfield (1959) in the large-deflexion analysis of certain strips with lateral thickness variation, plates which taper linearly to zero at their edges do not exhibit these boundary layers; indeed, the occurrence of a boundary layer, whether at the edge or elsewhere, depends on there being an abrupt change in the rigidity or in the rate of change of rigidity; the rigidity of a plate of constant thickness is to be regarded as falling abruptly to zero at a free edge. Plates, whose rigidity and rate of change of rigidity vary smoothly everywhere and vanish at the (free) edges, do not exhibit localized regions of severely varying stress and they therefore lend themselves to exact large-deflexion analysis. Such plates have an application in the field of high-speed aerodynamics. Elliptical plates of lenticular section, which comprise the simplest class of such plates, were considered first by Mansfield (1965) in a large-deflexion analysis of their pre-buckling and post-buckling behaviour under certain temperature variations in their plane and through their thickness. Now it is well known that in the small-deflexion régime there is often a close relationship between the buckling modes of plates, whether thermally or mechanically induced, and the vibrational modes; this is again apparent in the present large-deflexion studies.

2. Symbols

$2a$	major axis of ellipse
$2b$	minor axis of ellipse
A, B	terms introduced in equation (27)
c_1, c_2, c_3	arbitrary constants
D, D_0	flexural rigidity of plate defined by equation (4)
E	Young's modulus
f, g	arbitrary functions
$F(k_i, \alpha_j)$	incomplete elliptic integral of first kind
h, h_0	thickness of plate defined by equation (3)
H	term introduced in equation (33)
k	term introduced in equation (49)
$k_1, \ldots, k_4$	terms introduced in equations (44), (51), (82) and (84)
$K(k_i)$	complete elliptic integral of the first kind with modulus k_i
m	term introduced in equation (115)
p, q, r, s	terms introduced in equations (77) and (82)
t	time
U^*	strain energy in plate
U	nondimensional measure of U^* introduced in equation (68)
U_1	maximum (initial) value of U
U_2	value of U introduced in equation (73)
w	deflexion of plate measured from a reference plane

x, y	Cartesian coordinates in plane of plate, Ox lying on major axis
$\alpha_1, \ldots, \alpha_5$	terms introduced in equations (44), (51), (82), (84) and (86)
β	term introduced in equation (8) defining the middle surface forces
γ	parameter defined by equation (63) or (93)
$\gamma_1, \ldots, \gamma_4$	roots of equation (75)
$\epsilon_1, \epsilon_2, \epsilon_3$	terms defining small-deflexion modes, equations (15) and (20)
$\bar{\epsilon}_1, \bar{\epsilon}_2, \bar{\epsilon}_3$	values of $\epsilon_1, \epsilon_2, \epsilon_3$ for a flat plate
ζ	b/a
η	term introduced in equation (89)
θ	term introduced in equation (113) defining initial velocity ratio
κ	nondimensional curvature
$\kappa_x, \kappa_y, \kappa_{xy}$	nondimensional curvatures introduced in equation (7)
$\kappa_X, \kappa_Y, \kappa_{XY}$	maximum or zero-time values of $\kappa_x, \kappa_y, \kappa_{xy}$
λ	term introduced in equation (24)
Λ	parameter defined by equation (63) or (93)
μ	term introduced in equations (5), (7) and defined in equation (9)
ν	Poisson's ratio, assumed to be 0·3 in numerical calculations
ρ	density of plate material
$\sigma_x, \sigma_y, \tau_{xy}$	direct and shear stresses in plate
τ	non-dimensional measure of time, defined in equation (9)
Φ	force function introduced in equation (1)
Ω	nondimensional frequency, 2π/(increase in τ during one cycle)
Ω_0	values of Ω defined by equation (63) or (93)
∇^2	Laplacian operator
$\Diamond^4$	bilinear operator defined after equation (2)

Suffix 0 after w, κ_x, κ_y, κ_{xy} refers to the undisturbed state
Suffix d, b, or t, after Ω or ϵ refers to dishing, bending or torsion mode
Suffix e or c after Ω refers to extensional or curling mode
Suffix s or u after γ or U refers to the stable or unstable equilibrium state
Asterisk * after β or κ refers to critical buckling conditions
A dot denotes differentiation with respect to τ.

3. Analysis

Within the spirit of large-deflexion plate theory the governing equations may be expressed (Mansfield 1962) in the form

$$\nabla^2\left(\frac{1}{h}\nabla^2\Phi\right) - (1+\nu)\,\Diamond^4\left(\frac{1}{h}, \Phi\right) + \tfrac{1}{2}E\{\Diamond^4(w,w) - \Diamond^4(w_0,w_0)\} = 0 \tag{1}$$

and

$$\nabla^2\{D\nabla^2(w-w_0)\} + \rho h\frac{\partial^2 w}{\partial t^2} = (1-\nu)\,\Diamond^4(D, w-w_0) + \Diamond^4(\Phi, w), \tag{2}$$

where the diamond operator, $\Diamond$ (pronounced 'die') is defined by

$$\begin{aligned}\Diamond^4(f,g) &\equiv \tfrac{1}{2}\{(\nabla^2 f)(\nabla^2 g) + \nabla^2(f\nabla^2 g + g\nabla^2 f)\} - \tfrac{1}{4}\{\nabla^4(fg) + f\nabla^4 g + g\nabla^4 f\}\\ &\equiv \frac{\partial^2 f}{\partial x^2}\frac{\partial^2 g}{\partial y^2} - 2\frac{\partial^2 f}{\partial x\,\partial y}\frac{\partial^2 g}{\partial x\,\partial y} + \frac{\partial^2 f}{\partial y^2}\frac{\partial^2 g}{\partial x^2}.\end{aligned}$$

In these equations h is the plate thickness, E is Young's modulus, ν is Poisson's ratio, ρ is the density of the plate material, D is the plate rigidity, w is the deflexion and Φ is the force function from which the middle-surface (membrane) stresses are to be derived from the relations

$$h\sigma_x = \frac{\partial^2\Phi}{\partial y^2}, \quad h\sigma_y = \frac{\partial^2\Phi}{\partial x^2}, \quad h\tau_{xy} = -\frac{\partial^2\Phi}{\partial x\,\partial y}.$$

The introduction of the force function assures equilibrium in the plane of the plate, while compatibility of strains is assured by equation (1). Equation (2) is the equation of equilibrium normal to the plane of the plate. These equations are simply generalizations of von Kármán's large-deflexion equations taking account of varying thickness and rigidity.

The thickness of the plate varies parabolically across a diameter, vanishing along the boundary according to the equation

$$h = h_0\left(1-\frac{x^2}{a^2}-\frac{y^2}{b^2}\right), \tag{3}$$

where h_0 is the thickness at the centre and a, b are the semi-axes of the plate. The rigidity D is given by

$$\left.\begin{aligned} D &= D_0\left(1-\frac{x^2}{a^2}-\frac{y^2}{b^2}\right)^3, \\ \text{where} \qquad D_0 &= \frac{Eh_0^3}{12(1-\nu^2)}. \end{aligned}\right\} \tag{4}$$

In its undisturbed state the plate is free from stress and its mid-plane is either flat or uniformly curved according to the equation

$$w_0 = -\mu\{\tfrac{1}{2}\kappa_{x,0}(x^2-\tfrac{1}{6}a^2)+\kappa_{xy,0}xy+\tfrac{1}{2}\kappa_{y,0}(y^2-\tfrac{1}{6}b^2)\}, \tag{5}$$

where μ is a dimensional constant, introduced for convenience and defined later (equation (9)), and $\kappa_{x,0}$ etc. are nondimensional measures of the curvatures; the grouping of the terms $(x^2-\frac{1}{6}a^2)$, $(y^2-\frac{1}{6}b^2)$ is chosen such that

$$\iint_A hw_0\,\mathrm{d}x\,\mathrm{d}y = 0. \tag{6}$$

3·1. *Method of solution*

The method of solution is in two distinct phases. The first phase is an inverse one in that general expressions are assumed for describing the spatial variation of w and Φ. These expressions (three for w and one for Φ) satisfy the edge conditions and are shown to be capable of satisfying the governing coupled nonlinear equations (1) and (2). In the second phase the solution is completed by proper choice of the corresponding variations with time.

3·2. *General expressions for w and* Φ

The point has already been made that the nonlinearities arising from large deflexions are of practical significance only for the lower modes. We therefore confine our attention to the three 'fundamental' modal components—two bending and one twisting—and search for a solution in the form

$$w = -\mu\{\tfrac{1}{2}\kappa_x(x^2-\tfrac{1}{6}a^2)+\kappa_{xy}xy+\tfrac{1}{2}\kappa_y(y^2-\tfrac{1}{6}b^2)\}, \tag{7}$$

where κ_x, κ_{xy}, κ_y are functions only of time. It may be verified that each term in equation (7) satisfies equation (6) with w_0 replaced by w, and hence ensures that the c.g. of the plate remains stationary.

The general form of equation (7) is similar to that considered by Mansfield (1965) and in like manner we make the tentative assumption that the force function Φ is of the form

$$\Phi = \beta D \tag{8}$$

where β, which is nondimensional, is a function only of time. This is tantamount to assuming that while the *magnitude* of the middle-surface stresses varies with time, their *distribution* does not.

3·2·1. *Stresses in the plate*

The force function given by equation (8) yields the following middle-surface stresses

$$\sigma_x = -\frac{\beta E h_0^2}{2(1-\nu^2)\,b^2}\left(1-\frac{x^2}{a^2}-5\frac{y^2}{b^2}\right),$$

$$\sigma_y = -\frac{\beta E h_0^2}{2(1-\nu^2)\,a^2}\left(1-5\frac{x^2}{a^2}-\frac{y^2}{b^2}\right),$$

$$\tau_{xy} = -\frac{2\beta E h_0^2 xy}{(1-\nu^2)\,a^2 b^2}.$$

The bending stresses vary linearly through the thickness of the plate. On the face which is in the direction of positive w the bending stresses are given by

$$\sigma_x = \frac{\mu E h}{2(1-\nu^2)}\{\kappa_x-\kappa_{x,0}+\nu(\kappa_y-\kappa_{y,0})\},$$

$$\sigma_y = \frac{\mu E h}{2(1-\nu^2)}\{\kappa_y-\kappa_{y,0}+\nu(\kappa_x-\kappa_{x,0})\},$$

$$\tau_{xy} = \frac{\mu E h}{2(1+\nu)}\{\kappa_{xy}-\kappa_{xy,0}\}.$$

3·2·2. *Edge conditions*

At the edge of the plate there are no applied forces or moments and these conditions are satisfied because, at the plate boundary,

$$D = \frac{\partial D}{\partial n} = \Phi = \frac{\partial \Phi}{\partial n} = 0,$$

where n is measured normal to the boundary.

It remains to show that these simple expressions for w and Φ are, in fact, capable of satisfying the governing differential equations and hence of providing the true solution. First, however, we define the dimensional constant μ, and hence the nondimensional curvature parameters introduced in equations (5) and (7), and introduce a nondimensional measure of time:

$$\left.\begin{aligned} \mu &= \frac{h_0}{ab}\left(\frac{4+2\nu+5(\zeta^2+\zeta^{-2})}{1-\nu^2}\right)^{\frac{1}{2}}, \\ \text{where}\quad \zeta &= b/a, \\ \text{and}\quad \tau &= \frac{12}{ab}\left(\frac{D_0}{\rho h_0}\right)^{\frac{1}{2}} t. \end{aligned}\right\} \tag{9}$$

A dot will denote differentiation with respect to τ.

3·3. *Satisfaction of the governing equations*

The spatial satisfaction of equations (1) and (2) by the assumed forms for w and Φ is readily shown by direct substitution. Thus, referring to equation (1), it is to be noted that

$$\nabla^2\left(\frac{1}{h}\nabla^2\Phi\right) = \frac{12\beta D_0}{h_0 a^2 b^2}\{2+5(\zeta^2+\zeta^{-2})\},$$

$$\Diamond^4\left(\frac{1}{h},\,\Phi\right) = \frac{-24\beta D_0}{h_0 a^2 b^2},$$

$$\tfrac{1}{2}\Diamond^4(w,w) = \mu^2(\kappa_x\kappa_y-\kappa_{xy}^2),$$

$$\tfrac{1}{2}\Diamond^4(w_0,w_0) = \mu^2(\kappa_{x,0}\kappa_{y,0}-\kappa_{xy,0}^2).$$

Equation (1) therefore contains only terms which are functions of time and independent of x, y; it can be written nondimensionally in the form

$$\beta = \kappa_{x,0}\kappa_{y,0}-\kappa_{xy,0}^2-\kappa_x\kappa_y+\kappa_{xy}^2. \tag{10}$$

Referring to equation (2) it is to be noted that

$$\nabla^2(w-w_0) = \mu(\kappa_{x,0}+\kappa_{y,0}-\kappa_x-\kappa_y),$$

$$\nabla^2 D = \frac{6D_0}{a^2b^2}\left(1-\frac{x^2}{a^2}-\frac{y^2}{b^2}\right)\{(1+5\zeta^2)\,(x^2-\tfrac{1}{6}a^2)+(1+5\zeta^{-2})\,(y^2-\tfrac{1}{6}b^2)\}.$$

$$(1-\nu)\,\Diamond^4(D,w-w_0)+\Diamond^4(\Phi,w) = \Diamond^4\{D,(1-\nu+\beta)\,w-(1-\nu)\,w_0\},$$

and

$$\Diamond^4\{D,\tfrac{1}{2}c_1(x^2-\tfrac{1}{6}a^2)+c_2xy+\tfrac{1}{2}c_3(y^2-\tfrac{1}{6}b^2)\}$$
$$= \frac{6D_0}{a^2b^2}\left(1-\frac{x^2}{a^2}-\frac{y^2}{b^2}\right)\{(c_1+5\zeta^2c_3)\,(x^2-\tfrac{1}{6}a^2)-8c_2xy+(c_3+5\zeta^{-2}c_1)\,(y^2-\tfrac{1}{6}b^2)\}.$$

Thus, confining attention to the spatial variations, each term in equation (2) varies as the product of $(1-x^2/a^2-y^2/b^2)$ and one of the 'modal components' $(x^2-\frac{1}{6}a^2)$, xy or $(y^2-\frac{1}{6}b^2)$. For the equation to be satisfied it follows that the coefficients of terms which vary in like manner must vanish, and this gives rise to three equations which can be expressed nondimensionally in the form

$$(5\zeta^2+\nu)\,(\kappa_{x,0}-\kappa_x)+(1-5\nu\zeta^2)\,(\kappa_{y,0}-\kappa_y)+\beta(\kappa_x+5\zeta^2\kappa_y) = 12\ddot{\kappa}_x, \tag{11 a}$$

$$(1+5\nu\zeta^{-2})\,(\kappa_{x,0}-\kappa_x)+(5\zeta^{-2}+\nu)\,(\kappa_{y,0}-\kappa_y)+\beta(5\zeta^{-2}\kappa_x+\kappa_y) = 12\ddot{\kappa}_y, \tag{11 b}$$

$$(1-\nu)\,(\kappa_{xy,0}-\kappa_{xy})-\beta\kappa_{xy} = 3\ddot{\kappa}_{xy}. \tag{11 c}$$

A significant feature of equations (10) and (11) is that the only deflexion components involved are κ_x, κ_y and κ_{xy}. Thus, when the initial conditions involve only these components, so does the subsequent motion; higher modes are not introduced.

3·4. *Initial conditions*

Thus far the analysis has shown that, for the class of plates considered here, equations (1) and (2) reduce to equations (10) and (11 a, b, c) in which β, κ_x, κ_{xy}, κ_y are functions only of time. The further integration of these equations—described earlier as the second phase of

the solution—introduces the conditions at zero time. A variety of such initial conditions can be envisaged, but attention here is confined to two basic forms, namely

$$\left.\begin{aligned} &[\kappa_x, \kappa_{xy}, \kappa_y]_{\tau=0} = \kappa_{x,0}, \kappa_{xy,0}, \kappa_{y,0} \\ \text{with}\quad &[\dot\kappa_x, \dot\kappa_{xy}, \dot\kappa_y]_{\tau=0} \text{ having specified values,} \end{aligned}\right\} \tag{12}$$

which corresponds to the application to the undisturbed plate of a specified impulse, and

$$\left.\begin{aligned} &[\dot\kappa_x, \dot\kappa_{xy}, \dot\kappa_y]_{\tau=0} = 0 \\ \text{with}\quad &[\kappa_x, \kappa_{xy}, \kappa_y]_{\tau=0} \text{ having specified values,} \end{aligned}\right\} \tag{13}$$

which corresponds to the release of a specified restraint.

It will be realized that, because of the nonlinearity, an analytical solution of equations (10) and (11) is not generally possible and it is often necessary to introduce numerical values at an early stage. Furthermore, in order to obtain a clear picture of the nature of the plate vibrations it is advisable to consider first the simplest types of vibration, such as small-deflexion vibrations of a flat plate, before considering the more complex nonlinear types.

4. Small-deflexion modes

In the small-deflexion régime the behaviour of the plate is linear and it possesses normal modes of vibration. The properties of such normal modes (e.g. independence and superposition) are well known and these introductory remarks are purely cautionary to emphasize that in the large-deflexion régime the concept of a normal mode has a much reduced significance.

4·1. *Flat elliptical plate*

If the plate in its undisturbed state is flat the terms $\kappa_{x,0}$, etc., are zero and equation (10) then shows that when small-deflexion vibrations are being considered the term β is to be neglected in equation (11). The governing (linear) equations are therefore

$$\left.\begin{aligned} (5\zeta^2+\nu)\,\kappa_x + (1+5\nu\zeta^2)\,\kappa_y + 12\ddot\kappa_x &= 0, \\ (1+5\nu\zeta^{-2})\,\kappa_x + (5\zeta^{-2}+\nu)\,\kappa_y + 12\ddot\kappa_y &= 0, \\ (1-\nu)\,\kappa_{xy} + 3\ddot\kappa_{xy} &= 0. \end{aligned}\right\} \tag{14}$$

Normal modes may be determined by writing

$$(\kappa_x, \kappa_y, \kappa_{xy}) = (\epsilon_1, \epsilon_2, \epsilon_3)\,\mathrm{e}^{\mathrm{i}\Omega\tau} \tag{15}$$

where Ω is a nondimensional measure of the frequency. Substitution of equation (15) in equation (14) gives

$$\begin{pmatrix} 5\zeta^2+\nu-12\Omega^2 & 1+5\nu\zeta^2 & 0 \\ 1+5\nu\zeta^{-2} & 5\zeta^{-2}+\nu-12\Omega^2 & 0 \\ 0 & 0 & 4(1-\nu)-12\Omega^2 \end{pmatrix} \begin{pmatrix} \epsilon_1 \\ \epsilon_2 \\ \epsilon_3 \end{pmatrix} = 0.$$

The three modes thus defined are best described by the terms *dishing*, *bending* and *torsion* and accordingly, for ease of identification, we introduce the corresponding suffices d, b and t.

The torsion mode is the simplest, in which

$$\left.\begin{aligned} \epsilon_1^t : \epsilon_2^t : \epsilon_3^t &= 0:0:1 \\ \text{so that the modal contour lines are rectangular hyperbolas, and} \\ \Omega_t &= \{\tfrac{1}{3}(1-\nu)\}^{\frac{1}{2}}. \end{aligned}\right\} \tag{16}$$

In the dishing and bending modes the amplitude ratios are given by

$$\epsilon_1 : \epsilon_2 : \epsilon_3 = 1 + 5\nu\zeta^2 : 12\Omega^2 - (5\zeta^2 + \nu) : 0, \tag{17}$$

where

$$24\zeta^2\Omega_d^2 = 5(1+\zeta^4) + 2\nu\zeta^2 + \{25(1-\zeta^4)^2 + 4\zeta^4(1+5\nu)^2 + 20\nu\zeta^2(1-\zeta^2)^2\}^{\frac{1}{2}}, \tag{18}$$

$$24\zeta^2\Omega_b^2 = 5(1+\zeta^4) + 2\nu\zeta^2 - \{25(1-\zeta^4)^2 + 4\zeta^4(1+5\nu)^2 + 20\nu\zeta^2(1-\zeta^2)^2\}^{\frac{1}{2}}. \tag{19}$$

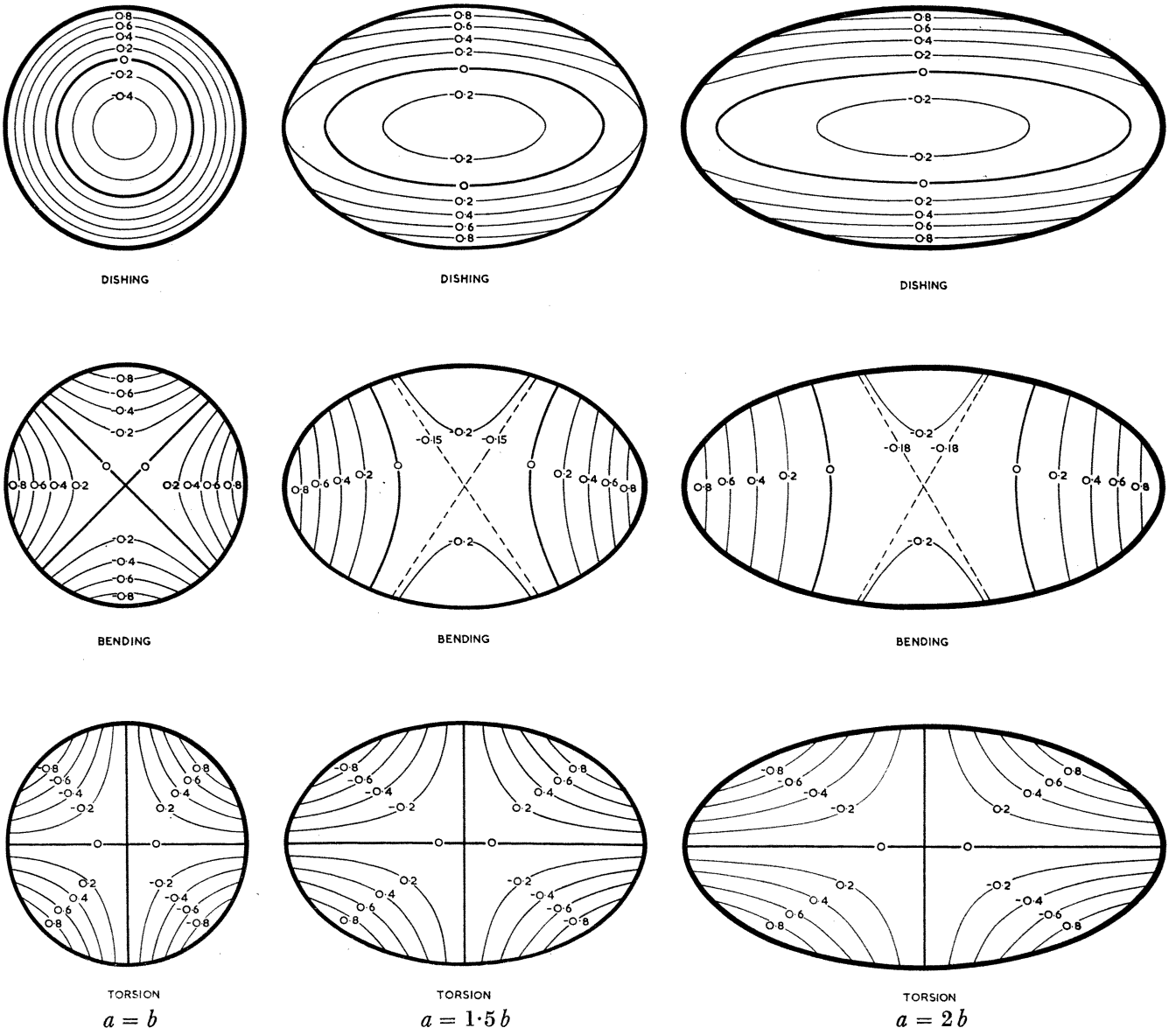

FIGURE 1. Small-deflexion modal contour lines.

It may be verified that for the dishing mode $\epsilon_1 \epsilon_2 > 0$ and the modal contour lines are therefore ellipses, while for the bending mode $\epsilon_1 \epsilon_2 < 0$ and the modal contour lines are hyperbolas. Modal contour lines for the dishing, bending and torsion modes are shown in figure 1 for

various values of ζ. As ζ varies from 1 to 0 the ratio $\epsilon_2^b/\epsilon_1^b$ varies from -1 to $-\nu$, this latter value corresponding to the anticlastic curvature due to the Poisson's ratio effect in the bending of a long strip. [The association of the term *bending* with a significant degree of anticlastic curvature is to be noted. When the anticlastic curvature is very small, or zero, we use the term *curling*.]

Figure 2 shows the variation of Ω_d, Ω_b and Ω_t with ζ. It is to be noted that

$$\Omega_d > \Omega_t \geqslant \Omega_b,$$

the equality sign occurring for the circular plate ($\zeta = 1$) where, as a by-product of the rotational symmetry, the torsion and bending modes—$w_t \propto xy$, $w_b \propto (x^2 - y^2)$—are effectively identical.

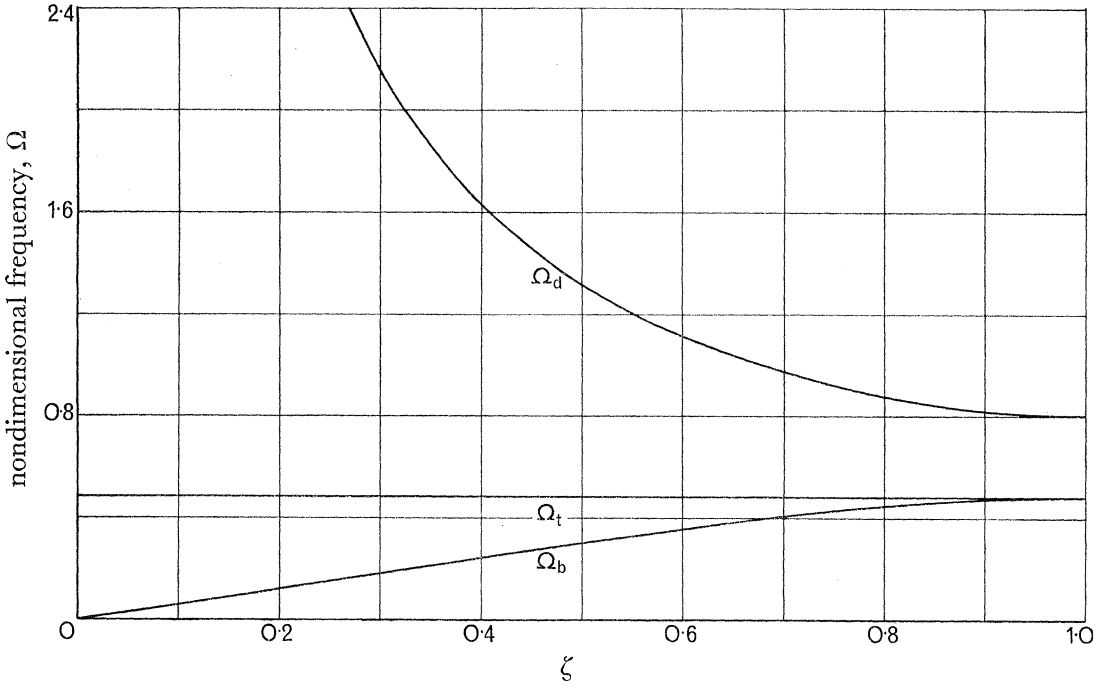

FIGURE 2. Small-deflexion dishing, bending and torsion frequencies.

4·2. *Curved elliptical plate*

The small-deflexion modes of a curved plate are of the form

$$(\kappa_x - \kappa_{x,0}, \kappa_y - \kappa_{y,0}, \kappa_{xy} - \kappa_{xy,0}) = (\epsilon_1, \epsilon_2, \epsilon_3)\, e^{i\Omega\tau} \tag{20}$$

and equation (10) shows that the middle-surface forces cannot now be neglected, for we have

$$\beta = -(\kappa_{y,0}\epsilon_1 + \kappa_{x,0}\epsilon_2 - 2\kappa_{xy,0}\epsilon_3)\, e^{i\Omega\tau} + O(\epsilon^2). \tag{21}$$

Substitution of equations (20) and (21) in equation (11) yields the following equation for the modes and frequencies

$$\left[\begin{pmatrix} 5\zeta^2+\nu & 1+5\nu\zeta^2 & 0 \\ 1+5\nu\zeta^{-2} & 5\zeta^{-2}+\nu & 0 \\ 0 & 0 & 4(1-\nu) \end{pmatrix} + \begin{pmatrix} \kappa_{x,0}+5\zeta^2\kappa_{y,0} \\ \kappa_{y,0}+5\zeta^{-2}\kappa_{x,0} \\ -4\kappa_{xy,0} \end{pmatrix} (\kappa_{y,0},\ \kappa_{x,0},\ -2\kappa_{xy,0})\right] \begin{pmatrix} \epsilon_1 \\ \epsilon_2 \\ \epsilon_3 \end{pmatrix} = 12\Omega^2 \begin{pmatrix} \epsilon_1 \\ \epsilon_2 \\ \epsilon_3 \end{pmatrix}. \tag{22}$$

The effect of curvature is, in general, to cause a higher natural frequency than for the corresponding flat plate. There are, however, exceptions to this rule which occur when the curvatures are such that

$$(\kappa_{y,0}, \kappa_{x,0}, -2\kappa_{xy,0}) \begin{pmatrix} \bar{\epsilon}_1 \\ \bar{\epsilon}_2 \\ \bar{\epsilon}_3 \end{pmatrix} = 0, \tag{23}$$

where $(\bar{\epsilon}_1, \bar{\epsilon}_2, \bar{\epsilon}_3)$ defines a mode for the flat plate. In such a case the curved plate possesses the same mode and corresponding natural frequency as the flat plate; also, as would be expected, middle-surface forces do not occur and the term β is zero. The simplest case for

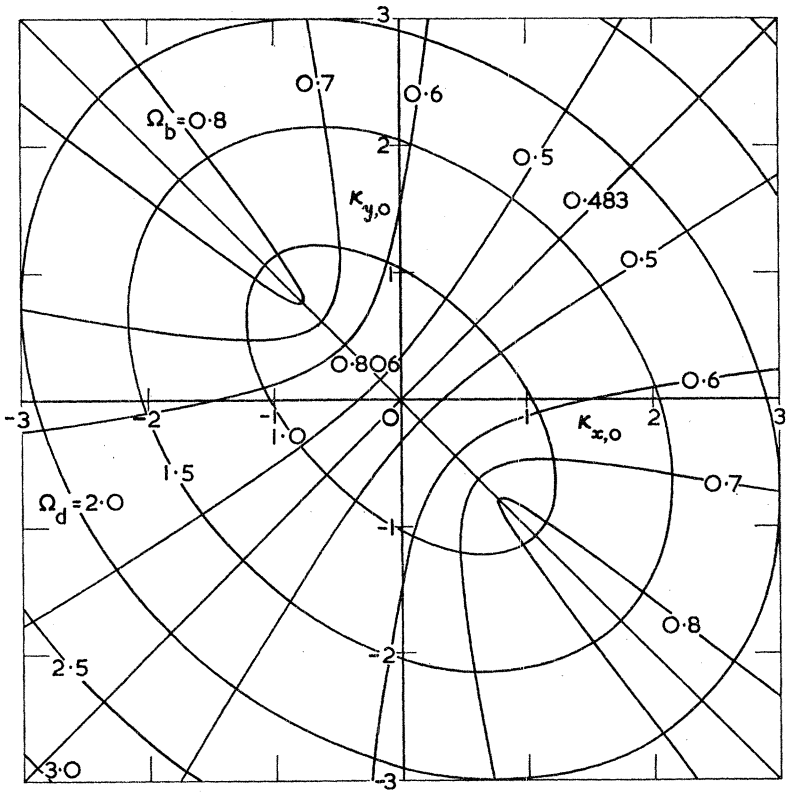

FIGURE 3. Variation of frequencies with initial curvatures; $\kappa_{xy,0} = 0$, $\zeta = 1$.

which equation (23) is satisfied occurs when $\kappa_{xy,0}$ is zero; the fact that Ω_t is then independent of $\kappa_{x,0}$ and $\kappa_{y,0}$ is immediately apparent from equation (22). The variation of Ω_d and Ω_b with $\kappa_{x,0}$ and $\kappa_{y,0}$, with $\kappa_{xy,0}$ zero, is shown in figures 3 and 4 for plates in which $\zeta = 1$ and $\frac{1}{2}$.

4·2·1. *Plate with large curvatures*

Apart from the special cases which satisfy equation (23) a proportional increase in the curvatures causes an increase in the natural frequencies, but to obtain an idea of the extent of the increases in frequency we consider here the asymptotic behaviour of a plate in which

$$(\kappa_{x,0}, \kappa_{y,0}, \kappa_{xy,0}) = \lambda(\kappa'_{x,0}, \kappa'_{y,0}, \kappa'_{xy,0}), \text{ say,} \tag{24}$$

as $\lambda \to \infty$. This is in the realm of shallow shell theory and, in order not to violate the assumption of shallowness, it is preferable to regard the increase in the nondimensional curvature

symbols as caused by a decrease in thickness rather than an increase in actual curvature. With this proviso in mind we substitute equation (24) in equation (22) and first search for a solution in which Ω is of order λ. The limiting form of equation (22) is doubly degenerate and accordingly there is only one such root; it is given by

$$12\Omega_e^2 \sim 5\zeta^{-2}\kappa_{x,0}^2 + 2\kappa_{x,0}\kappa_{y,0} + 5\zeta^2\kappa_{y,0}^2 + 8\kappa_{xy,0}^2, \tag{25}$$

and the corresponding mode shape is given by

$$\epsilon_1 : \epsilon_2 : \epsilon_3 = \kappa_{x,0} + 5\zeta^2\kappa_{y,0} : \kappa_{y,0} + 5\zeta^{-2}\kappa_{x,0} : -4\kappa_{xy,0}. \tag{26}$$

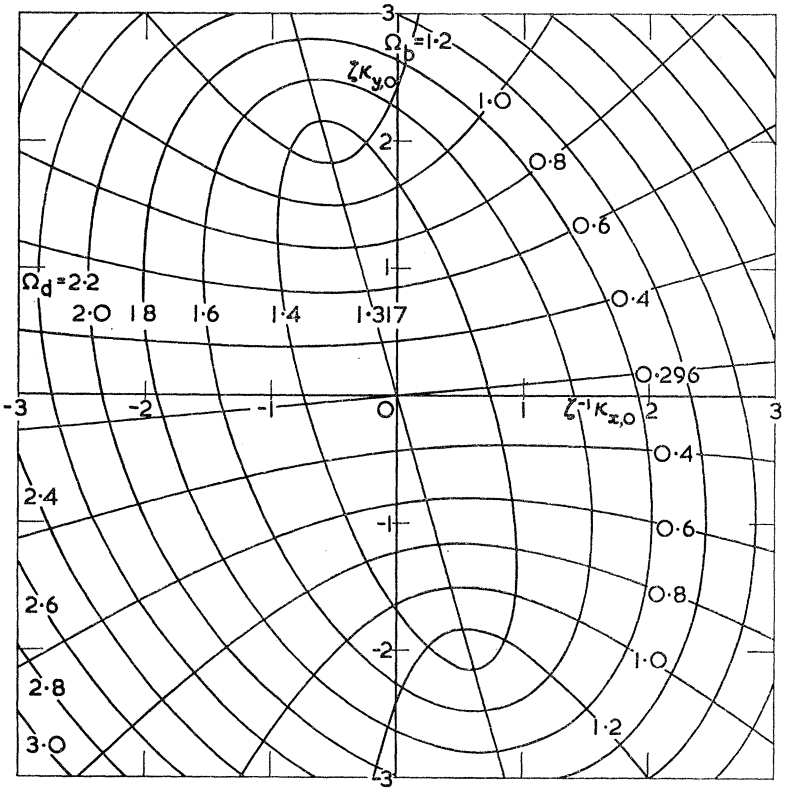

FIGURE 4. Variation of frequencies with initial curvatures; $\kappa_{xy,0} = 0$, $\zeta = \frac{1}{2}$.

This is an *extensional* mode in that it is governed by the in-plane stiffness of the plate rather than the flexural stiffness. Note that this extensional mode cannot necessarily be identified with the terms dishing, bending or torsion, for by suitable choice of the initial curvatures any desired mode shape may be obtained. The two other modes are flexural in character and are obtained by searching for solutions of equation (22) in which Ω remains finite as $\lambda \to \infty$. The resulting quadratic in Ω^2 simplifies to

$$\left.\begin{aligned} 3A\Omega^4 - \Omega^2\{A(1-\nu) + 6B + 10\kappa_{xy,0}^2(\zeta - \zeta^{-1})^2\} + 2B(1-\nu) = 0, \\ \text{where} \qquad A = 5\zeta^{-2}\kappa_{x,0}^2 + 2\kappa_{x,0}\kappa_{y,0} + 5\zeta^2\kappa_{y,0}^2 + 8\kappa_{xy,0}^2, \\ B = \kappa_{x,0}^2 - 2\nu\kappa_{x,0}\kappa_{y,0} + \kappa_{y,0}^2 + 2(1+\nu)\kappa_{xy,0}^2. \end{aligned}\right\} \tag{27}$$

These asymptotic frequencies depend on the ratios, rather than the magnitudes, of the initial curvatures and are plotted against $\kappa_{x,0}/\kappa_{xy,0}$ and $\kappa_{y,0}/\kappa_{xy,0}$ in figure 5 for a plate in

which $\zeta = \frac{1}{2}$. This presentation loses its significance if $\kappa_{xy,0}$ is zero when, as shown below, the frequencies assume a particularly simple form.

Plates with no initial twist. When $\kappa_{xy,0}$ is zero equation (27) factorizes to give

$$\Omega_t^2 = \tfrac{1}{3}(1-\nu) \tag{28}$$

and

$$\Omega^2 = \frac{2(\kappa_{x,0}^2 - 2\nu\kappa_{x,0}\kappa_{y,0} + \kappa_{y,0}^2)}{5\zeta^{-2}\kappa_{x,0}^2 + 2\kappa_{x,0}\kappa_{y,0} + 5\zeta^2\kappa_{y,0}^2}. \tag{29}$$

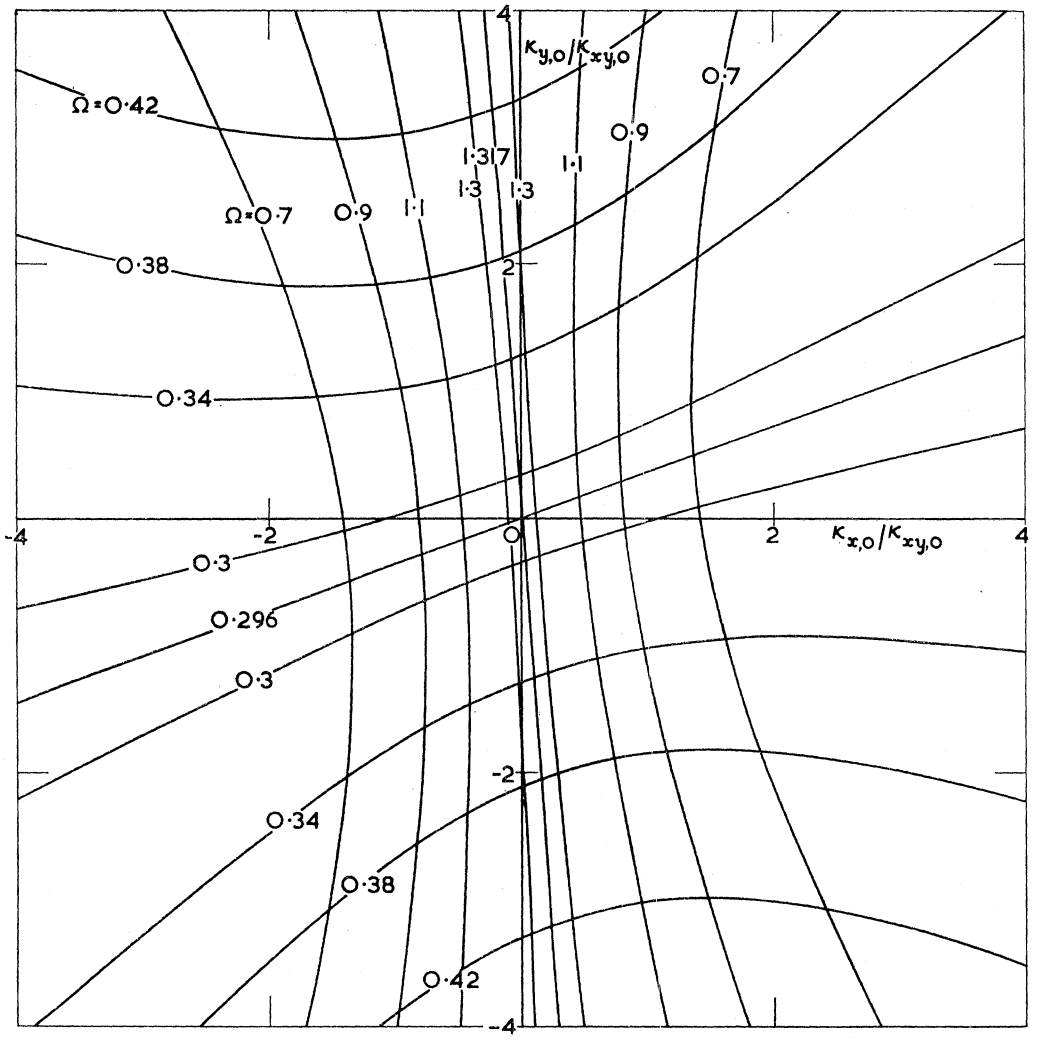

FIGURE 5. Variation of asymptotic frequencies with curvature ratios: $\zeta = \frac{1}{2}$.

This simplification is possible because equation (23) is now satisfied by the flat plate torsion mode which is therefore a mode for the curved plate. The frequency corresponding to equation (29) is plotted against $\kappa_{x,0}/\kappa_{y,0}$ for various values of ζ in figure 6. The mode shape corresponding to equation (29) is given by

$$\epsilon_1 : \epsilon_2 : \epsilon_3 = \kappa_{x,0} : -\kappa_{y,0} : 0 \tag{30}$$

and we note that this is not necessarily associated with either the bending or dishing mode.

Thus when $\kappa_{y,0}$, say, is zero the component ϵ_2 vanishes and the mode is best described as a purely *curling* mode whose frequency is given simply by

$$\Omega_c^2 = \tfrac{2}{5}\zeta^2. \tag{31}$$

This curling frequency is the same as the fundamental frequency of a free-free beam whose stiffness and inertia vary in the same manner as in the plate; indeed, the actual curling frequency—as opposed to the nondimensional frequency—is independent of the plate width b.

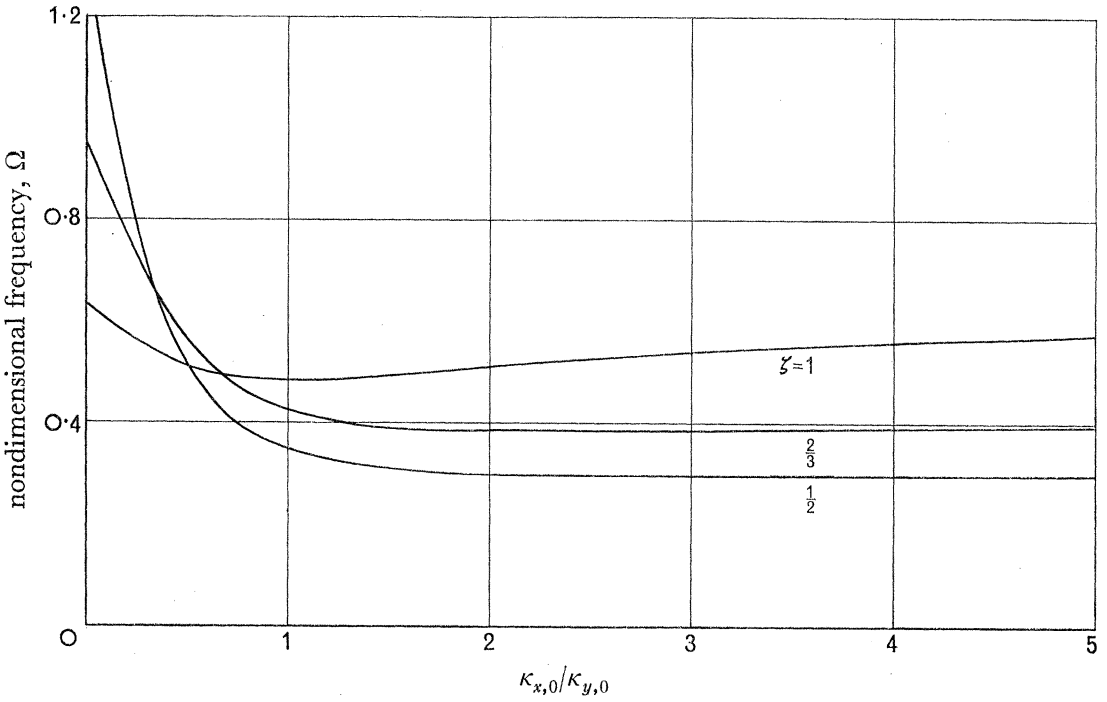

FIGURE 6. Variation of asymptotic frequencies with curvature ratios; $\kappa_{xy,0} = 0$.

4·2·2. *Variation of modes with initial curvature*

The analysis of § 4·2·1 shows that as the initial curvature parameters tend to infinity one of the modes becomes extensional while two remain flexural in character, but the asymptotic analysis presented there does not tell us which of the three flat plate flexural modes changes its character. Thus it is convenient to envisage a continuous family of plates specified by equation (24) in which λ increases uniformly from zero to infinity. Associated with this family of plates there are therefore three families of modes; by tracing the development of these modes with λ a complete picture of the mode behaviour is obtained.

Circular plate. Because of the cumbersome nature of the general analysis it is expedient to restrict attention first to the circular plate for then, without loss of generality, we may take $\kappa_{xy,0} = 0$. This also means that the shape and frequency of the torsion mode do not vary with λ, and we are left to consider only the dishing and bending modes for which equation (22) yields

$$12\Omega^4 - \Omega^2\{10 + 2\nu + \lambda^2(5\kappa'^2_{x,0} + 2\kappa'_{x,0}\kappa'_{y,0} + 5\kappa'^2_{y,0})\} + 2\{1 - \nu^2 + \lambda^2(\kappa'^2_{x,0} - 2\nu\kappa'_{x,0}\kappa'_{y,0} + \kappa'^2_{y,0})\} = 0. \tag{32}$$

PHILOSOPHICAL TRANSACTIONS OF THE ROYAL SOCIETY A MATHEMATICAL, PHYSICAL & ENGINEERING SCIENCES

The roots of this equation may be cast in the form

$$24\Omega^2 = 10+2\nu+\lambda^2(5\kappa'^2_{x,0}+2\kappa'_{x,0}\kappa'_{y,0}+5\kappa'^2_{y,0})\pm H^{\frac{1}{2}}, \tag{33}$$

where $$H = [2+10\nu+\lambda^2\{3(\kappa'_{x,0}+\kappa'_{y,0})^2-2(\kappa'_{x,0}-\kappa'_{y,0})^2\}]^2+24\lambda^4(\kappa'^2_{x,0}-\kappa'^2_{y,0})^2.$$

By considering the behaviour as $\lambda\to\infty$, we see that the extensional mode is associated with the positive value of $H^{\frac{1}{2}}$. Now as $\lambda\to 0$ this extensional mode is traced back to its origin in the flat plate mode whose frequency is given by

$$\Omega^2 = \tfrac{1}{2}(1+\nu) \tag{34}$$

and this identifies it as the dishing mode. (See equation (18) with $\zeta = 1$.)

The fact that the origin of the extensional mode does not depend on the ratio of the initial curvature is perhaps surprising, particularly in that it must be reconciled with the fact that if

$$\kappa'_{x,0} = -\kappa'_{y,0} \tag{35}$$

the dishing mode and frequency are the same as for the flat plate, in virtue of equation (23); furthermore, from equation (26) the extensional mode shape coincides with that of the bending mode. This apparent contradiction can only be resolved if, at some value of λ, the dishing and bending modes interchange. Such interchange can only occur if the bending and dishing frequencies coincide so that there is a state of modal indeterminacy. A frequency coincidence only occurs if the parameter H in equation (33) vanishes, and accordingly we consider this possibility in greater detail.

The parameter H is the sum of two squares and it can therefore vanish only when each of these components vanishes. The second component vanishes when

$$\kappa'_{x,0} = \pm\kappa'_{y,0},$$

but the plus sign is inadmissible because it results in an essentially positive and nonzero value of H. Taking the negative sign gives

$$H = (2+10\nu-8\kappa^2_{x,0})^2,$$

and this vanishes when $$\kappa^2_{x,0} = \tfrac{1}{4}(1+5\nu), \tag{36}$$

at which point $$\Omega^2_{\mathrm{d}} = \Omega^2_{\mathrm{b}} = \tfrac{1}{2}(1+\nu). \tag{37}$$

The apparent contradiction is thus resolved. The actual mode variation is well illustrated by considering a small dishing component superposed on the initial curvatures of equation (35) such that

$$\kappa_{x,0} = (1+\delta)\kappa,$$
$$\kappa_{y,0} = -(1-\delta)\kappa, \text{ say.}$$

The variation of the frequencies with κ is shown in figure 7 for $\delta = 0{\cdot}03, 0{\cdot}1$. In the vicinity of $\kappa = \frac{1}{2}(1+5\nu)^{\frac{1}{2}}$ there are abrupt changes in the shapes of the lower and higher frequency modes.

A numerical example. The analysis so far has been in terms of nondimensional curvature parameters. In order to give a clearer physical picture of the influence of initial curvatures on the small-deflexion frequencies we now express equation (36) in terms of deflexions and plate thicknesses.

From equation (9) with $\zeta = 1$ and $\nu = 0{\cdot}3$,

$$\mu = 4h_0/a^2,$$

whence, from equation (5),

$$[w_0]_{x=0,\,y=0} - [w_0]_{x=\pm a,\,y=0} = 2h_0\kappa_{x,0},$$
$$= 1{\cdot}58h_0$$

in virtue of equation (36), a result which is independent of the radius of the plate. Finally, we note that equation (37) implies a 67 % increase in bending frequency compared with that for the corresponding flat plate.

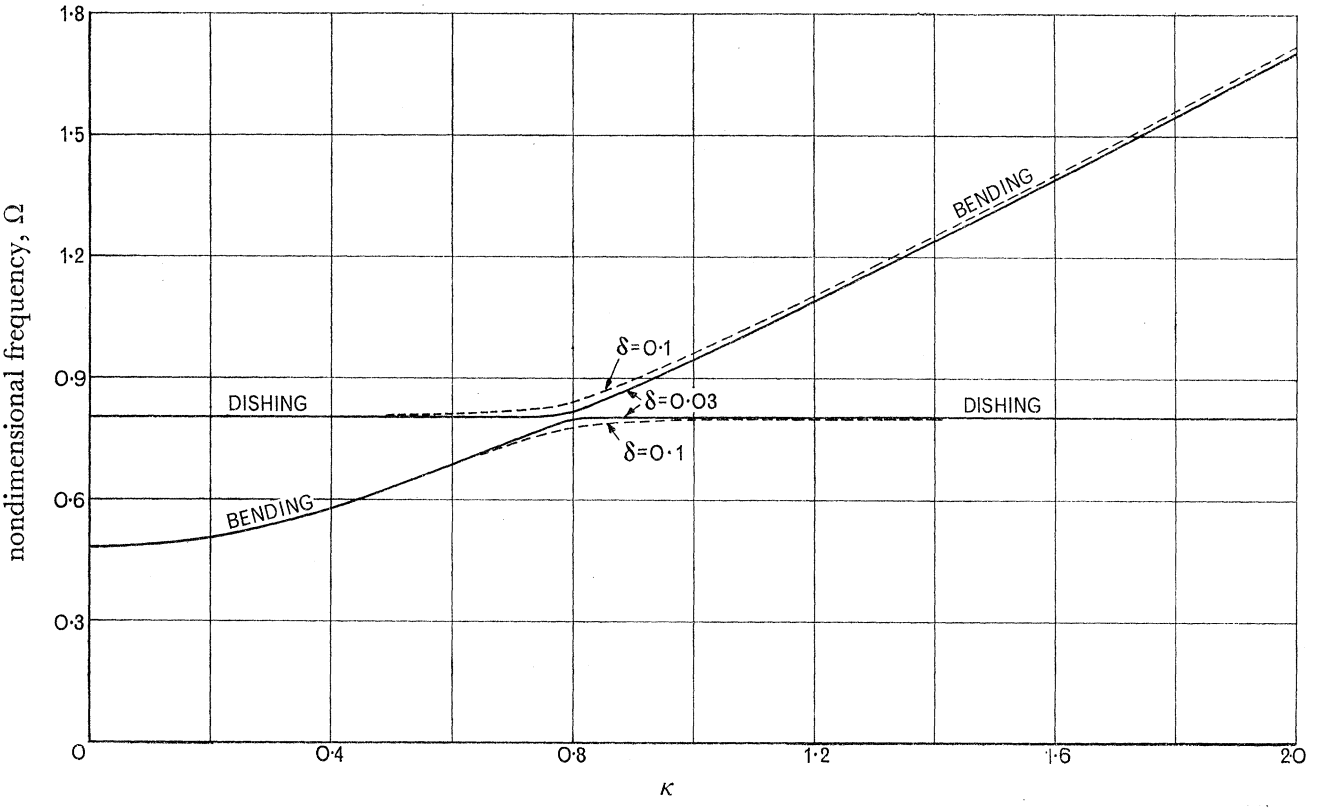

FIGURE 7. Frequency and mode variation with initial curvature: $\kappa_{x,0} = (1+\delta)\kappa$, $\kappa_{y,0} = -(1-\delta)\kappa$. Circular plate ($\zeta = 1$).

Elliptical plate. For the elliptical plate it may likewise be shown that the extensional mode has its origin in the flat plate dishing mode. Indeed, this follows from the fact that the frequency curves (Ω against λ) 'cross over' only in exceptional circumstances, and when this occurs there is a state of modal indeterminacy and a corresponding ambiguity in interpreting the paths of the curves. We have resolved this ambiguity by considering the limiting behaviour, as in the previous discussion of the circular plate.

Figure 8 is an illustrative example which shows the variation of the frequencies and mode shapes with $\kappa_{x,0}$ for a plate in which

$$\zeta = \tfrac{2}{3}$$

and

$$\kappa_{x,0} : \kappa_{y,0} : \kappa_{xy,0} = \epsilon_1^{\mathrm{d}} : -1{\cdot}05\epsilon_2^{\mathrm{d}} : 0{\cdot}05\epsilon_2^{\mathrm{d}}$$

where $(\epsilon_1^{\mathrm{d}}, \epsilon_2^{\mathrm{d}}, 0)$ is the dishing mode for the flat plate. This ratio between the initial curvatures has been chosen because it contains small perturbations from the relation

$$\kappa_{x,0} : \kappa_{y,0} : \kappa_{xy,0} = \epsilon_1^{\mathrm{d}} : -\epsilon_2^{\mathrm{d}} : 0$$

which satisfies equation (23) for the dishing and torsion modes. There are accordingly in figure 8 two regions in which abrupt changes occur in the mode shapes associated with each of the frequency curves.

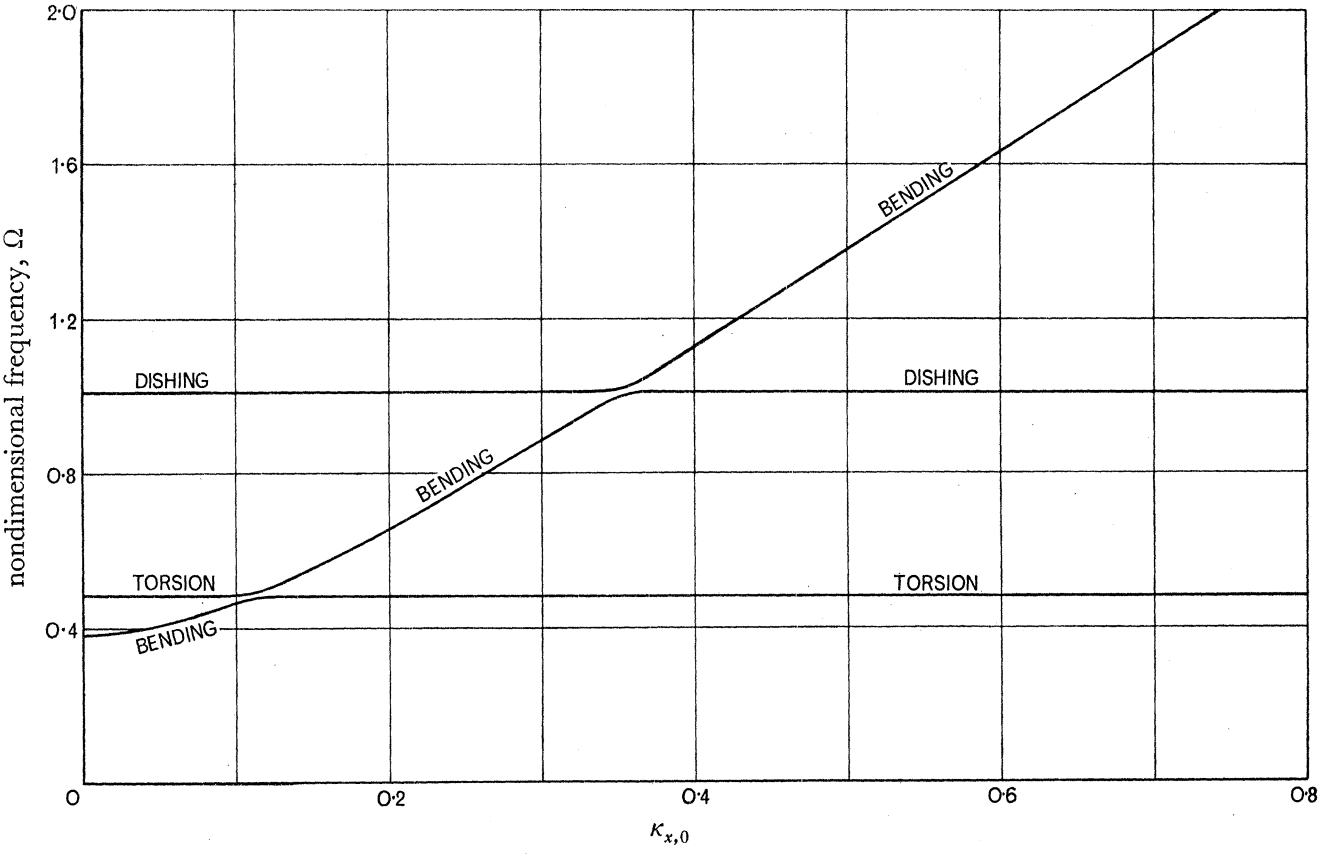

FIGURE 8. Frequency and mode variation with initial curvature: $\kappa_{x,0}:\kappa_{y,0}:\kappa_{xy,0} = \epsilon_1^{\mathrm{d}}: -1{\cdot}05\epsilon_2^{\mathrm{d}}: 0{\cdot}05\epsilon_2^{\mathrm{d}}$, elliptical plate ($\zeta = \frac{2}{3}$).

5. LARGE-DEFLEXION VIBRATIONS

It has already been mentioned that the concept of a mode has a much reduced significance in the large-deflexion régime. This is because of the nonlinear coupling effects which preclude the superposition of different modes, and hence preclude the analysis of a complex vibration by means of some normality principle. However, as Rosenberg (1964) points out, the concept of a mode as a free equiperiodic vibration—i.e. one in which

$$w(x, y, t) = w(x, y, t+T),$$

where T is the period of vibration—has some practical significance in that resonance of a structure occurs in the neighbourhood of the frequencies of such vibrations. Of course, in a nonlinear system the modal frequency is dependent on the amplitude so that for 'optimum' resonance conditions the frequency of the disturbing agency should match the varying modal frequency. The simplest type of nonlinear mode—being most closely related to a mode in a linear system—is the 'free vibration in unison' defined here by the relation

$$w(x, y, t) = w(x, y) f(t).$$

We will shortly consider examples of such simple nonlinear modes, but they are the exception rather than the rule. Indeed, if we postulate that each small-deflexion mode has a continued existence—in one form or another—in the large-deflexion régime, we find that we must dispense with the requirement of vibration in unison and adopt the following less restrictive definition of a mode:

(i) the motion is equiperiodic,

(ii) in each complete cycle there are two times at which all the velocities vanish,

(iii) there is at least one component of the vibration which varies monotonically between the states at which all the velocities vanish.

Items (i) and (ii) alone would be too general because they include, for example, all small-deflexion vibrations compounded of two or more modes whose periods have a common factor. Item (iii) has been introduced in an attempt to avoid this difficulty. From a practical standpoint it would not have been satisfactory to stipulate that *all* components of the vibration vary monotonically because, as will be shown later, this would often exclude the most important large-deflexion equiperiodic vibrations, namely those which have the lowest frequency for a given level of energy. Note also that in a small-deflexion modal vibration all particles pass through the equilibrium position at the same time, whereas in the large-deflexion régime this is generally not so unless the plate is initially flat or the mode is a vibration in unison.

Finally, some general observations on the form of equations (10) and (11): These contain no first derivatives with respect to τ because there is no damping and the plate is elastic. Accordingly, for every large-deflexion free vibration there is another in which the sign of τ is reversed. In particular, if in any free vibration the plate becomes instantaneously at rest the subsequent motion is a mirror-image of the previous motion; the plate 'retraces its steps'. In addition, if the plate is initially flat the equations are unaltered by a change in sign of the curvatures, so that if the plate passes through the (flat) equilibrium position at zero time, say, the subsequent motion is determined by the relations

$$\kappa_x(\tau) = -\kappa_x(-\tau), \quad \kappa_y(\tau) = -\kappa_y(-\tau), \quad \kappa_{xy}(\tau) = -\kappa_{xy}(-\tau).$$

5·1. *Flat circular plate*

For the flat circular plate equations (11 *a*, *b*, *c*) simplify considerably, particularly if the sums and differences of (*a*) and (*b*) are considered, so that

$$2(\ddot{\kappa}_x+\ddot{\kappa}_y)+(1+\nu)\,(\kappa_x+\kappa_y)-\beta(\kappa_x+\kappa_y) = 0, \tag{38a}$$

$$3(\ddot{\kappa}_x-\ddot{\kappa}_y)+(1-\nu)\,(\kappa_x-\kappa_y)+\beta(\kappa_x-\kappa_y) = 0, \tag{38b}$$

$$3\ddot{\kappa}_{xy}+(1-\nu)\,\kappa_{xy}+\beta\kappa_{xy} = 0, \tag{38c}$$

where, from equation (10)

$$\beta = \kappa_{xy}^2-\kappa_x\kappa_y. \tag{39}$$

The particular merit of writing the equations in this form is that it is immediately apparent that there exist vibrations characterized by

$$\left.\begin{aligned}\kappa_x &= \kappa_y,\\ \kappa_{xy} &= 0,\end{aligned}\right\} \tag{40}$$

so that only the dishing mode is present, or

$$\left.\begin{aligned}\kappa_x &= -\kappa_y,\\ \kappa_{xy} &= 0,\end{aligned}\right\} \tag{41}$$

so that only the bending mode is present, or

$$\kappa_x = \kappa_y = 0, \tag{42}$$

so that only the torsion mode is present.

5·1·1. *The dishing mode*

Equations (38 *b*, *c*) are satisfied by equation (40) above, and equations (38 *a*) and (39) are satisfied if

$$2\ddot{\kappa}_x + (1+\nu)\kappa_x + \kappa_x^3 = 0. \tag{43}$$

The relation between κ_x, τ (or κ_y, τ) can be expressed in terms of incomplete elliptic integrals, whose precise form depends on the initial conditions. If these are such that

$$[\dot{\kappa}_x]_{\tau=0} = 0,$$

and

$$[\kappa_x]_{\tau=0} = \kappa_X, \text{ say,}$$

then

$$\left.\begin{aligned}\tau &= \left(\frac{2}{1+\nu+\kappa_X^2}\right)^{\frac{1}{2}} \int_0^{\alpha_1} \frac{\mathrm{d}\psi}{(1-k_1^2\sin^2\psi)^{\frac{1}{2}}}\\ &= \left(\frac{2}{1+\nu+\kappa_X^2}\right)^{\frac{1}{2}} F(k_1, \alpha_1),\end{aligned}\right\} \tag{44}$$

where

$$\left.\begin{aligned}k_1^2 &= \frac{\kappa_X^2}{2(1+\nu+\kappa_X^2)},\\ \alpha_1 &= \cos^{-1}(\kappa_x/\kappa_X),\end{aligned}\right\}$$

and $F(k_1, \alpha_1)$ is the incomplete elliptic integral of the first kind. The motion is periodic and the frequency is given by

$$\Omega_{\mathrm{d}}^2 = \frac{\pi^2(1+\nu+\kappa_X^2)}{8\{K(k_1)\}^2}, \tag{45}$$

where $K(k_1), = F(k_1, \frac{1}{2}\pi)$, is the complete elliptic integral of the first kind with modulus k_1.

The velocity of the plate is a maximum as it passes through the equilibrium position where it is given by

$$[\dot{\kappa}_x]_{\kappa_x=0} = \kappa_X\{\tfrac{1}{2}(1+\nu) + \tfrac{1}{4}\kappa_X^2\}^{\frac{1}{2}}. \tag{46}$$

By means of equation (46) the solution can be adapted to accommodate initial conditions in which κ_x is zero and $\dot{\kappa}_x$ is specified.

5.1.2. *The bending and torsion modes*

In the small-deflexion régime the bending and torsion modes for the flat circular plate are essentially the same, differing only in their orientation to the (arbitarily chosen) reference axes. This is a result of the rotational symmetry of the plate and, as such, is valid in the large-deflexion régime. Thus for the bending mode, equations (38) and (39) are satisfied by equation (41) if κ_x satisfies the equation

$$3\ddot{\kappa}_x + (1-\nu)\kappa_x + \kappa_x^3 = 0. \tag{47}$$

PHILOSOPHICAL TRANSACTIONS OF THE ROYAL SOCIETY A MATHEMATICAL, PHYSICAL & ENGINEERING SCIENCES

Similarly the torsion mode, equation (42), is a solution if κ_{xy} satisfies the equation

$$3\ddot{\kappa}_{xy}+(1-\nu)\kappa_{xy}+\kappa_{xy}^3=0. \tag{48}$$

By the same token, a linear combination of the form

$$\left.\begin{aligned}\kappa_x &= \kappa, \text{ say}\\ \kappa_y &= -\kappa,\\ \kappa_{xy} &= k\kappa,\end{aligned}\right\} \tag{49}$$

is a solution if κ satisfies the equation

$$3\ddot{\kappa}+(1-\nu)\kappa+(1+k^2)\kappa^3=0, \tag{50}$$

but if the reference axes are chosen to coincide with the principal axes of curvature, or with the axes of maximum twist, the form of equation (50) reduces to that of equation (47) or (48).

The bending and torsion modes have much in common with the dishing mode and, as no generality is lost, the discussion is limited to the torsion mode. Thus, if the initial conditions are such that

$$[\dot{\kappa}_{xy}]_{\tau=0}=0,$$

and

$$[\kappa_{xy}]_{\tau=0}=\kappa_{XY}, \text{ say}$$

then

$$\left.\begin{aligned}\tau &= \left(\frac{3}{1-\nu+\kappa_{XY}^2}\right)^{\frac{1}{2}}F(k_2,\alpha_2),\\ \text{where}\quad k_2^2 &= \frac{\kappa_{XY}^2}{2(1-\nu+\kappa_{XY}^2)},\\ \alpha_2 &= \cos^{-1}(\kappa_{xy}/\kappa_{XY}).\end{aligned}\right\} \tag{51}$$

The motion is periodic and the frequency is given by

$$\Omega_{\mathrm{t}}^2=\frac{\pi^2(1-\nu+\kappa_{XY}^2)}{12\{K(k_2)\}^2}. \tag{52}$$

The velocity of the plate is a maximum as it passes through the equilibrium position where it is given by

$$[\dot{\kappa}_{xy}]_{\kappa_{xy}=0}=\kappa_{XY}\{\tfrac{1}{3}(1-\nu)+\tfrac{1}{6}\kappa_{XY}^2\}^{\frac{1}{2}}. \tag{53}$$

5·1·3. *Stability of the dishing, bending and torsion modes*

In discussing the stability of the dishing, bending and torsion modes it is instructive to consider first the mode behaviour when the maximum curvature is very large. When

$$\kappa_X^2,\ \kappa_Y^2 \quad \text{or} \quad \kappa_{XY}^2 \gg 1$$

equations (45) and (52) show that the frequencies vary asymptotically in direct proportion to the amplitudes

$$\left.\begin{aligned}\Omega_{\mathrm{d}} &\sim \frac{\pi\sqrt{(2\pi)}}{\{\Gamma(\frac{1}{4})\}^2}|\kappa_X| = 0{\cdot}599\,|\kappa_X|,\\ \Omega_{\mathrm{t}} &\sim 0{\cdot}489\,|\kappa_{XY}| = 0{\cdot}599(\tfrac{2}{3})^{\frac{1}{2}}|\kappa_{XY}|.\end{aligned}\right\} \tag{54}$$

The reason for this is that the motion is now governed by the middle-surface forces which arise because the mode shape is not a developable surface; in other words, the β term in the governing equations has assumed a dominating role. The middle-surface forces vary as the

square of the plate curvature and their normal component which acts as a restoring force therefore varies as the cube of the curvature. It is this highly nonlinear behaviour which causes the frequency to vary in proportion to the maximum curvature. Note that this asymptotic variation of frequency with maximum curvature, given by equation (54), has a marked similarity to the asymptotic variation of the small-deflexion frequency with initial curvature in the extensional mode, given by equation (25) with $\zeta = 1$:

$$\Omega_e \sim |\kappa_{x,0}|$$

for the dishing mode of a dished plate, and

$$\Omega_e \sim (\tfrac{2}{3})^{\frac{1}{2}} |\kappa_{xy,0}|$$

for the torsion mode of a twisted plate.

The point has already been made that as the maximum curvatures increase, the dishing, bending and torsion modes become extensional in character. Now in a plate subjected to static loads there are critical values of the middle-surface forces at which buckling occurs. It is therefore natural to consider the stability of these modes in the expectation that this may be related in some manner to the occurrence of static buckling.

Stability of the dishing mode. Consider now a circular plate vibrating in a large-deflexion dishing mode which is perturbed by a small bending component, say. We wish to determine the conditions required for the growth of such perturbation. Such growth is, of course, limited because it depends on a transfer of energy from the primary mode. Now in the stages immediately following the introduction of the perturbation it may be assumed that the middle surface forces are sensibly unaffected by the perturbation, so that equation (39) simplifies to

$$\beta \approx -\kappa_x^2, \tag{55}$$

where κ_x is given by the analysis of § 5·1·1. Equation (38 *b*), which governs the behaviour of the perturbation, may now be written in the form

$$(\ddot{\kappa}_x - \ddot{\kappa}_y)/(\kappa_x - \kappa_y) \approx -\tfrac{1}{3}(1 - \nu - \kappa_x^2). \tag{56}$$

Thus when

$$\kappa_x^2 < 1 - \nu$$

the sign of $(\ddot{\kappa}_x - \ddot{\kappa}_y)$ is opposite to that of $(\kappa_x - \kappa_y)$, resulting in a stable oscillatory behaviour of the perturbation. But if at any stage in the dishing vibration

$$\kappa_x^2 > 1 - \nu$$

the sign of $(\ddot{\kappa}_x - \ddot{\kappa}_y)$ is the same as that of $(\kappa_x - \kappa_y)$, resulting in a growth of the perturbation. Now the maximum value of κ_x is κ_X and accordingly the criterion for the stability of the dishing mode is that

$$\left.\begin{aligned} \kappa_X^2 &< \kappa_X^{*2}, \\ \text{where} \quad \kappa_X^{*2} &= 1 - \nu. \end{aligned}\right\} \tag{57}$$

It is to be noted that when $\kappa_X^2 = \kappa_X^{*2}$

the middle surface forces are such that

$$\beta = -(1 - \nu) \tag{58}$$

which is the critical value at which static buckling occurs in a plate subjected to a pressure distribution similar to the inertia distribution in the dishing mode. There is, however, an

important distinction between the static and dynamic cases; in the static case the middle surface forces maintain the values they have at the onset of buckling, whereas in the dynamic case the buckling tendency is resisted by the inertia of the plate, and middle-surface forces in excess of the static buckling values are developed. Indeed, if there is no perturbation the buckling tendency is completely suppressed.

This simplified stability analysis does not, of course, provide any quantitative information on the plate vibration. To provide such information figures 9 to 12 have been prepared. These show the variation of κ_x and κ_y with τ for plates released from nearly dished states in which

$$\kappa_X - \kappa_Y = 0{\cdot}01(\kappa_X + \kappa_Y),$$

or

$$\kappa_X - \kappa_Y = 0{\cdot}02(\kappa_X + \kappa_Y)$$

and $\frac{1}{2}(\kappa_X+\kappa_Y)/\kappa_X^* = 1{\cdot}5$ in figures 9, 10, and 3 in figures 11, 12. When $\frac{1}{2}(\kappa_X+\kappa_Y) \leqslant \kappa_X^*$ there is no tendency for the bending perturbation to increase, but when $\frac{1}{2}(\kappa_X+\kappa_Y) > \kappa_X^*$ the bending perturbation increases—though not indefinitely—and the resulting vibration loses its repetitive character. A comparison of figures 9 and 10 shows that a doubling of the initial perturbation does not affect the magnitude of the subsequent maximum perturbation, although it hastens its occurrence. Figures 9 to 12 are obtained from a numerical integration of the governing differential equations because no analytical solution exists. When such numerical integration is required the general technique in this paper is to write the three second order equations (11 a, b, c) as six first order equations in κ_x, $\dot{\kappa}_x$, κ_y, etc., and then to employ the Runge–Kutta step-by-step method. All results are doubly checked by retracing the vibration to its initiation and by repeating the calculation with a halved time interval.

Stability of the bending and torsion modes. The determination of the stability criterion for the bending and torsion modes is similar to that for the dishing mode. It is found that the criterion for the stability of the torsion mode is that

$$\left.\begin{aligned} \kappa_{XY}^2 &< \kappa_{XY}^{*2}, \\ \text{where} \quad \kappa_{XY}^{*2} &= 1+\nu. \end{aligned}\right\} \tag{59}$$

Further, when $\kappa_{XY}^2 = \kappa_{XY}^{*2}$
the middle-surface forces are such that

$$\beta = 1+\nu, \tag{60}$$

which is the critical value at which static buckling occurs in a plate subjected to a pressure distribution similar to the inertia distribution in the torsion mode. The criterion for the stability of the bending mode is obtained by substituting $\frac{1}{2}(\kappa_X-\kappa_Y)$ for κ_{XY} above.

5·1·4. *The curling modes*

We have already seen that with increase in amplitude the dishing, bending and torsion modes become extensional in character. Further, if certain critical curvatures are exceeded these modes become unstable. Indeed, for the highly dished cases in figures 11 and 12 the instability is such that at certain subsequent times (e.g. $\tau \approx 15$ figure 11 and $\tau \approx 7$, 12 and 17 in figure 12) when the plate is almost at rest the strain energy is largely flexural. This suggests that there may be modes—in the sense described in § 5—which are largely flexural in

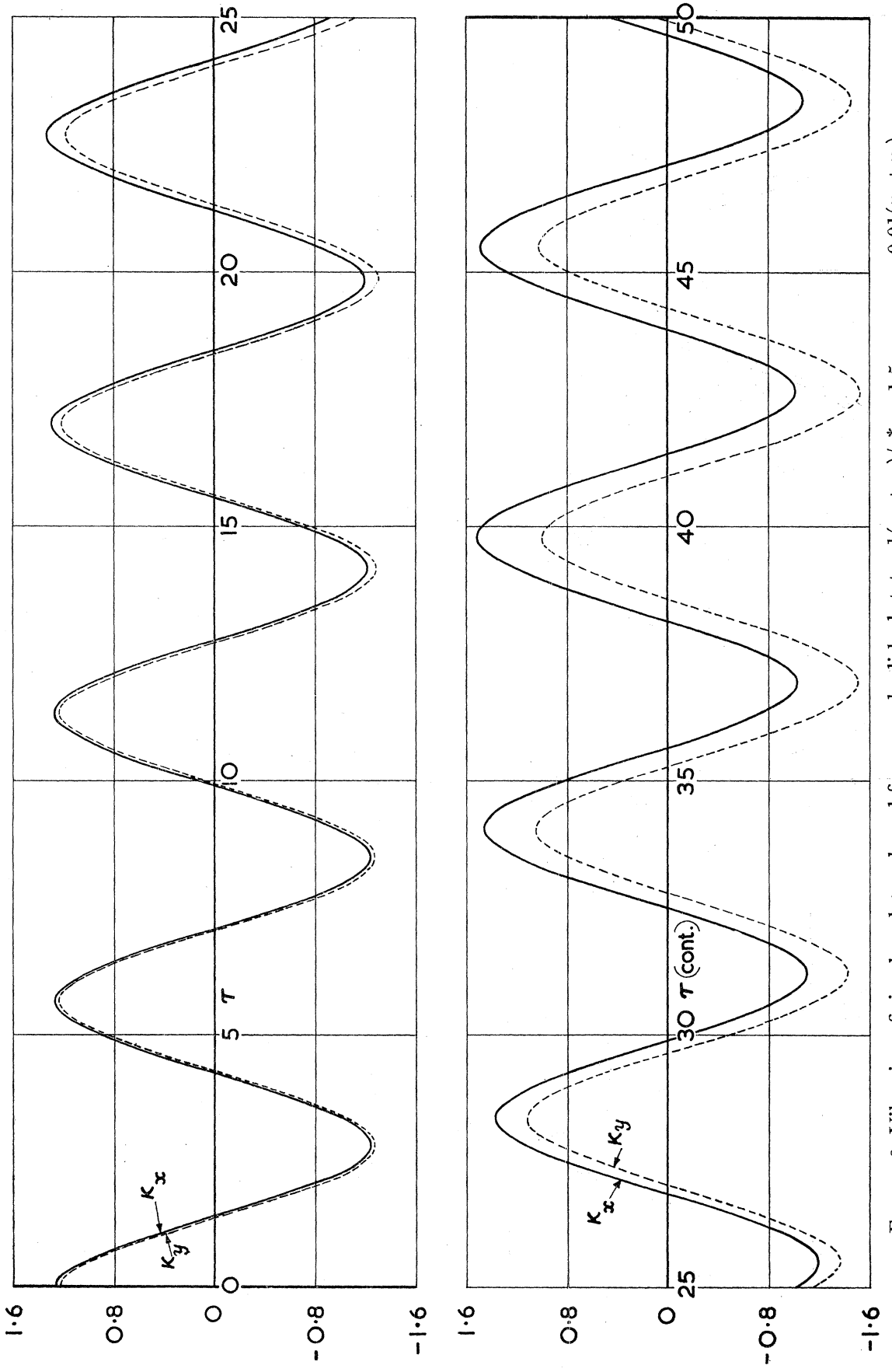

FIGURE 9. Vibration of circular plate released from nearly dished state: $\frac{1}{2}(\kappa_X+\kappa_Y)/\kappa_X^* = 1{\cdot}5$, $\kappa_X-\kappa_Y = 0{\cdot}01(\kappa_X+\kappa_Y)$.

PHILOSOPHICAL TRANSACTIONS OF THE ROYAL SOCIETY A MATHEMATICAL, PHYSICAL & ENGINEERING SCIENCES

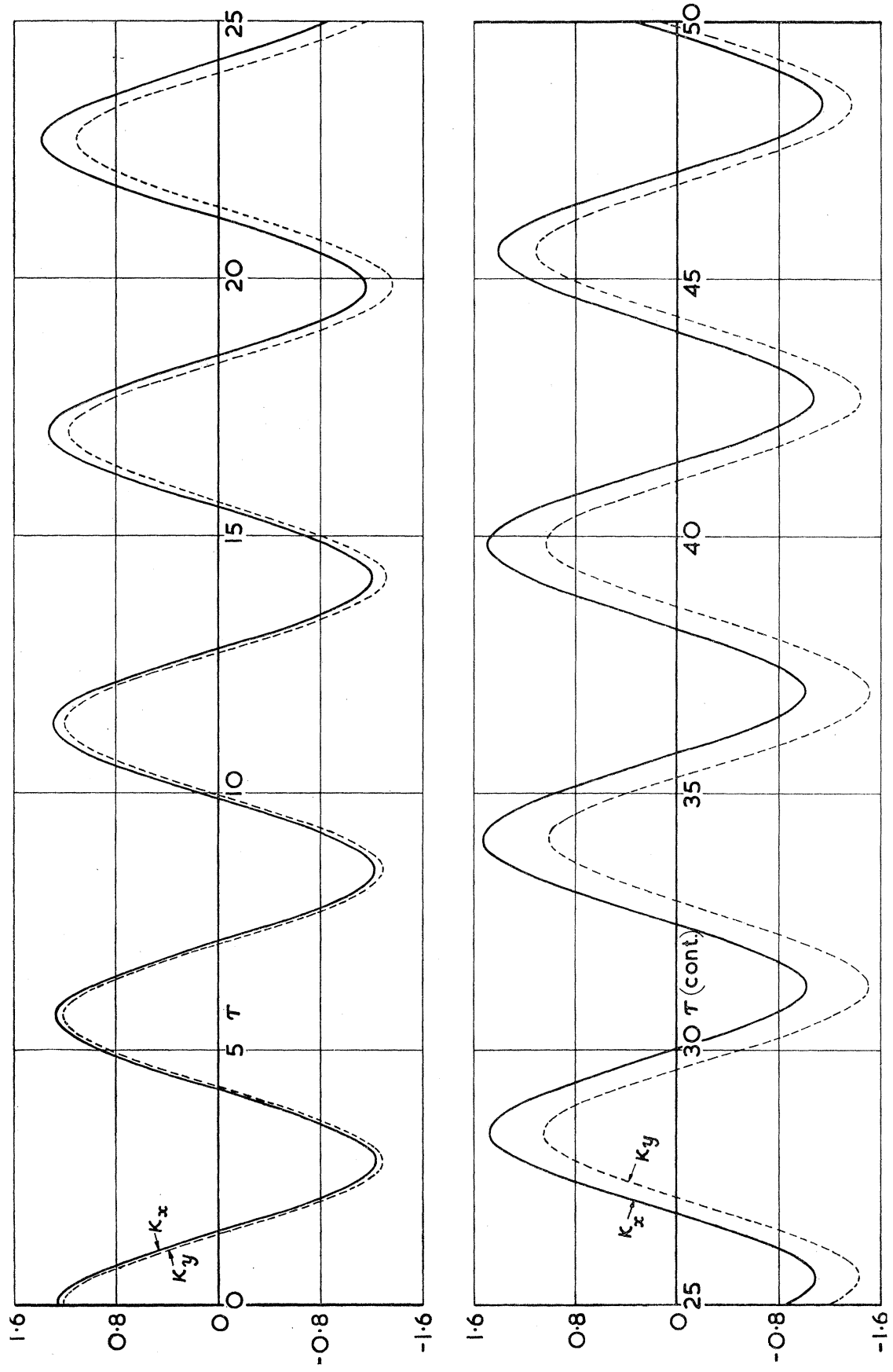

FIGURE 10. Vibration of circular plate released from nearly dished state; $\frac{1}{2}(\kappa_X+\kappa_Y)/\kappa_X^*=1{\cdot}5$, $\kappa_X-\kappa_Y=0{\cdot}02(\kappa_X+\kappa_Y)$.

PHILOSOPHICAL TRANSACTIONS OF THE ROYAL SOCIETY A MATHEMATICAL, PHYSICAL & ENGINEERING SCIENCES

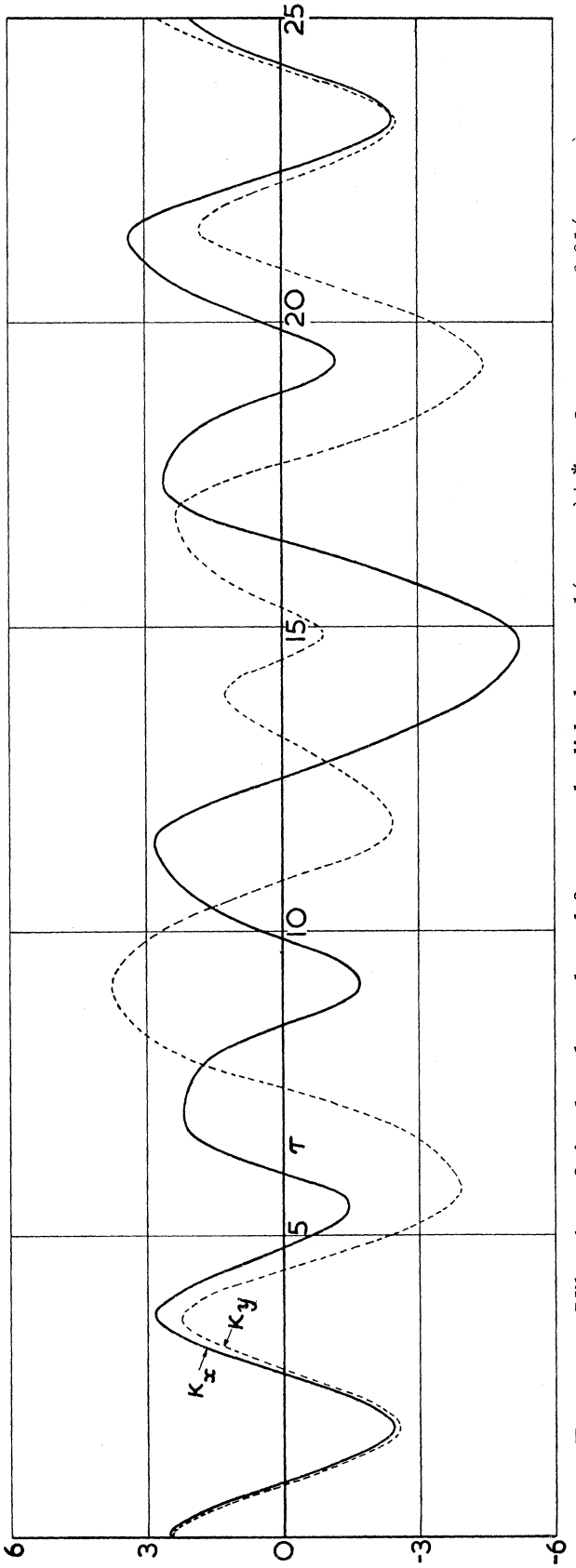

FIGURE 11. Vibration of circular plate released from nearly dished state; $\frac{1}{2}(\kappa_X+\kappa_Y)/\kappa_X^*=3$, $\kappa_X-\kappa_Y=0{\cdot}01(\kappa_X+\kappa_Y)$.

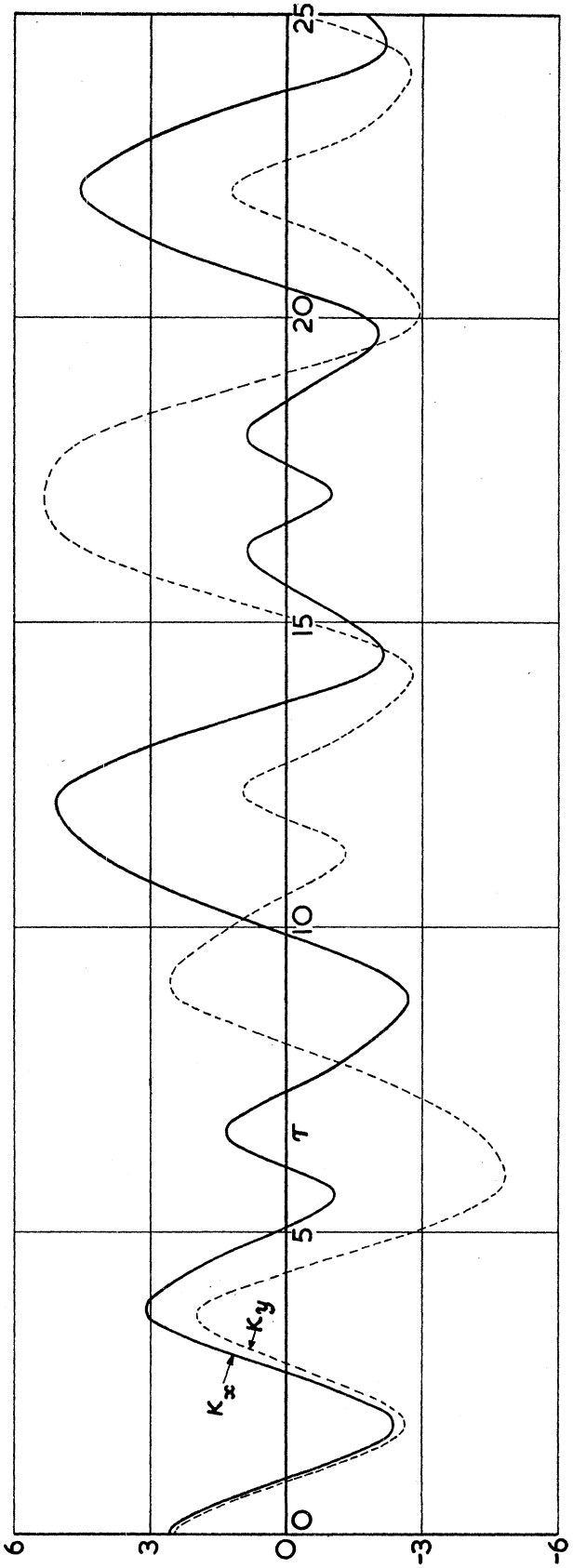

FIGURE 12. Vibration of circular plate released from nearly dished state; $\frac{1}{2}(\kappa_X+\kappa_Y)/\kappa_X^*=3$, $\kappa_X-\kappa_Y=0{\cdot}02(\kappa_X+\kappa_Y)$.

PHILOSOPHICAL TRANSACTIONS OF THE ROYAL SOCIETY A MATHEMATICAL, PHYSICAL & ENGINEERING SCIENCES

character throughout their motion, but whose existence is only possible when the energy of the vibrating plate exceeds a certain value. Now any large-deflexion mode which is predominantly flexural in character will approximate to the curling mode, introduced after equation (30), for this is the only type of deformation in which there is no straining of the

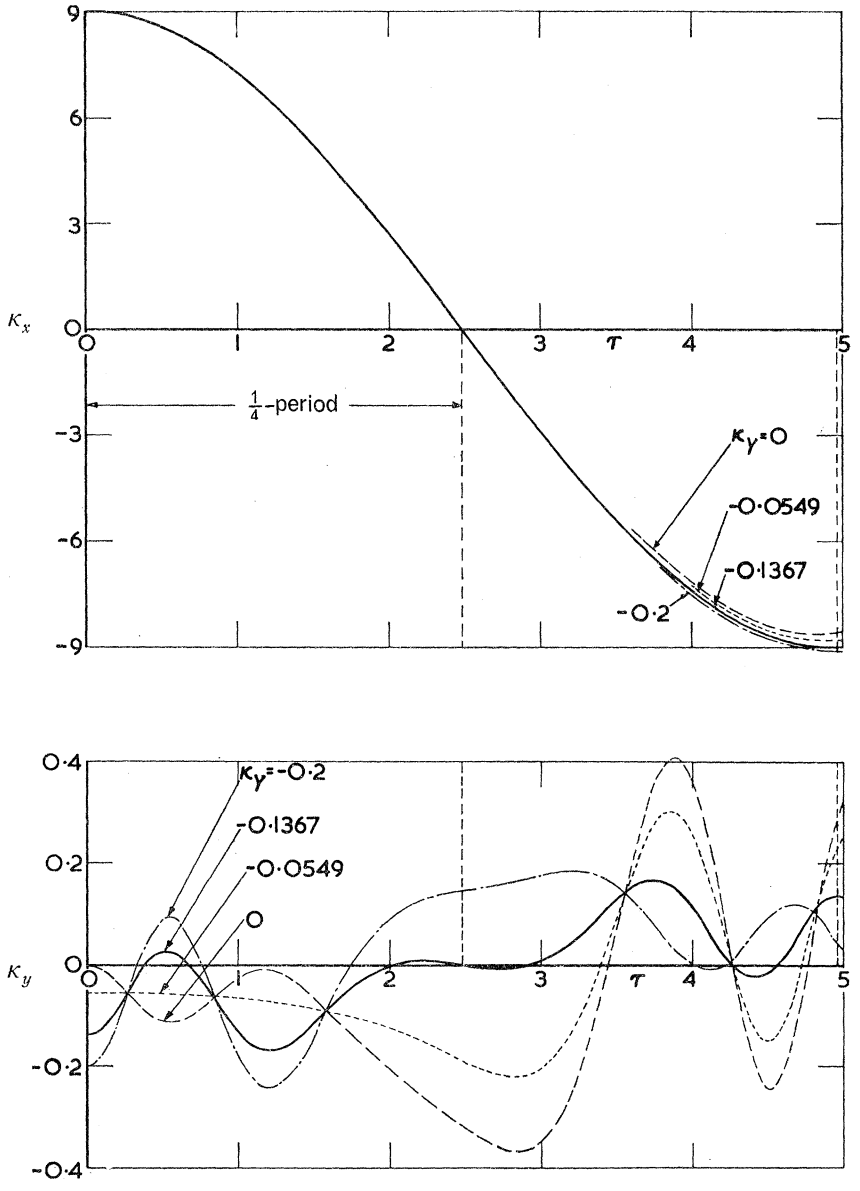

FIGURE 13. Vibrations in and near a curling mode, circular plate, $\kappa_X = 9$.

middle surface. With this underlying concept in mind we now consider a series of vibrations in which the plate is released from nearly curled states in which

$$\kappa_X \gg \kappa_Y, \text{ say}$$

and

$$\kappa_{XY} = 0.$$

Figure 13 shows the subsequent variations of κ_x and κ_y with time for $\kappa_X = 9$, with κ_Y taking various values between $-0{\cdot}2$ and 0. The variation of κ_x does not depend significantly on the

(small) value of κ_Y, but the variation of κ_y shows some interesting features. The 'smoothest' initial variation occurs when $\kappa_Y = -0{\cdot}0549$, and this is the value that the plate would have if subjected to a static loading similar to the inertia loading in a purely curling vibration. This value of κ_Y is obtained by equating to zero the left hand side of equation (11 *b*), whence

$$\kappa_Y = \frac{-2\kappa_X(1+5\nu)}{5+\nu+5\kappa_X^2+\{(5+\nu+5\kappa_X^2)^2-4\kappa_X^2(1+5\nu)\}^{\frac{1}{2}}}. \tag{61}$$

For other values of κ_Y the variation of κ_y with time is best described as a high frequency vibration superposed on the 'smooth' variation. Thus, confining attention to the first $\frac{1}{4}$-period range it is seen that the period and the amplitude of these superposed vibrations increase with time. The reason for this is that they are predominantly extensional vibrations —similar to those considered in § 4·2·1—and their frequency varies approximately as the curvature κ_x; the increase in amplitude is similarly related to the reduction of effective stiffness in the plate as the curvature κ_x decreases. Finally, we note that when $\kappa_Y = -0{\cdot}1367$ the curvatures κ_x and κ_y vanish simultaneously, at $\tau = 2{\cdot}478$, and the motion is periodic. Furthermore, the frequency in this curling mode is only 0·2 % greater than that given by equation (31).

Figure 14 is similar to figure 13 except that $\kappa_X = 5$ and κ_Y takes various values between $-0{\cdot}2$ and $+0{\cdot}15$. The smoothest initial variation now occurs when $\kappa_Y = -0{\cdot}0963$ and the curling mode occurs when $\kappa_Y = +0{\cdot}0555$. Thus, in the curling mode the sign of κ_Y differs from that when $\kappa_X = 9$. The reason for this is that the superposed κ_y vibrations are less rapid, because of the reduced value of κ_X, and change sign once less often during each $\frac{1}{4}$-period.

5·1·5. *Presentation of results*

The modal relations between κ_X and κ_Y for the dishing, bending and curling modes are shown in figure 15 where, because the plate is circular, there is symmetry about the lines $\kappa_X = \pm\kappa_Y$. It is seen that there is a *series* of curling modes associated with separate 'tongues' in the κ_X, κ_Y plane, which become extensional in character for large values of $|\kappa_X\kappa_Y|$. A further point of interest occurs at the intersection of the first curling mode with the bending mode; at that point $(-0{\cdot}836, +0{\cdot}836)$ the magnitude of κ_X, κ_Y coincides with the critical magnitude in the dishing mode (see point a) above which the dishing mode becomes unstable. Furthermore, the intersection is at a point of modal indeterminacy, in that the frequency of a small dishing component superposed on the bending mode coincides with the frequency of the bending mode itself.

The variation of frequency with amplitude is shown in figure 16 where the points a, ..., h correspond to those in figure 15, enabling the various curves to be identified. It is seen that when $\kappa_Y > 0{\cdot}836$ the lowest frequency is that associated with the curling mode and, except in certain localized regions, it is insensitive to changes in amplitude.

Figures 17 a, ..., h show the variations of κ_x, κ_y with time, in modes corresponding to the points a, ..., h in figures 15 and 16; points a and b are at the points of limiting stability discussed in § 5·1·3.

5·1·6. *Stability of the curling modes*

To obtain some idea of the stability of the curling modes figures 18 to 21 have been prepared. These show the variation of κ_x, κ_y and β with time up to $\tau = 25$ for circular plates

released from states which differ from modal relations by varying amounts. Figures 18, 19, 20 are for $\kappa_X = 9$ and, respectively, $\kappa_Y = -0{\cdot}13$, $-0{\cdot}1$, 0, values which may be compared with $-0{\cdot}1367$ for the curling mode. It is seen that the resulting vibrations are sensitive to variations in κ_Y, although these variations are small in comparison with κ_X. Figure 21 is for

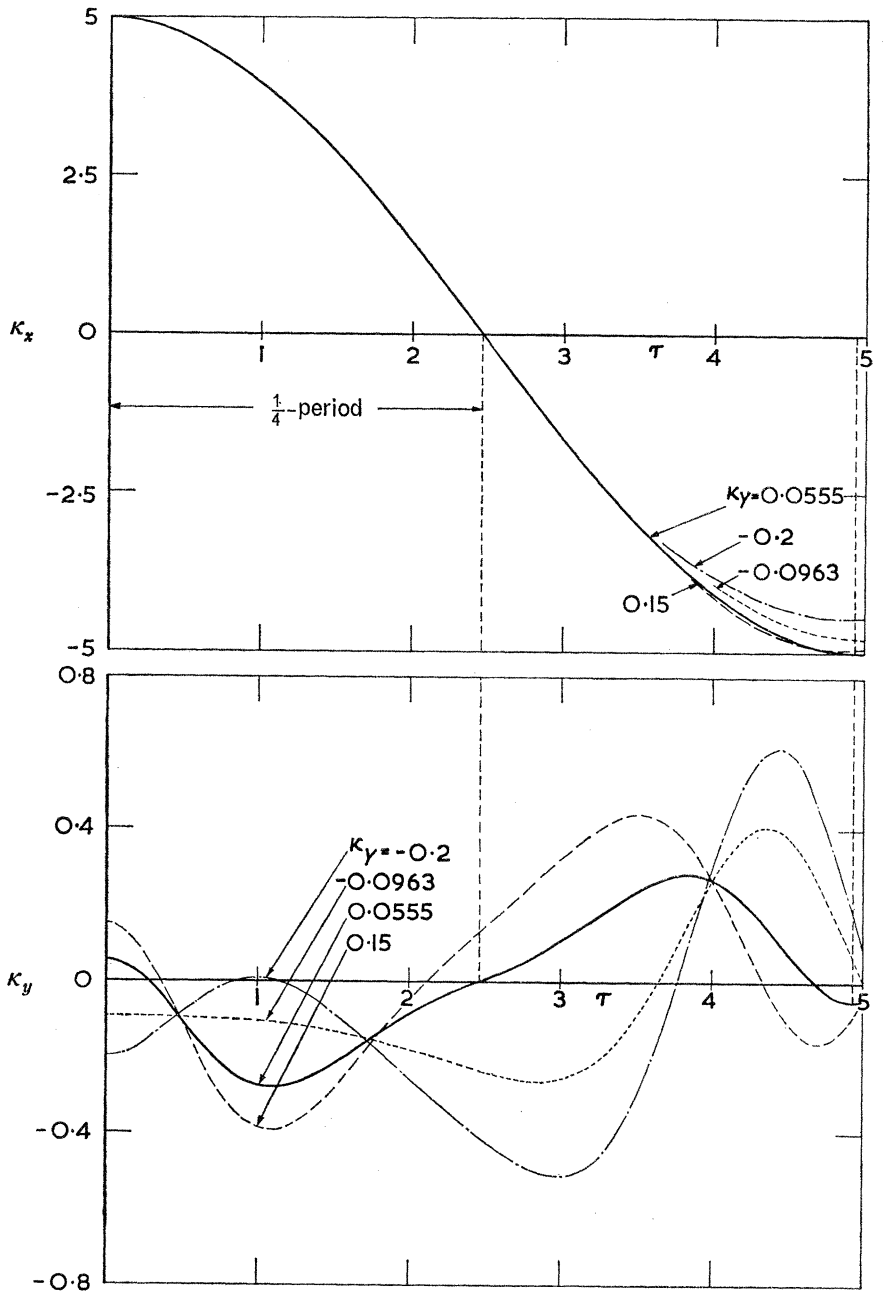

FIGURE 14. Vibrations in and near a curling mode, circular plate, $\kappa_X = 5$.

$\kappa_X = 10$ and $\kappa_Y = 0$, compared with $-0{\cdot}263$ for the curling mode. The resulting vibration is much more unstable than that in figure 20, and this is due to the greater departure from the modal relation which is, itself, reflected in the varying curvature near point h in figure 15.

5·2. *Dishing modes of a dished circular plate*

In this section we consider another 'vibration in unison', namely the large-deflexion dishing mode of an initially dished circular plate. For such a plate the governing differential equation is obtained from equations (10) and (11) by writing

$$\kappa_{x,0} = \kappa_{y,0}, \qquad \kappa_{xy,0} = 0,$$

$$\kappa_x = \kappa_y, \qquad \kappa_{xy} = 0$$

whence, in terms of κ_x,

$$2\ddot{\kappa}_x + (1+\nu)(\kappa_x - \kappa_{x,0}) + \kappa_x(\kappa_x^2 - \kappa_{x,0}^2) = 0. \tag{62}$$

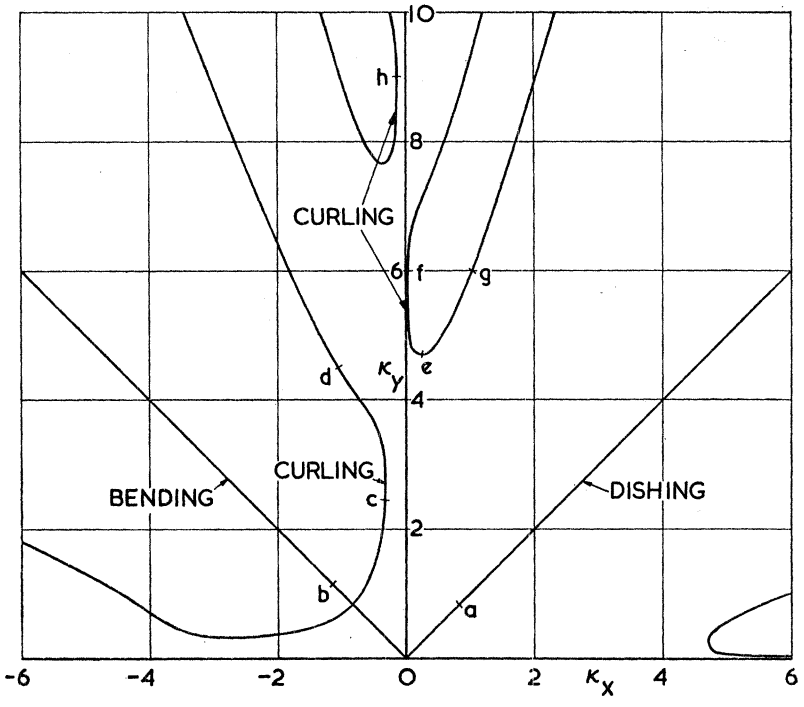

FIGURE 15. Modal relation between κ_X, κ_Y: circular plate.

It is convenient to define $\kappa_{x,0}$ positive, which involves no loss of generality.

Now although the terms in equation (62) are nondimensional there are certain advantages, particularly a unification with the analysis of § 5·3, in introducing the following parameters

$$\left.\begin{aligned} \Lambda &= 3\kappa_{x,0}/2(1+\nu+2\kappa_{x,0}^2)^{\frac{1}{2}}, \\ \gamma &= (\kappa_x - \kappa_{x,0})/(1+\nu+2\kappa_{x,0}^2)^{\frac{1}{2}}, \\ \Omega_0^2 &= \tfrac{1}{2}(1+\nu+2\kappa_{x,0}^2), \end{aligned}\right\} \tag{63}$$

where Λ is a measure of the dishing curvature in the undisturbed state, and varies between zero and $\frac{3}{4}\sqrt{2}$, γ is a measure of the displacement about the undisturbed state, and, from the analysis of § 4·2, Ω_0 is the nondimensional frequency appropriate to small deflexions in the dishing mode. In terms of these parameters equation (62) reduces to

$$\ddot{\gamma} + \Omega_0^2\gamma(1+2\Lambda\gamma+\gamma^2) = 0, \tag{64}$$

which may be integrated as follows.

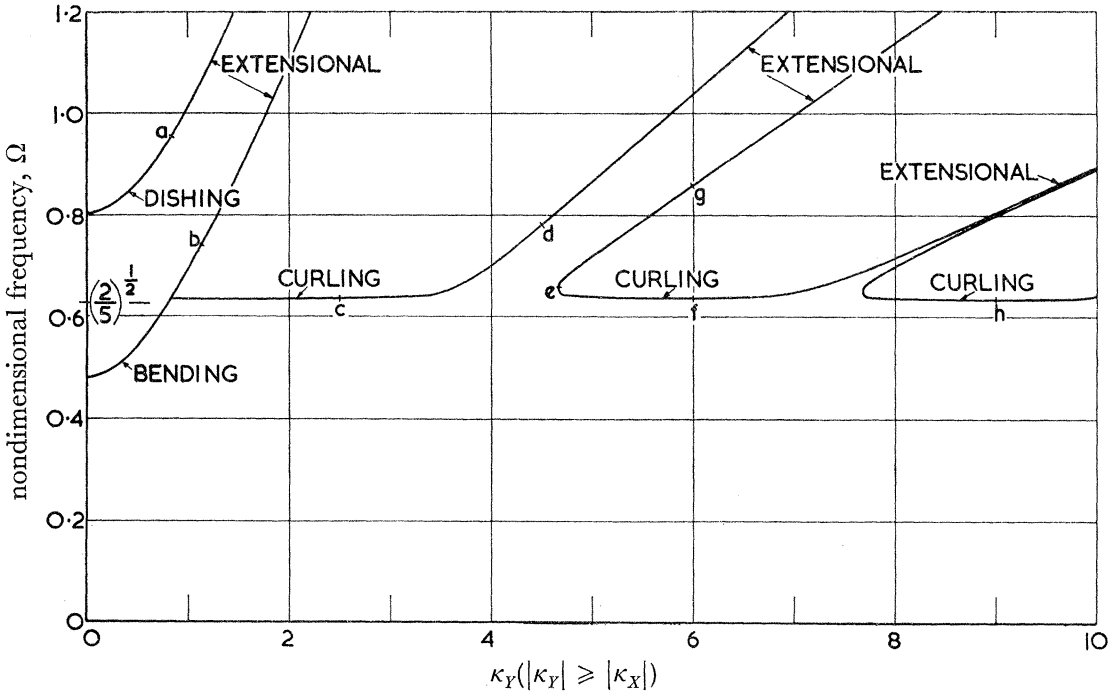

FIGURE 16. Frequency variation with amplitude, circular plate.

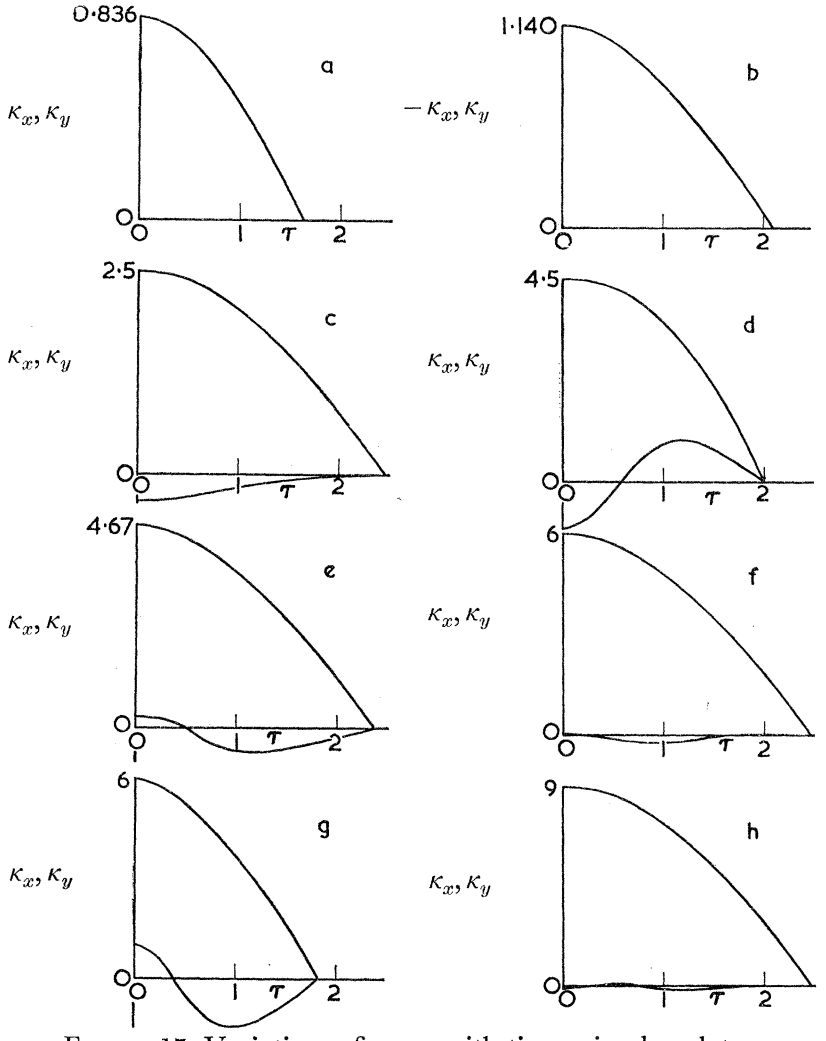

FIGURE 17. Variations of κ_x, κ_y with time; circular plate.

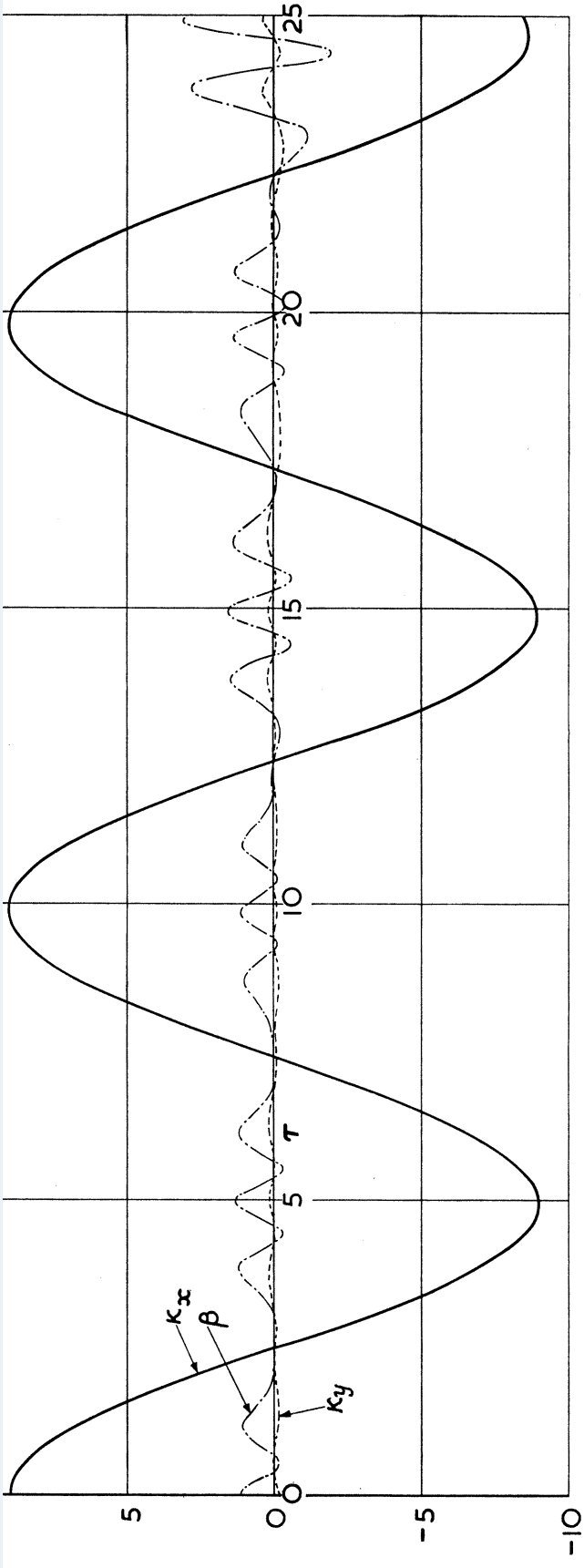

FIGURE 18. Vibration of circular plate released from nearly curled state; $\kappa_X = 9$, $\kappa_Y = -0{\cdot}13$.

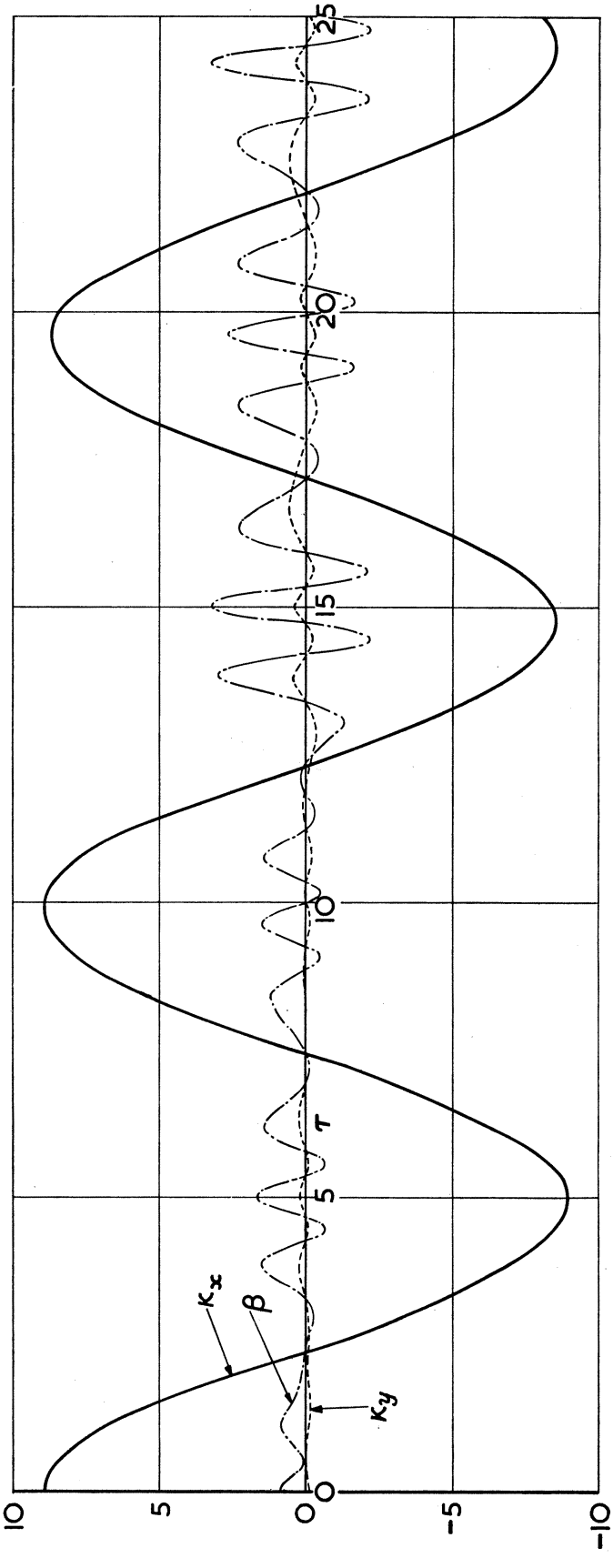

FIGURE 19. Vibration of circular plate released from nearly curled state; $\kappa_X = 9$, $\kappa_Y = -0{\cdot}1$.

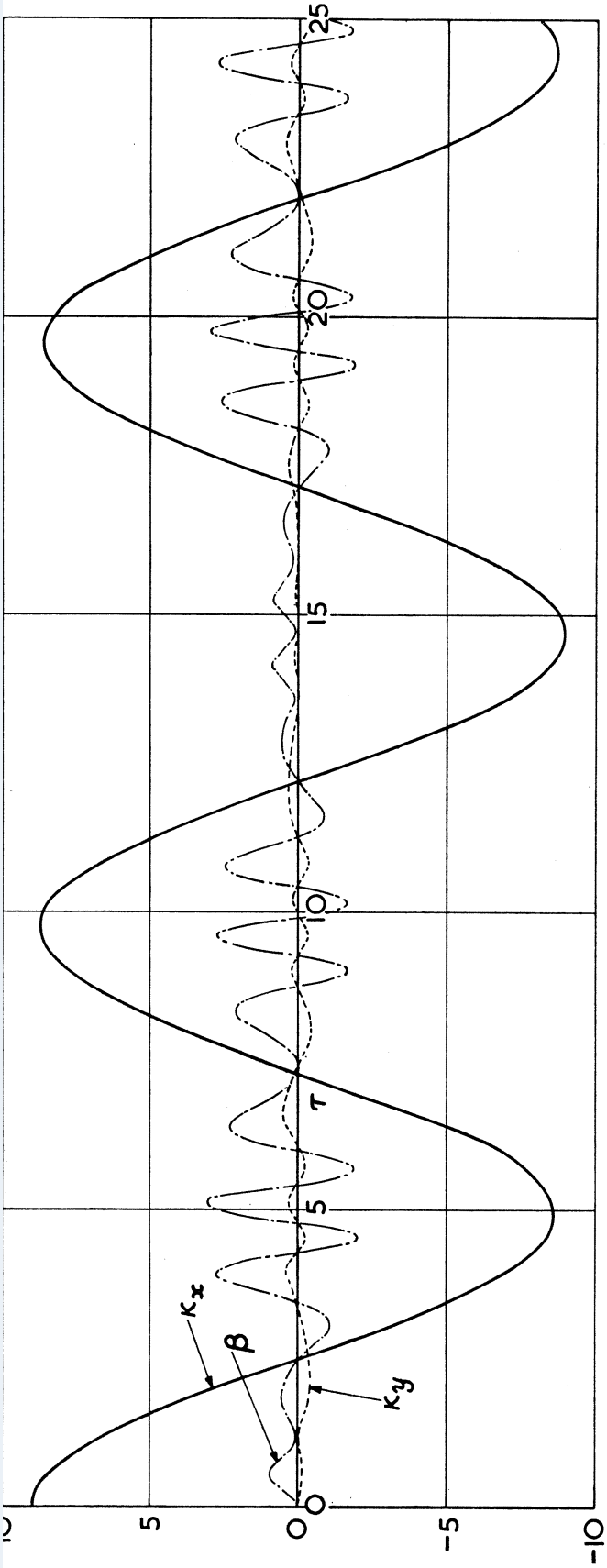

FIGURE 20. Vibration of circular plate released from purely curled state; $\kappa_X = 9$, $\kappa_Y = 0$.

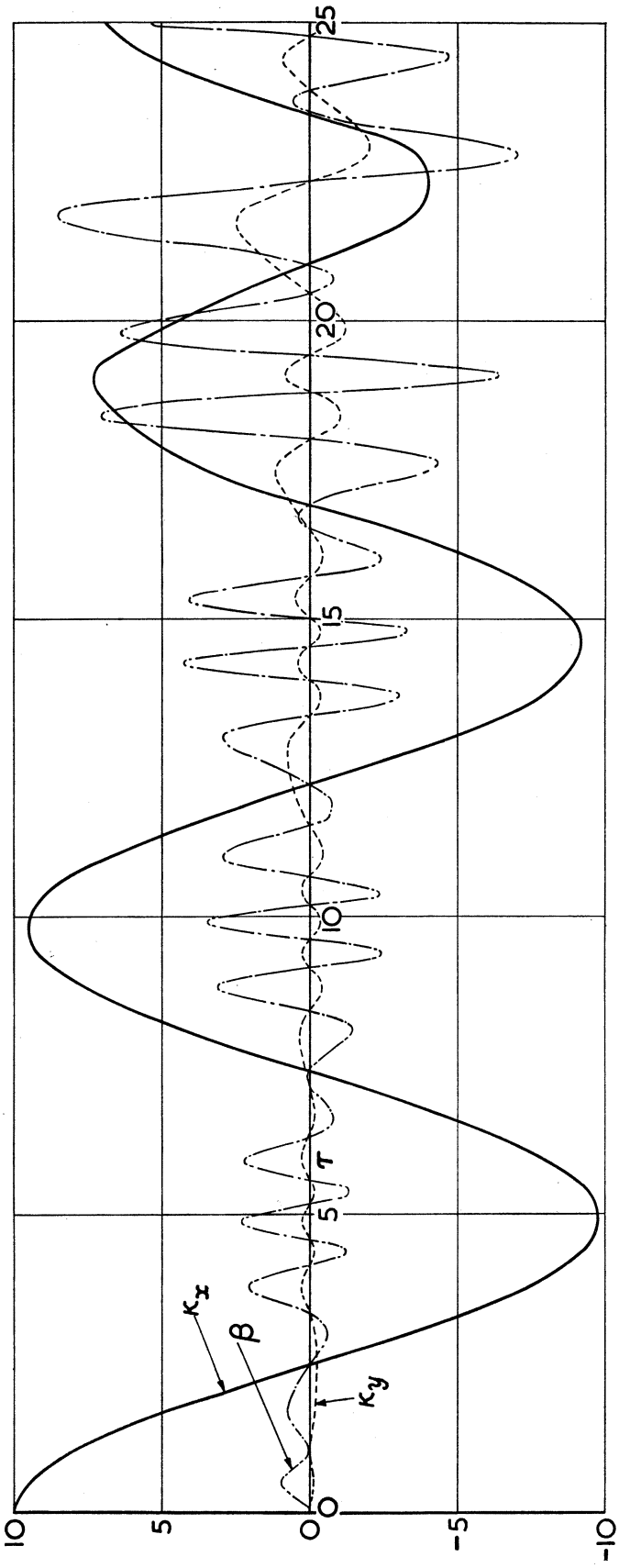

FIGURE 21. Vibration of circular plate released from purely curled state; $\kappa_X = 10$, $\kappa_Y = 0$.

PHILOSOPHICAL TRANSACTIONS OF THE ROYAL SOCIETY A MATHEMATICAL, PHYSICAL & ENGINEERING SCIENCES

Expressing $\ddot{\gamma}$ in the form $\dot{\gamma}\,\mathrm{d}\dot{\gamma}/\mathrm{d}\gamma$ leads immediately to a first integration of the form

$$\tfrac{1}{2}(\dot{\gamma})^2 = -\Omega_0^2 \int \gamma(1+2\Lambda\gamma+\gamma^2)\,\mathrm{d}\gamma$$

$$= \tfrac{1}{4}\Omega_0^2[U_1-(2\gamma^2+\tfrac{8}{3}\Lambda\gamma^3+\gamma^4)], \tag{65}$$

where the constant of integration U_1 depends upon the initial conditions. If the plate is released from rest when $\gamma = \gamma_1$, say, the constant is given by

$$U_1 = 2\gamma_1^2+\tfrac{8}{3}\Lambda\gamma_1^3+\gamma_1^4. \tag{66}$$

The further integration of equation (65) yields

$$\Omega_0\tau = \sqrt{2}\int_{\gamma_1}^{\gamma} \frac{\mathrm{d}\gamma}{[U_1-(2\gamma^2+\tfrac{8}{3}\Lambda\gamma^3+\gamma^4)]^{\frac{1}{2}}}. \tag{67}$$

This is an elliptic integral whose form depends markedly on the value of Λ and the amplitude of vibration.

5·2·1. *Strain energy in the plate*

Before considering equation (67) in further detail it is convenient to determine the strain energy in the plate, for this is intimately related to the coefficient U_1. Furthermore, consideration of the strain energy variation with γ provides a simple physical insight into the different types of dishing mode—and hence into the proper interpretation of equation (67).

The strain energy in the plate U^* is the sum of that due to bending and that due to straining of the middle surface.

$$U^* = \tfrac{1}{2}\int\int D[\{\nabla^2(w-w_0)\}^2-(1-\nu)\,\Diamond^4(w-w_0, w-w_0)]\,\mathrm{d}A$$

$$+\tfrac{1}{2}\int\int \frac{1}{Eh}\{(\nabla^2\Phi)^2-(1+\nu)\,\Diamond^4(\Phi,\Phi)\}\,\mathrm{d}A$$

$$= \tfrac{1}{8}\pi D_0 ab\mu^2[(\kappa_x+\kappa_y-\kappa_{x,0}-\kappa_{y,0})^2-2(1-\nu)\{(\kappa_x-\kappa_{x,0})(\kappa_y-\kappa_{y,0})-(\kappa_{xy}-\kappa_{xy,0})^2\}+\beta^2] \tag{68}$$

Thus, for the initially dished circular plate,

$$\left.\begin{aligned} U^* &= \tfrac{1}{2}\pi D_0 a^2\mu^2\Omega_0^4 U, \text{ say,} \\ U &= 2\gamma^2+\tfrac{8}{3}\Lambda\gamma^3+\gamma^4, \end{aligned}\right\} \tag{68a}$$

where

which is nondimensional. Thus we have identified the term in the square bracket in equations (65) and (67) as the difference between the initial (nondimensional) strain energy U_1 and the current strain energy U. Indeed, equation (65) is simply a statement of energy conservation:

$$\text{kinetic energy}+\text{strain energy} = \text{constant},$$

and the integrand in equation (67) is a measure of the plate velocity. Note that the maximum value of the plate velocity occurs when γ is zero, and is given by

$$(\dot{\gamma}_0)^2 = \tfrac{1}{2}\Omega_0^2 U_1. \tag{69}$$

Consider now the variation of U with γ. If $0<\Lambda<1$ the function U has only one minimum, at γ zero, as typified by the curve for $\Lambda = 0{\cdot}97$ in figure 22*a*. If $\Lambda > 1$ the function U possesses two minima as typified by the curve for $\Lambda = 1{\cdot}04$ in figure 22*b*. These points of

PHILOSOPHICAL TRANSACTIONS OF THE ROYAL SOCIETY A MATHEMATICAL, PHYSICAL & ENGINEERING SCIENCES

minimum strain energy correspond to stable equilibrium positions; the condition that $\Lambda > 1$ implies that $\kappa_{x,0} > 2(1+\nu)^{\frac{1}{2}}$ which is the condition (Mansfield 1965) for the existence of a stable 'snapped-through' state in which

$$\kappa_x = \kappa_y = -\tfrac{1}{2}\kappa_{x,0} - \tfrac{1}{2}\{\kappa_{x,0}^2 - 4(1+\nu)\}^{\frac{1}{2}}$$

or, in terms of γ, Λ,

$$\gamma = -\Lambda - (\Lambda^2-1)^{\frac{1}{2}} = \gamma_s, \text{ say.} \tag{70}$$

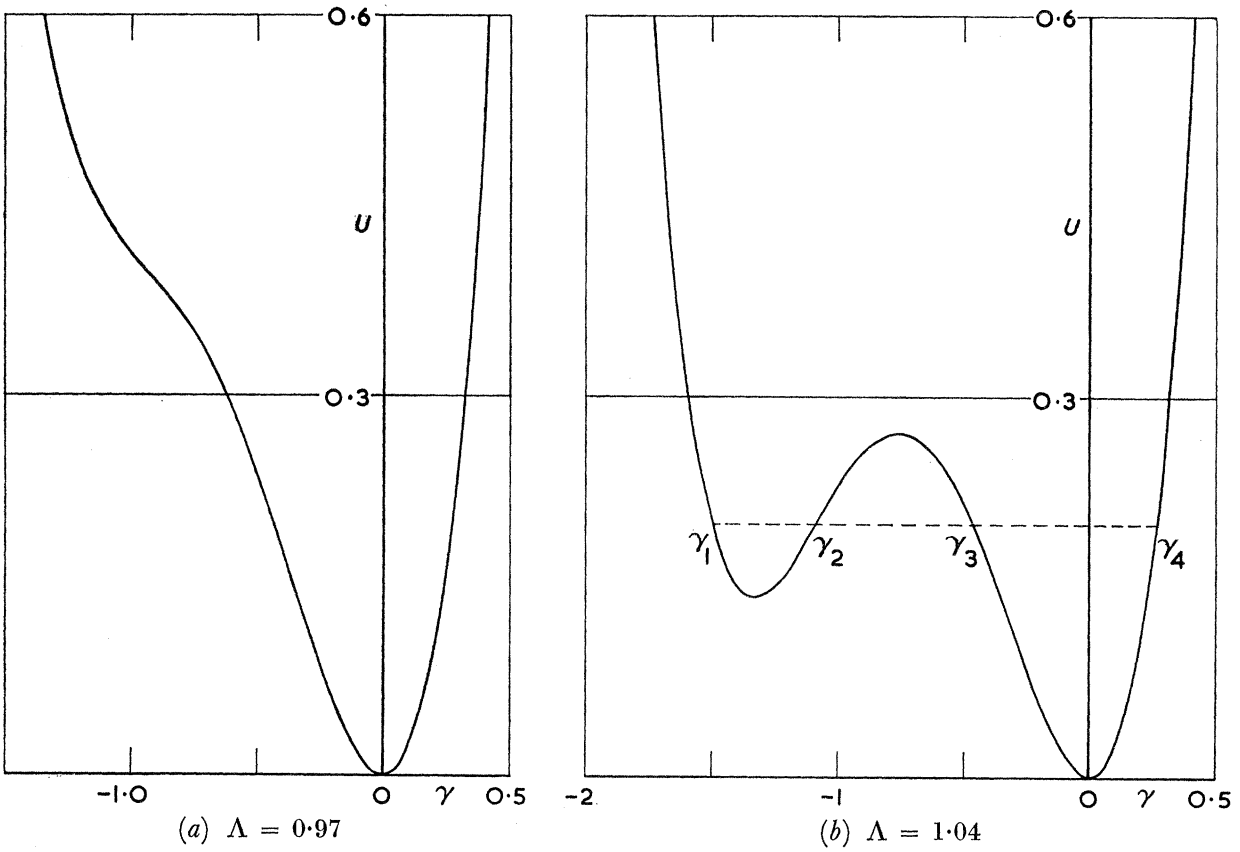

FIGURE 22 (*a* and *b*). Variation of strain energy U with displacement γ.

By the same token an unstable equilibrium position of maximum strain energy occurs when

$$\gamma = -\Lambda + (\Lambda^2-1)^{\frac{1}{2}} = \gamma_u, \text{ say.} \tag{71}$$

The strain energy in the plate at these stable and unstable equilibrium positions is given by

$$\left.\begin{aligned} U_s &= -1 + 4\Lambda^2 - \tfrac{8}{3}\Lambda^4 - \tfrac{8}{3}\Lambda(\Lambda^2-1)^{\frac{3}{2}}, \\ U_u &= -1 + 4\Lambda^2 - \tfrac{8}{3}\Lambda^4 + \tfrac{8}{3}\Lambda(\Lambda^2-1)^{\frac{3}{2}}. \end{aligned}\right\} \tag{72}$$

The significance of these energy expressions becomes apparent when we consider what happens when the plate is released from a state of rest at (γ_1, U_1). At a subsequent time when the plate is at (γ, U) the kinetic energy is proportional to $(U_1 - U)$. The motion is therefore analogous to that of a frictionless bead acted on by gravity and constrained to follow the (γ, U) curve. In this analogy the change in strain energy $(U_1 - U)$ corresponds to the velocity of the bead. The analogy also shows that the plate next comes to rest at the point (γ_2, U_2) say, where

$$U_2 = U_1. \tag{73}$$

The limits of vibration are thus determined by those states which possess the same strain energy. In general there are only two such states, but when

$$\left.\begin{aligned} &\Lambda > 1 \\ \text{and} \quad &U_s < U < U_u \end{aligned}\right\} \tag{74}$$

there are four states, as shown in figure 22*b* where they are identified by the suffixes $1, \ldots, 4$. Vibrations may then occur with limits of γ_1, γ_2 or γ_3, γ_4, the former corresponding to vibrations about the stable snapped-through state.

Consider now the solution of equation (73). Substitution from equations (66) and (68) shows that γ_2 is a root of the equation

$$2\gamma^2+\tfrac{8}{3}\Lambda\gamma^3+\gamma^4 = 2\gamma_1^2+\tfrac{8}{3}\Lambda\gamma_1^3+\gamma_1^4, \tag{75}$$

from which the factor $(\gamma-\gamma_1)$ may be extracted to yield

$$2(\gamma+\gamma_1)+\tfrac{8}{3}\Lambda(\gamma^2+\gamma\gamma_1+\gamma_1^2)+(\gamma+\gamma_1)\,(\gamma^2+\gamma_1^2) = 0. \tag{76}$$

We have, of course, already determined the conditions for the presence of one or three real roots of this cubic. The three real roots have been denoted by $\gamma_2, \gamma_3, \gamma_4$ and we have adopted the convention that $\gamma_1 < \gamma_2 < \gamma_3 < \gamma_4$; when there is only one real root it is convenient to introduce further notation, namely that equation (76) is cast in the form

$$(\gamma-\gamma_2)\,\{(\gamma-r)^2+s^2\} = 0, \tag{77}$$

where r, s are real.

Although the roots of equation (76) are most readily determined by numerical methods the following special cases yield simple analytical solutions.

Case in which $U_1 = U_s$. In this case $(\gamma-\gamma_s)$ appears as a double root and equation (75) is therefore of the form

$$\{\gamma+\Lambda+(\Lambda^2-1)^{\frac{1}{2}}\}^2\,(\gamma-\gamma_3)\,(\gamma-\gamma_4) = 0, \tag{78}$$

whence, by equating coefficients of powers of γ in equations (75) and (78),

$$\gamma_{3,4} = -\tfrac{1}{3}\Lambda+(\Lambda^2-1)^{\frac{1}{2}}\mp\tfrac{2}{3}\{\Lambda^2-3\Lambda(\Lambda^2-1)^{\frac{1}{2}}\}^{\frac{1}{2}}. \tag{79}$$

Case in which $U_1 = U_u$. In this case $(\gamma-\gamma_u)$ appears as a double root of equation (75) and accordingly

$$\gamma_{1,4} = -\tfrac{1}{3}\Lambda-(\Lambda^2-1)^{\frac{1}{2}}\mp\tfrac{2}{3}\{\Lambda^2-3\Lambda(\Lambda^2-1)^{\frac{1}{2}}\}^{\frac{1}{2}}. \tag{80}$$

Case in which $\Lambda = 1$, $U_1 = U_s = U_u$. This is a special case in which the plate is at a point of neutral stability at $\gamma = -1$, so that the factor $(\gamma+1)$ appears as a triple root of equation (75) and hence

$$\gamma_{1,2,3} = -1, \quad \gamma_4 = \tfrac{1}{3}. \tag{81}$$

5.2.2. *Elliptic integral representation of the solution*

We are now in a position to express equation (67) in terms of elliptic integrals, and hence to determine the frequency of vibration, etc. We consider first those

cases which are *not* covered by condition (74) and which can therefore be cast in the form

$$\left.\begin{aligned}\Omega_0\tau &= \sqrt{2}\int_{\gamma_1}^{\gamma}\frac{\mathrm{d}\gamma}{[(\gamma-\gamma_1)(\gamma_2-\gamma)\{(\gamma-r)^2+s^2\}]^{\frac{1}{2}}}\\ &= (2/pq)^{\frac{1}{2}}F(k_3,\alpha_3),\\ \text{where}\quad k_3 &= \frac{1}{2}\left\{\frac{(\gamma_2-\gamma_1)^2-(p-q)^2}{pq}\right\}^{\frac{1}{2}},\\ \alpha_3 &= 2\cot^{-1}\left\{\frac{q(\gamma_2-\gamma)}{p(\gamma-\gamma_1)}\right\}^{\frac{1}{2}},\\ p^2 &= (r-\gamma_2)^2+s^2,\\ q^2 &= (r-\gamma_1)^2+s^2.\end{aligned}\right\} \tag{82}$$

The $\frac{1}{2}$-period of vibration is given by

$$\begin{aligned}\Omega_0[(\tau)_{\gamma_2}-(\tau)_{\gamma_1}] &= (2/pq)^{\frac{1}{2}}\{F(k_3,\pi)-F(k_3,0)\}\\ &= 2(2/pq)^{\frac{1}{2}}K(k_3).\end{aligned}$$

The frequency Ω is thus given by

$$\left(\frac{\Omega}{\Omega_0}\right)^2 = \frac{\pi^2 pq}{8\{K(k_3)\}^2}. \tag{83}$$

Those cases which *are* covered by condition (74) yield two solutions, depending on whether the vibration is about the stress-free equilibrium position or about the snapped-through equilibrium position. Vibrations about the stress-free equilibrium position are determined by

$$\left.\begin{aligned}\Omega_0\tau &= \sqrt{2}\int_{\gamma_3}^{\gamma}\frac{\mathrm{d}\gamma}{[(\gamma-\gamma_1)(\gamma-\gamma_2)(\gamma-\gamma_3)(\gamma_4-\gamma)]^{\frac{1}{2}}}\\ &= 2\left(\frac{2}{(\gamma_4-\gamma_2)(\gamma_3-\gamma_1)}\right)^{\frac{1}{2}}F(k_4,\alpha_4),\\ \text{where}\quad k_4 &= \left\{\frac{(\gamma_2-\gamma_1)(\gamma_4-\gamma_3)}{(\gamma_3-\gamma_1)(\gamma_4-\gamma_2)}\right\}^{\frac{1}{2}},\\ \alpha_4 &= \sin^{-1}\left\{\frac{(\gamma_4-\gamma_2)(\gamma-\gamma_3)}{(\gamma_4-\gamma_3)(\gamma-\gamma_2)}\right\}^{\frac{1}{2}}.\end{aligned}\right\} \tag{84}$$

The frequency Ω is given by

$$\left(\frac{\Omega}{\Omega_0}\right)^2 = \frac{\pi^2(\gamma_4-\gamma_2)(\gamma_3-\gamma_1)}{32\{K(k_4)\}^2}. \tag{85}$$

Vibrations about the snapped-through state are given by

$$\left.\begin{aligned}\Omega_0\tau &= \sqrt{2}\int_{\gamma_1}^{\gamma}\frac{\mathrm{d}\gamma}{[(\gamma-\gamma_1)(\gamma_2-\gamma)(\gamma_3-\gamma)(\gamma_4-\gamma)]^{\frac{1}{2}}}\\ &= 2\left(\frac{2}{(\gamma_4-\gamma_2)(\gamma_3-\gamma_1)}\right)^{\frac{1}{2}}F(k_4,\alpha_5),\\ \text{where}\quad \alpha_5 &= \sin^{-1}\left\{\frac{(\gamma_4-\gamma_2)(\gamma-\gamma_1)}{(\gamma_2-\gamma_1)(\gamma_4-\gamma)}\right\}^{\frac{1}{2}}.\end{aligned}\right\} \tag{86}$$

PHILOSOPHICAL TRANSACTIONS OF THE ROYAL SOCIETY A MATHEMATICAL, PHYSICAL & ENGINEERING SCIENCES

It follows that the frequency is again given by equation (85). This means that *for a given level of energy* the frequency of vibration about the snapped-through state is the same as that about the stress-free state. The maximum value of the plate velocity occurs at $\gamma = \gamma_s$ and is given by

$$(\dot{\gamma}_s)^2 = \tfrac{1}{2}\Omega_0^2(U_1 - U_s). \tag{87}$$

The elliptic integrals presented here simplify, as follows, for the special cases discussed in § 5·2·1 which exhibit repeated roots of equation (75).

Case in which $U_1 = U_s$. The term k_2 in equation (84) is now zero and the solution can be cast in the form

$$\frac{\gamma - \gamma_3}{\gamma - \gamma_s} = \left(\frac{\gamma_4 - \gamma_3}{\gamma_4 - \gamma_s}\right) \sin\left[\tfrac{1}{2}\Omega_0 \tau \{\tfrac{1}{2}(\gamma_4 - \gamma_s)\,(\gamma_3 - \gamma_s)\}^{\frac{1}{2}}\right] \tag{88}$$

where $\gamma_{3,4}$ are given by equation (79).

Case in which $U_1 = U_u$. There are two cases to consider in which, in theory, the plate eventually reaches the unstable equilibrium state γ_u after release from γ_1 or γ_4—given by equation (80). For the plate released from γ_1 the term k_2 in equation (86) is unity and the solution can be cast in the form

$$\left.\begin{aligned} \Omega_0 \tau \{\tfrac{1}{2}(\gamma_4 - \gamma_u)\,(\gamma_u - \gamma_1)\}^{\frac{1}{2}} &= \ln\left(\frac{1+\eta}{1-\eta}\right), \\ \text{where} \qquad \eta &= \left\{\frac{(\gamma_4 - \gamma_u)\,(\gamma - \gamma_1)}{(\gamma_u - \gamma_1)\,(\gamma_4 - \gamma)}\right\}^{\frac{1}{2}}. \end{aligned}\right\} \tag{89}$$

If the plate is released from γ_4 the solution is

$$\Omega_0 \tau \{\tfrac{1}{2}(\gamma_4 - \gamma_u)\,(\gamma_u - \gamma_1)\}^{\frac{1}{2}} = \ln\left(\frac{\eta+1}{\eta-1}\right). \tag{90}$$

Case in which $\Lambda = 1$, $U_1 = U_s = U_u$. If the plate is released from the state $\gamma_4 = \frac{1}{3}$, it will eventually reach the state of neutral stability at $\gamma = -1$, according to the relation

$$\gamma = \frac{12}{9 + 2\Omega_0^2 \tau^2} - 1. \tag{91}$$

5·2·3. *Presentation of results*

Numerical results for the dishing modes of dished circular plates have been determined for a range of initial curvatures and amplitudes. Figures 23, 24 and 25 are phase-plane diagrams for $\Lambda = 0{\cdot}8$, $1{\cdot}0$, $1{\cdot}04$ respectively, in which $\dot{\gamma}/\Omega_0$ is plotted against γ for a variety of amplitudes of vibration; if the vibration were sinusoidal these curves would be circular. Figure 26 shows Ω/Ω_0 plotted against $[\dot{\gamma}/\Omega_0]_{\max.}$ for various values of Λ. The relationship between Ω/Ω_0 and the amplitude of vibration may, of course, be determined from figure 26 and the appropriate phase-plane diagram. The broken curves on figures 25 and 26 correspond to vibrations about the snapped-through state. Finally, we note that the values chosen for Λ, namely $0{\cdot}8$, $1{\cdot}0$ and $1{\cdot}04$, correspond to initial curvatures which are respectively $0{\cdot}406$, $1{\cdot}0$ and $1{\cdot}77$ times the critical initial curvature, $\kappa_{x,0} = 2(1+\nu)^{\frac{1}{2}}$, above which a stable snapped-through state is possible.

5·3. *Torsion modes of a twisted elliptical plate*

In this section we consider another 'vibration in unison', namely the large-deflexion torsion mode of an initially twisted elliptical plate. For such a plate the governing differential equation is obtained from equations (10) and (11) by writing

$$\kappa_{x,0} = \kappa_{y,0} = \kappa_x = \kappa_y = 0,$$

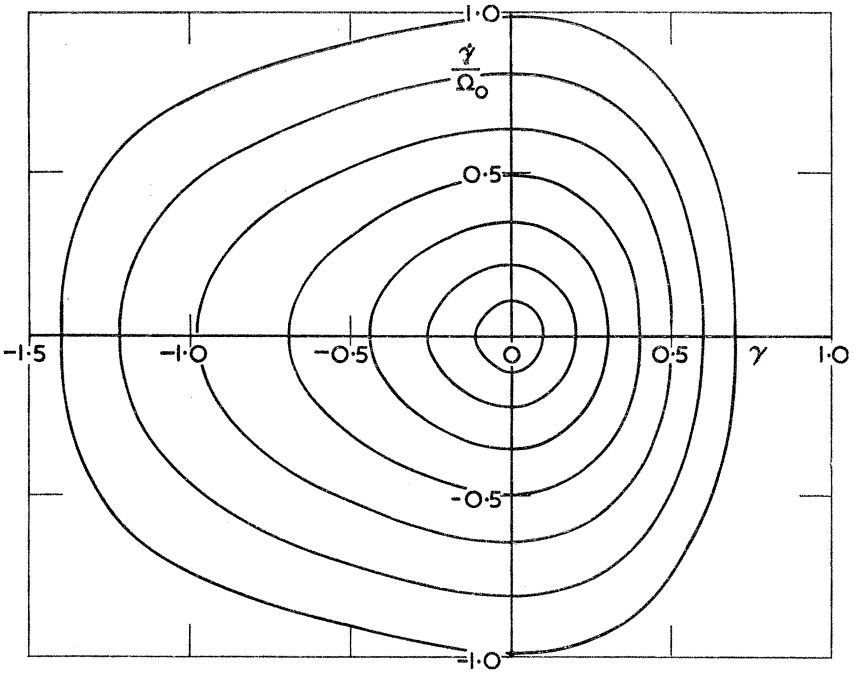

FIGURE 23. Phase-plane diagram, $\Lambda = 0{\cdot}8$.

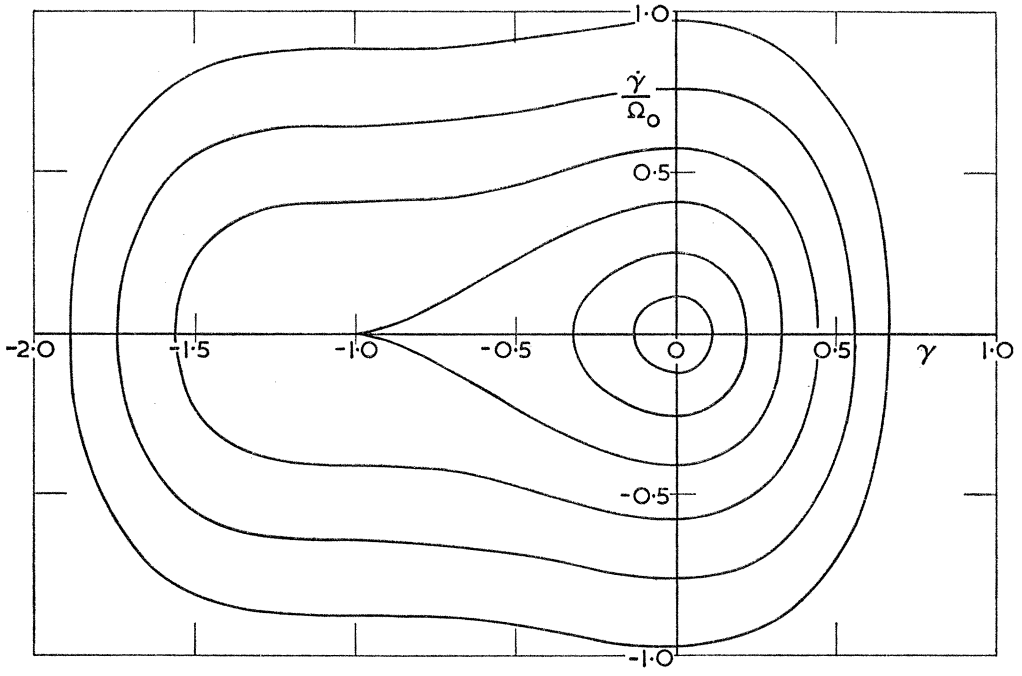

FIGURE 24. Phase-plane diagram, $\Lambda = 1{\cdot}0$.

whence
$$3\ddot{\kappa}_{xy} + (1-\nu)(\kappa_{xy} - \kappa_{xy,0}) + \kappa_{xy}(\kappa_{xy}^2 - \kappa_{xy,0}^2) = 0. \tag{92}$$

This equation can be written in the form of equation (64) by redefining the parameters Λ, γ and Ω_0 as follows:

$$\left.\begin{aligned} \Lambda &= 3\kappa_{xy,0}/2(1-\nu+2\kappa_{xy,0}^2)^{\frac{1}{2}}, \\ \gamma &= (\kappa_{xy} - \kappa_{xy,0})/(1-\nu+2\kappa_{xy,0}^2)^{\frac{1}{2}}, \\ \Omega_0^2 &= \tfrac{1}{3}(1-\nu+2\kappa_{xy,0}^2), \end{aligned}\right\} \tag{93}$$

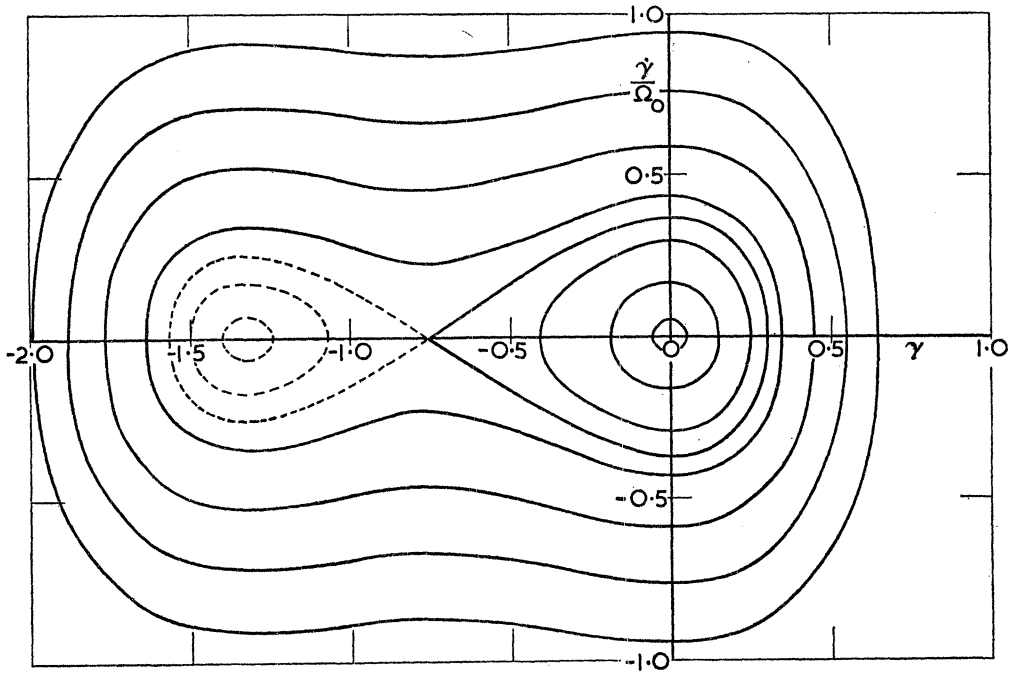

FIGURE 25. Phase-plane diagram, $\Lambda = 1{\cdot}04$.

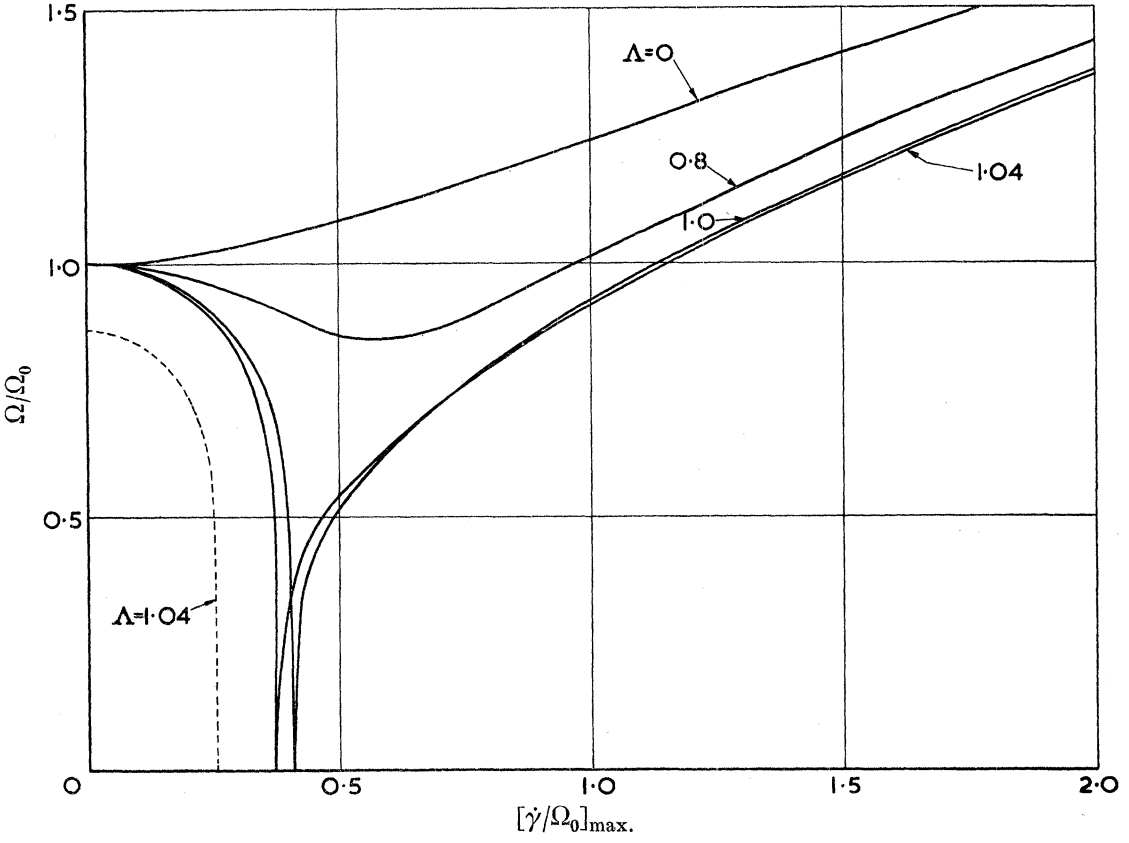

FIGURE 26. Variation of frequency with maximum velocity.

where Λ is now a measure of the twisting curvature in the undisturbed state and again varies between zero and $\frac{3}{4}\sqrt{2}$, γ is a measure of the displacement about the undisturbed state and, from the analysis of § 4·2, Ω_0 is the nondimensional frequency appropriate to small deflexions in the torsion mode. This redefinition means that the remaining analysis of § 5·2, including figures 23 to 26, is now valid for this torsion case. We note, in passing, that the condition that $\Lambda > 1$ implies that $\kappa_{xy,0} > 2(1-\nu)^{\frac{1}{2}}$ which is the condition for the existence of a stable snapped-through state of reversed twist in which

$$\kappa_{xy} = -\tfrac{1}{2}\kappa_{xy,0} - \tfrac{1}{2}\{\kappa_{xy,0}^2 - 4(1-\nu)\}^{\frac{1}{2}}. \tag{94}$$

5·4. *Flat elliptical plate*

5·4·1. *The torsion mode*

For the flat elliptical plate the only large-deflexion 'vibration in unison' is the torsion mode. The governing equation is the same as equation (48) for the circular plate and the corresponding analysis of § 5·1·2 is therefore valid for the ellipse. This does not mean that the actual vibration is not influenced by the ellipticity, because the nondimensional terms κ_{xy}, τ are themselves dependent on the plate dimensions.

5·4·2. *The dishing mode*

Before discussing the large-deflexion dishing mode of a flat elliptical plate it is instructive to consider the behaviour of a plate released from a state κ_X, κ_Y whose shape is appropriate to the small-deflexion dishing mode, equation (17), but whose magnitude is such that large-deflexion effects would be expected. Now large-deflexion effects become significant when β, which determines the middle-surface forces, cannot be neglected. Furthermore, static buckling of the plate occurs when

$$\left.\begin{aligned} \beta &= -(1-\nu) \\ &= \beta^*, \text{ say,} \end{aligned}\right\} \tag{58 bis}$$

and, with this in mind, we have chosen the magnitudes of κ_X, κ_Y to be such that the initial values of β are $\frac{1}{2}\beta^*$ and β^*. Figure 27 corresponds to the initial value of $\frac{1}{2}\beta^*$ and shows the variation of κ_x, κ_y and β with τ for a plate in which $\zeta = \frac{2}{3}$. It is seen that κ_x and κ_y do not vanish simultaneously—indeed, this is also reflected in the occurrence of small but positive values of β—and the motion cannot strictly be described as a mode. Furthermore, the initial (negative) value of β is sometimes exceeded in the subsequent motion which is, nevertheless, of a stable character. Figure 28 corresponds to the initial value of β^*. The subsequent motion shows much larger variations from a purely modal behaviour; peak (negative) values of β considerably in excess of β^* occur, and this tends to produce an unstable vibration with an interchange of extensional and flexural energies.

The values of κ_X, κ_Y necessary for a true dishing mode, for a plate in which $\zeta = \frac{2}{3}$, have been obtained by a trial-and-error process. For each value of κ_X, say, a series of values of κ_Y is chosen and the subsequent motions are determined by numerical integration of the governing equations. At the correct value of κ_Y the curvatures κ_x, κ_y vanish simultaneously at the $\frac{1}{4}$-period of vibration. The search for the dishing modes is, of course, helped by knowledge of the small-deflexion mode, and also by the asymptotic modal behaviour with

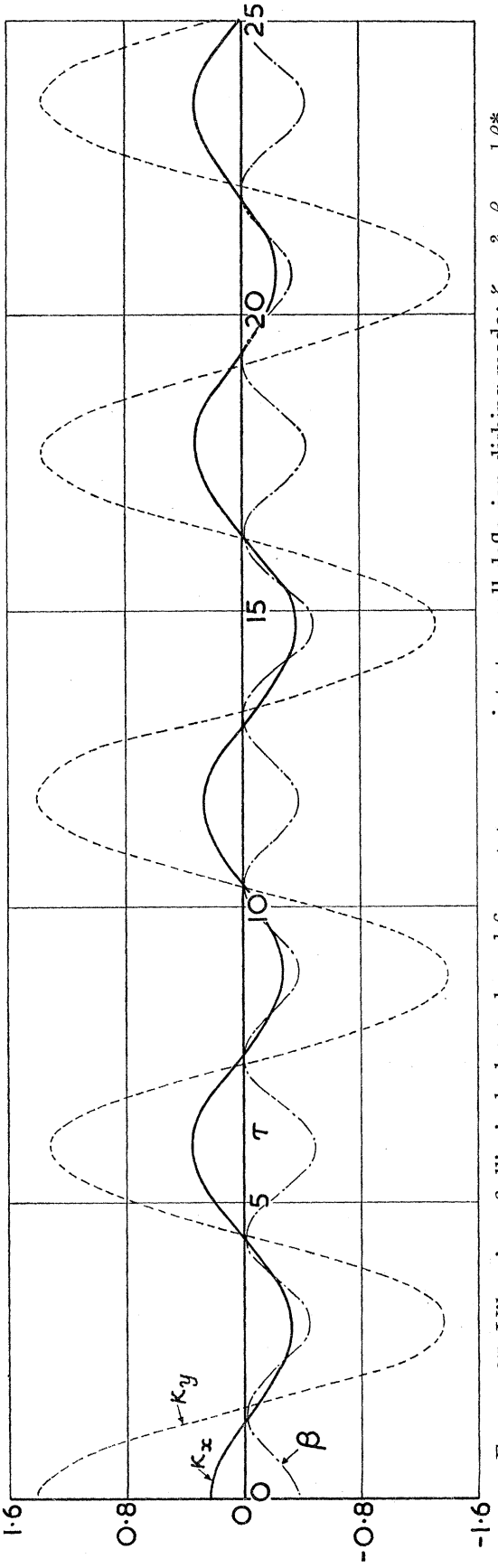

FIGURE 27. Vibration of elliptical plate released from state appropriate to small-deflexion dishing mode: $\zeta = \frac{2}{3}$, $\beta_0 = \frac{1}{2}\beta^*$.

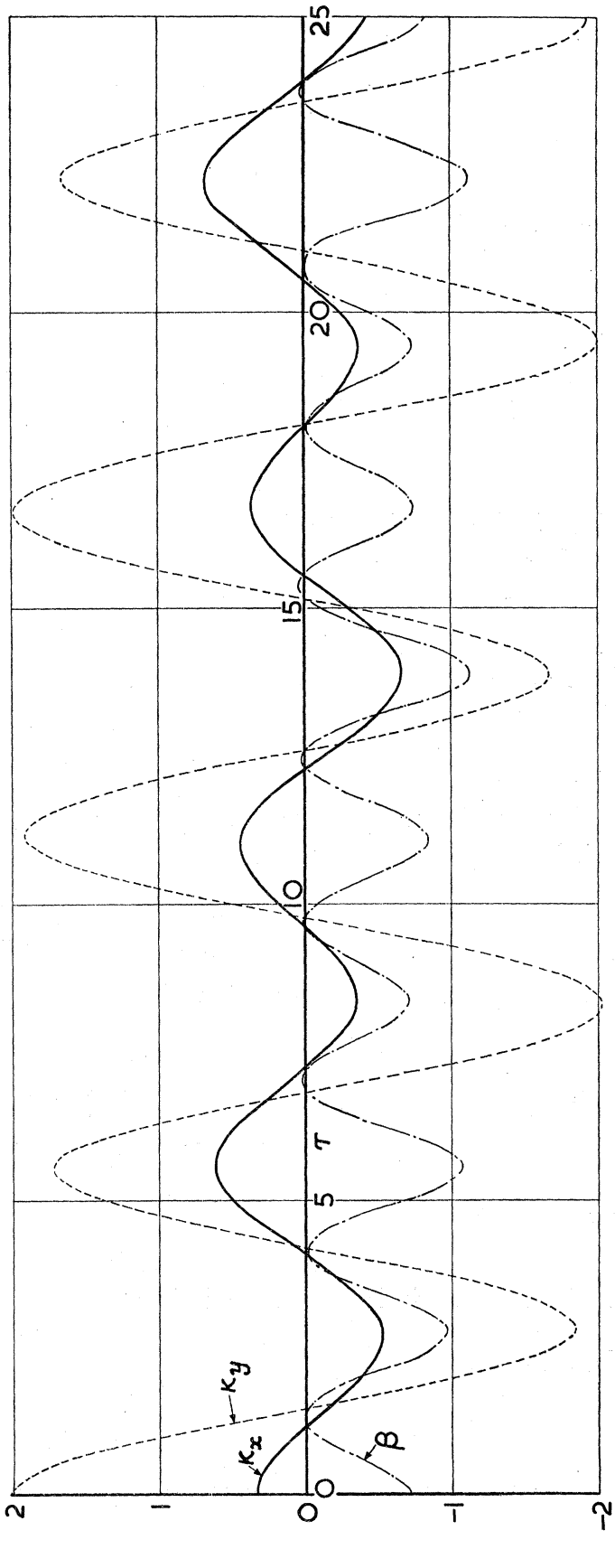

FIGURE 28. Vibration of elliptical plate released from state appropriate to small-deflexion dishing mode; $\zeta = \frac{2}{3}$, $\beta_0 = \beta^*$.

PHILOSOPHICAL TRANSACTIONS OF THE ROYAL SOCIETY A MATHEMATICAL, PHYSICAL & ENGINEERING SCIENCES

very large curvatures. The asymptotic behaviour is obtained by considering only the β terms on the left hand sides of equations (11 a, b):

$$\left.\begin{aligned} -\kappa_x\kappa_y(\kappa_x+5\zeta^2\kappa_y) &\sim 12\ddot{\kappa}_x,\\ -\kappa_x\kappa_y(5\zeta^{-2}\kappa_x+\kappa_y) &\sim 12\ddot{\kappa}_y.\end{aligned}\right\} \tag{95}$$

It can be verified that these asymptotic equations are satisfied by a 'vibration in unison' for which the term 'dishing' is more appropriate than hitherto, because the edge of the plate lies in an (oscillating) plane

$$\kappa_x \sim \zeta^2\kappa_y, \tag{96}$$

where

$$\kappa_x^3 \sim -2\zeta^2\ddot{\kappa}_x. \tag{97}$$

A comparison with the analysis for the asymptotic behaviour for the circular plate shows that the frequency again varies asymptotically in proportion to the amplitude

$$\Omega_{\mathrm{d}} \sim 0{\cdot}599\zeta^{-1}|\kappa_X|. \tag{98}$$

Finally we note that the asymptotic mode, equation (96) is also a 'similar' small-deflexion extensional mode for a plate with large initial curvatures, see § 4·2·1, where the term 'similar' is used to imply that

$$\epsilon_1 : \epsilon_2 : \epsilon_3 = \kappa_{x,0} : \kappa_{y,0} : \kappa_{xy,0}. \tag{99}$$

Furthermore, the corresponding small-deflexion extensional frequency for such a plate is given by

$$\Omega_{\mathrm{e}} \sim \zeta^{-1}|\kappa_{x,0}| \tag{100}$$

which is closely related to equation (98).

The velocity components of the plate $[\dot{\kappa}_x]_0$, $[\dot{\kappa}_y]_0$ as it passes through the equilibrium position may be determined from the relation

$$\left[\frac{\dot{\kappa}_x}{\dot{\kappa}_y}\right]_{\kappa_x=\kappa_y=0} = \lim \left[\frac{\kappa_x}{\kappa_y}\right]_{\kappa_x,\,\kappa_y\to 0} \tag{101}$$

and the equation of energy conservation

$$[\text{kinetic energy}]_{\kappa_x=\kappa_y=0} = [\text{strain energy}]_{\kappa_x=\kappa_X,\,\kappa_y=\kappa_Y}.$$

This equation corresponds to equation (69) for the circular plate, and reduces to

$$5\zeta^{-2}[\dot{\kappa}_x^2]_0+5\zeta^2[\dot{\kappa}_y^2]_0-2[\dot{\kappa}_x\dot{\kappa}_y]_0 = 2\{(\kappa_X+\kappa_Y)^2-2(1-\nu)\kappa_X\kappa_Y+\kappa_X^2\kappa_Y^2\}. \tag{102}$$

5·4·3. *The bending mode*

The analysis and computational technique for determining the large-deflexion bending mode of a flat elliptical plate are similar to those for the dishing mode, and accordingly we quote only the results. The asymptotic behaviour is obtained from an alternative solution of equation (95), namely

$$\kappa_x \sim -\zeta^2\kappa_y, \tag{103}$$

where

$$\kappa_x^3 \sim -3\zeta^2\ddot{\kappa}_x. \tag{104}$$

The frequency again varies asymptotically in proportion to the amplitude

$$\Omega_{\mathrm{b}} \sim 0{\cdot}489\zeta^{-1}|\kappa_X|. \tag{105}$$

The asymptotic mode, equation (103), is also a 'similar' small-deflexion extensional mode of a plate with large initial curvatures satisfying equation (99) for which

$$\Omega_e \sim (\tfrac{2}{3})^{\frac{1}{2}} \zeta^{-1} |\kappa_{x,0}|. \tag{106}$$

Equations (101) and (102) suffice to determine the velocity components of the plate as it passes through the equilibrium position.

It is of interest to note that with increasing curvature the character of the bending mode changes to a much greater extent than in the dishing mode. Indeed, from being a small-deflexion mode with κ_X the dominant curvature, it becomes a large-deflexion mode with κ_Y the dominant curvature—as in the dishing mode. However, simple physical reasoning suggests that there will be a large-deflexion mode in which κ_X is the dominant curvature, and this is indeed the case. It is the *curling* mode—similar to that discussed in § 5·1·4—and it is considered in § 5·4·4.

Stability of the torsion, dishing and bending modes. The stability characteristics of the torsion mode of an elliptical plate are similar to those of the circular plate, equations (59) and (60). Some information on the stability of the dishing mode has already been given in figures 27 and 28, where the initial values chosen for κ_X, κ_Y can be regarded as perturbations from the modal values. However, for the case in which initially $\beta = \beta^*$, the magnitude of the perturbations was unduly great, the curvatures being $\pm 20\,\%$ from the modal values; at this critical initial value of β a perturbation of this magnitude might be expected to have a marked destabilizing influence on the ensuing vibration.

5·4·4. *The curling modes*

The technique for determining curling modes is similar to that discussed in § 5·1·4 for the circular plate, but there is now no condition arising from the rotational symmetry of the plate, and separate computation is required for curling about the major and minor axes. The frequency for curling about the minor axis is given approximately by equation (31); similarly, that about the major axis is given by

$$\Omega_c^2 \approx \tfrac{2}{5}\zeta^{-2}. \tag{107}$$

Small twisting component superposed on curling mode. In § 5·1·4 the curling mode for the circular plate was regarded as a close neighbour of a 'smooth' vibration in which the smaller, transverse curvature was initially unchanging; in the curling mode the transverse curvature, and hence the middle surface forces, oscillate about their values in this 'smooth' vibration. There are similar relationships and features for the elliptical plate, but the point we wish to emphasize here is that during a curling vibration the *average* value of the middle-surface forces is *nonzero*. Now the torsional stiffness of a thin strip is altered by the presence of middle-surface forces—whether mechanically or thermally induced—and hence we would expect the frequency of a small twisting component superposed on a curling vibration to differ from its small-deflexion value. The actual behaviour is complex but the following approximate analysis goes some way in providing a physical understanding. With $\kappa_{x,0}$, etc., zero equations (11 a, b, c) may be cast in the form

$$(\beta - 5\zeta^2 - \nu)\,\kappa_x + (5\zeta^2\beta - 1 - 5\nu\zeta^2)\,\kappa_y = 12\ddot{\kappa}_x, \tag{108a}$$

$$(5\zeta^{-2}\beta - 1 - 5\nu\zeta^{-2})\,\kappa_x + (\beta - \nu - 5\zeta^{-2})\,\kappa_y = 12\ddot{\kappa}_y, \tag{108b}$$

$$(\beta + 1 - \nu)\,\kappa_{xy} + 3\ddot{\kappa}_{xy} = 0. \tag{108c}$$

If now we search for solutions in which κ_x is large in comparison with κ_y, κ_{xy}, equation (108*b*) yields

$$\beta \to \nu + \frac{\zeta^2}{5}, \tag{109}$$

provided also that $\ddot{\kappa}_y$ *is negligible*. Strictly speaking, therefore, this limiting form for β is appropriate to the 'smooth' vibration rather than the curling mode but, as explained previously, it is also the *average* value in an asymptotic curling mode. Substitution of equation (109) back into equation (108*a*) yields

$$-\tfrac{2}{5}\zeta^2\kappa_x + O(\kappa_y) = \ddot{\kappa}_x,$$

whose solution is

$$\kappa_x \to \kappa_X \cos\{(\tfrac{2}{5})^{\frac{1}{2}}\zeta\tau\}, \tag{110}$$

which thus provides a simple check on the analysis; indeed, equation (110) could have been used to derive equation (109). Finally, substitution into equation (108*c*) yields

$$(1+\tfrac{1}{5}\zeta^2)\,\kappa_{xy} + 3\ddot{\kappa}_{xy} = 0,$$

whose solution is

$$\kappa_{xy} = \kappa_{XY}\cos\Omega\tau,$$

where

$$\Omega^2 = \tfrac{1}{3}(1+\tfrac{1}{5}\zeta^2), \tag{111}$$

so that the frequency always exceeds the small-deflexion value given by

$$\Omega_t^2 = \tfrac{1}{3}(1-\nu). \tag{16 *bis*}$$

Note also that for the circular plate ($\zeta = 1$) the frequency given by equation (111) coincides with the curling frequency; this is because the effect of the small initial twist is confined to an alteration in the direction of the axis of curling. When $\zeta < 1$ the twisting frequency exceeds the curling frequency.

Although the above analysis is of an asymptotic character, it yields tolerable results for quite modest values of the nondimensional curling curvature. For example, figure 29 shows comparisons with the true variation with time of κ_x, κ_{xy} and β over the range $0 < \tau < 50$ for a plate in which $\zeta = \frac{2}{3}$ and, initially, $\kappa_X = 2{\cdot}297$, $\kappa_{XY} = 0{\cdot}080$, $\kappa_Y = 0{\cdot}0028$. These initial curvatures have been chosen because they correspond to a purely curled state with generators inclined at 2° from the minor axis of the ellipse; furthermore, the magnitude of the (nonzero) principal curvature, namely 2·300, is such that if the generators were parallel to the minor axis the subsequent motion would be repetitive. According to small-deflexion theory the (nondimensional) time interval between successive zeros of κ_{xy} is 6·51, whereas from equation (111) the interval is 5·22. In the example treated in figure 29 the *average* time interval is 5·60, successive intervals being $\frac{1}{2}$(5·40), 5·52, 6·01, 5·55, 5·40, 5·49, 5·99, 5·62 and 5·39.

5·4·5. *Presentation of results*

For the special case in which $\zeta = \frac{2}{3}$ the dishing, bending and curling modes have been determined over the range $|\kappa_X| \leqslant 4$, $|\kappa_Y| \leqslant 6$. The modal relations between κ_X and κ_Y are shown in figure 30 where, because the plate is flat, there is point-symmetry about the origin. The general pattern of curling modes associated with separate 'tongues' is similar to that for the circular plate, but there is no longer any intersection between the bending mode and a curling mode. The variation of frequency with amplitude is shown in figure 31 where the

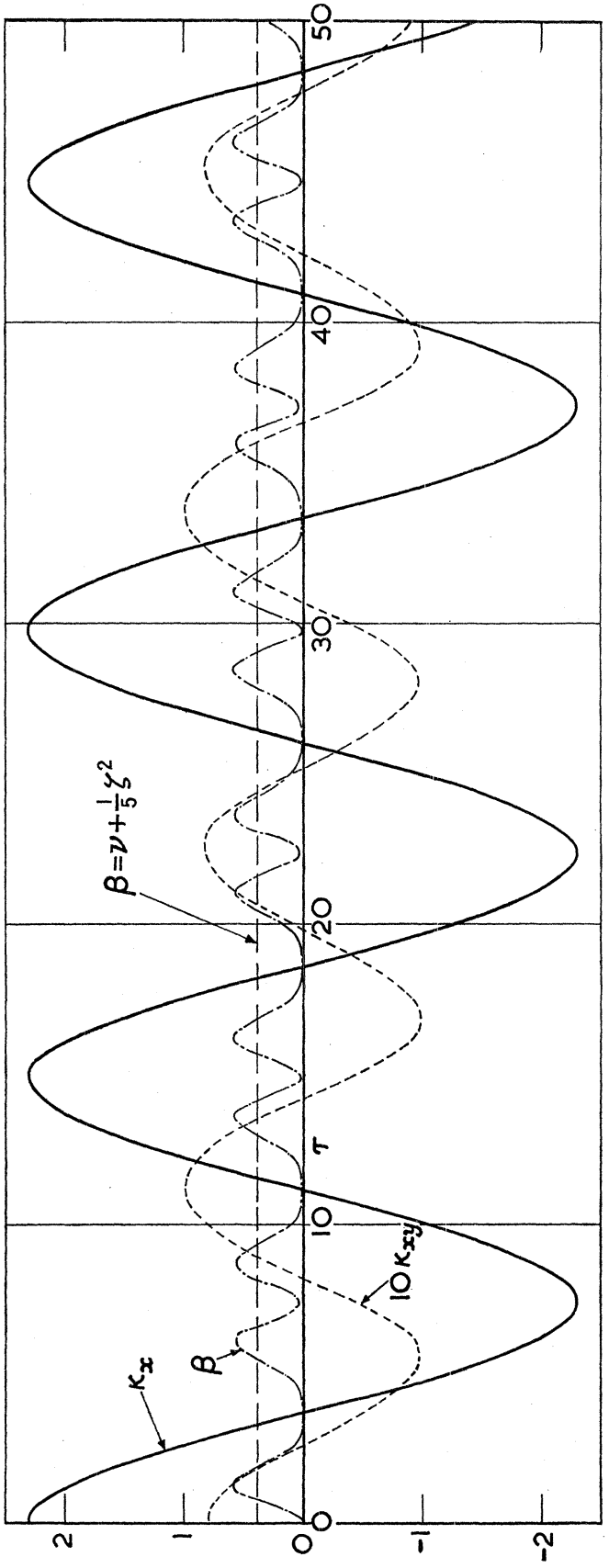

FIGURE 29. Small twisting component superposed on curling mode; $\zeta = \frac{2}{3}$, $\kappa_X = 2{\cdot}297$, $\kappa_{XY} = 0{\cdot}080$, $\kappa_Y = 0{\cdot}0028$.

PHILOSOPHICAL TRANSACTIONS OF THE ROYAL SOCIETY A MATHEMATICAL, PHYSICAL & ENGINEERING SCIENCES

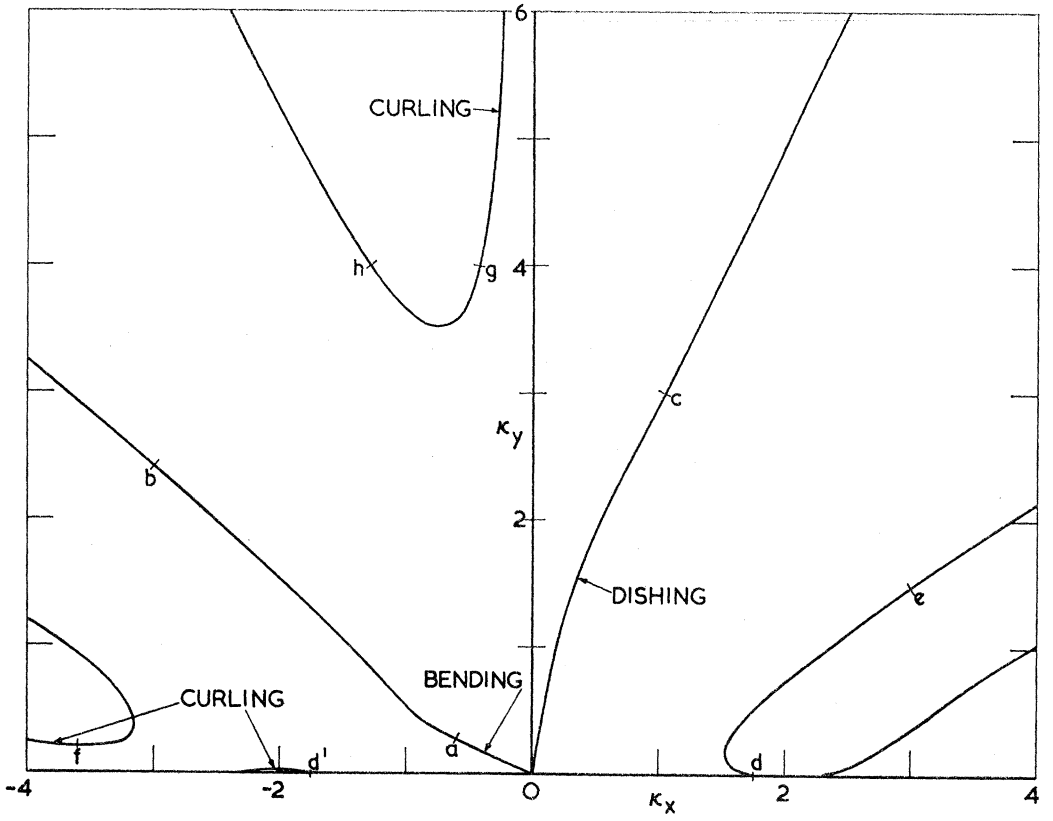

FIGURE 30. Modal relation between κ_X, κ_Y: elliptical plate, $\zeta = \frac{2}{3}$.

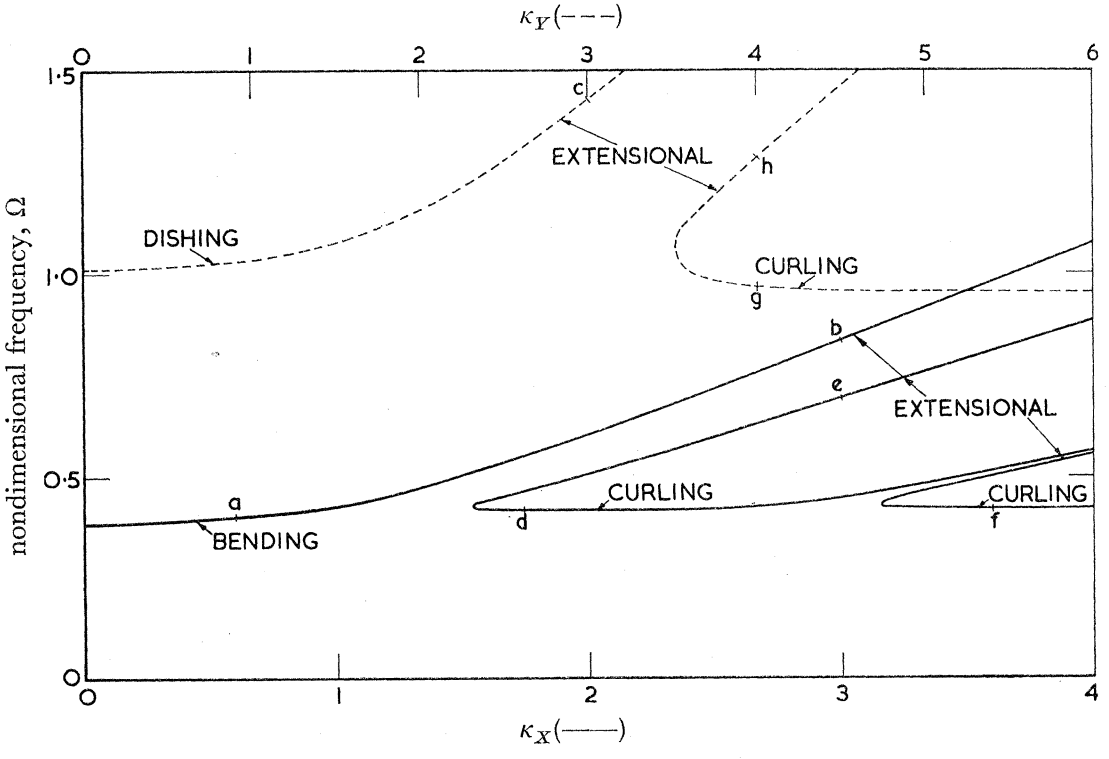

FIGURE 31. Frequency variation with amplitude, elliptical plate: $\zeta = \frac{2}{3}$.

points a, ..., h correspond to those of figure 30, enabling the various curves to be identified. Figures 32 a, ..., h show the variations of κ_x, κ_y with time, in modes corresponding to the points a, ..., h in figures 30 and 31.

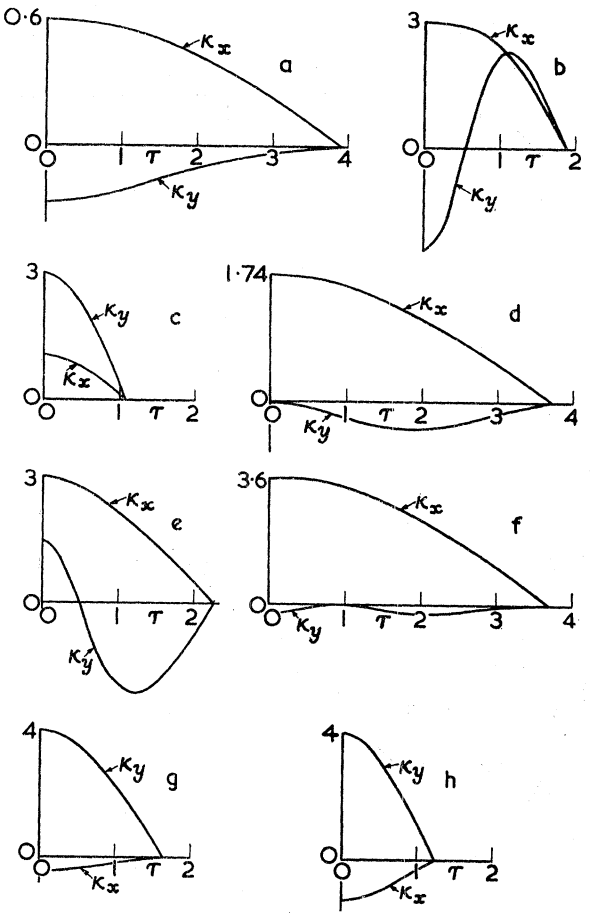

FIGURE 32. Variations of κ_x, κ_y with time; elliptical plate, $\zeta = \frac{2}{3}$.

5·5. *Curved elliptical plate*

Apart from the special cases considered in §§ 5·2 and 5·3 the large-deflexion vibrations of an initially curved elliptical plate are not 'in unison' and the governing equations must be integrated numerically. A wide variety of vibrations is possible and here we confine attention to those which exhibit the most interesting and important features.

5·5·1. *Bending vibration of a dished circular plate*

This case is considered because it is comparatively simple and because, from the analysis of § 4·2, the *small-deflexion* mode is independent of the magnitude of the initial dishing. Intuitively, we might therefore expect that the dishing curvature would introduce a measure of 'slackness' into the bending mode, so that, in comparison with the flat plate, a given amplitude of vibration would result in a smaller increase in frequency. To test this hypothesis we consider a circular plate in which

$$\kappa_{x,0} = \kappa_{y,0} = 1, \text{ say},$$

and search for modal relations along the following lines (shown chain-dotted in figure 33)

$$\kappa_Y = \pm i + \kappa_X \quad (i = 1, 2, 3),$$

for these are orthogonal to the small-deflexion modal relation and of fixed (bending) amplitude, namely $i\sqrt{2}$. The modal points so determined are identified by the points α_i in figure 33. Also shown in figure 33 are the relations between κ_x, κ_y during the corresponding

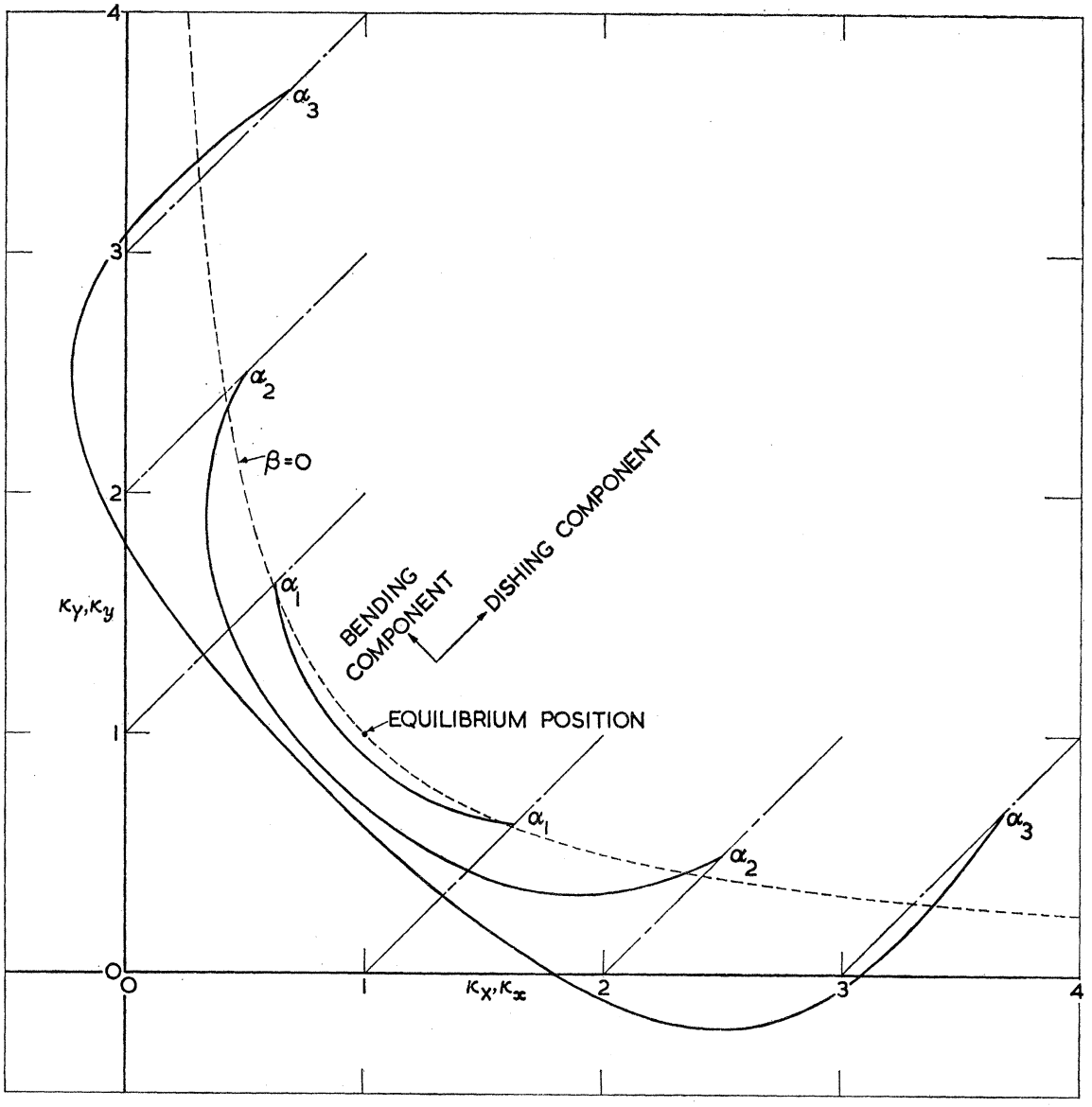

FIGURE 33. Bending vibrations of dished circular plate: curvature relations for different amplitudes.

modal vibrations; these are symmetrical about the line $\kappa_x = \kappa_y$. The broken line is the hyperbola along which β is zero; points to the left of this line correspond to positive values of β, with negative values to the right. It is to be noted that the vibrations are no longer 'in unison' as they are for the flat plate *nor, indeed, do they pass through the equilibrium position.* These are, of course, large-deflexion features but they are generally valid for all curved plates, exceptions being those cases considered in §§ 5·2 and 5·3.

TABLE 1. VARIATION OF Ω_b AND β WITH AMPLITUDE

i	0	1	2	3
Ω_b, flat plate	0·483	0·543	0·691	0·883
Ω_b, dished plate	0·483	0·490	0·510	0·586
$\beta_{min.}$, flat plate	0	0	0	0
$\beta_{max.}$, flat plate	0	0·25	1	2·25
$\beta_{min.}$, dished plate	0	−0·017	−0·256	−1·50
$\beta_{max.}$, dished plate	0	0·095	0·394	1·57

The corresponding frequencies are given in table 1 above, where they are compared with those of equal (bending) amplitude in the flat plate. The small-deflexion values are given by $i = 0$. It is seen that with increasing amplitude the increase in bending frequency for the dished plate is markedly less than for the flat plate. This comparative 'slackness' is due to the much reduced *overall* effect of the middle surface forces, specified by β. The extreme values of β in each cycle are also shown in table 1. Not only are the maximum values of β reduced but, for the amplitudes considered, the values of β at the limits of the vibration are of opposite sign to those for the flat plate so that they have a destabilizing influence. It follows that the 'slackness' is confined to regions of large amplitude where, because the velocities are small, the influence on the frequency is especially marked. When $i = 3$ the value of β at the stationary points α_3 is algebraically greater than the critical value $-(1-\nu)$, and this accounts for the reversal in the initial direction of the bending component. Needless to say, this particular vibration is unstable, but it does illustrate the point that an 'amplitude' may not necessarily be an uncontroversial method for specifying a nonlinear vibration.

5·5·2. *Modes containing a given amount of energy*

In the previous example modes of a given amplitude were determined, but this was facilitated by an element of symmetry in the problem. Without such symmetry the concept of a given amplitude tends to lose its significance or, at least, requires a more elaborate definition. In such instances it is useful to consider modes containing a given amount of energy.

As an illustrative example we consider a plate specified by

$$\zeta = \tfrac{2}{3}, \quad \kappa_{x,0} = 1, \quad \kappa_{y,0} = -2$$

and we search for modes in which

$$U^* = 0{\cdot}1625\pi D_0 ab\mu^2, \text{ say,}$$

which is one-sixth of the energy required to 'flatten' the plate. From equation (68) the curvatures κ_X and κ_Y thus satisfy the equation

$$(\kappa_X+\kappa_Y+1)^2-2(1-\nu)(\kappa_X-1)(\kappa_Y+2)+(\kappa_X\kappa_Y+2)^2 = 1{\cdot}3, \qquad (112)$$

which is shown by the broken line in figure 34. By considering the behaviour of the plate released from points on this curve of constant energy it is found that points a, a′ and b, b′ yield modes. The corresponding κ_x, κ_y relations are shown by the full lines and it is to be noted that these do not pass through the static equilibrium position nor do they possess any element of symmetry.

5·5·3. *Vibrations passing through the static equilibrium position*

The point has already been made that large-deflexion modes of curved plates do not, in general, pass through the static equilibrium position. Let us, however, relax the condition that in each cycle there are times at which all the velocities vanish, and then investigate the possibility of repetitive vibrations which pass through the static equilibrium position at least once in each cycle. Such 'modes' do not, in fact, exist as can be seen from the following

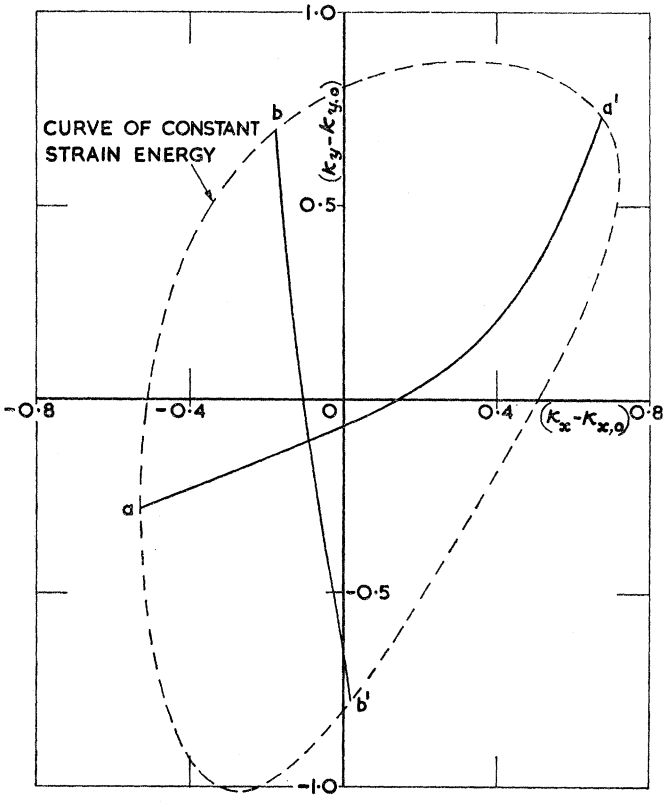

FIGURE 34. Modes associated with a given amount of energy: $\zeta = \frac{2}{3}$, $\kappa_{x,0} = 1$, $\kappa_{y,0} = -2$.

illustrative example which is identical to that considered in § 5·5·2 except that the plate is given an impulse from its equilibrium position, the resultant kinetic energy being equal to the previously considered strain energy. Furthermore, just as we previously considered the plate behaviour following release from all points on the strain energy curve, so we now consider its behaviour when the initial kinetic energy is associated with all initial velocity ratios. The initial velocities may thus be expressed in the form

$$\left.\begin{aligned}[\dot{\kappa}_x]_{\tau=0} &= v\cos\theta,\\ [\dot{\kappa}_y]_{\tau=0} &= v\sin\theta,\end{aligned}\right\} \tag{113}$$

where, from equation (102),

$$\begin{aligned} v^2(5\zeta^{-2}\cos^2\theta + 5\zeta^2\sin^2\theta - 2\sin\theta\cos\theta) &= 16U^*/\pi D_0 ab\mu^2\\ &= 2{\cdot}6 \text{ in this example.} \end{aligned} \tag{114}$$

The κ_x, κ_y relations for the cases of interest are shown in figures 35 $a, \ldots, d$ and 36 a, b. In figure 35 the plate curvatures follow paths which touch the bounding strain energy curve—shown again by a broken line—whence, because the plate is then instantaneously

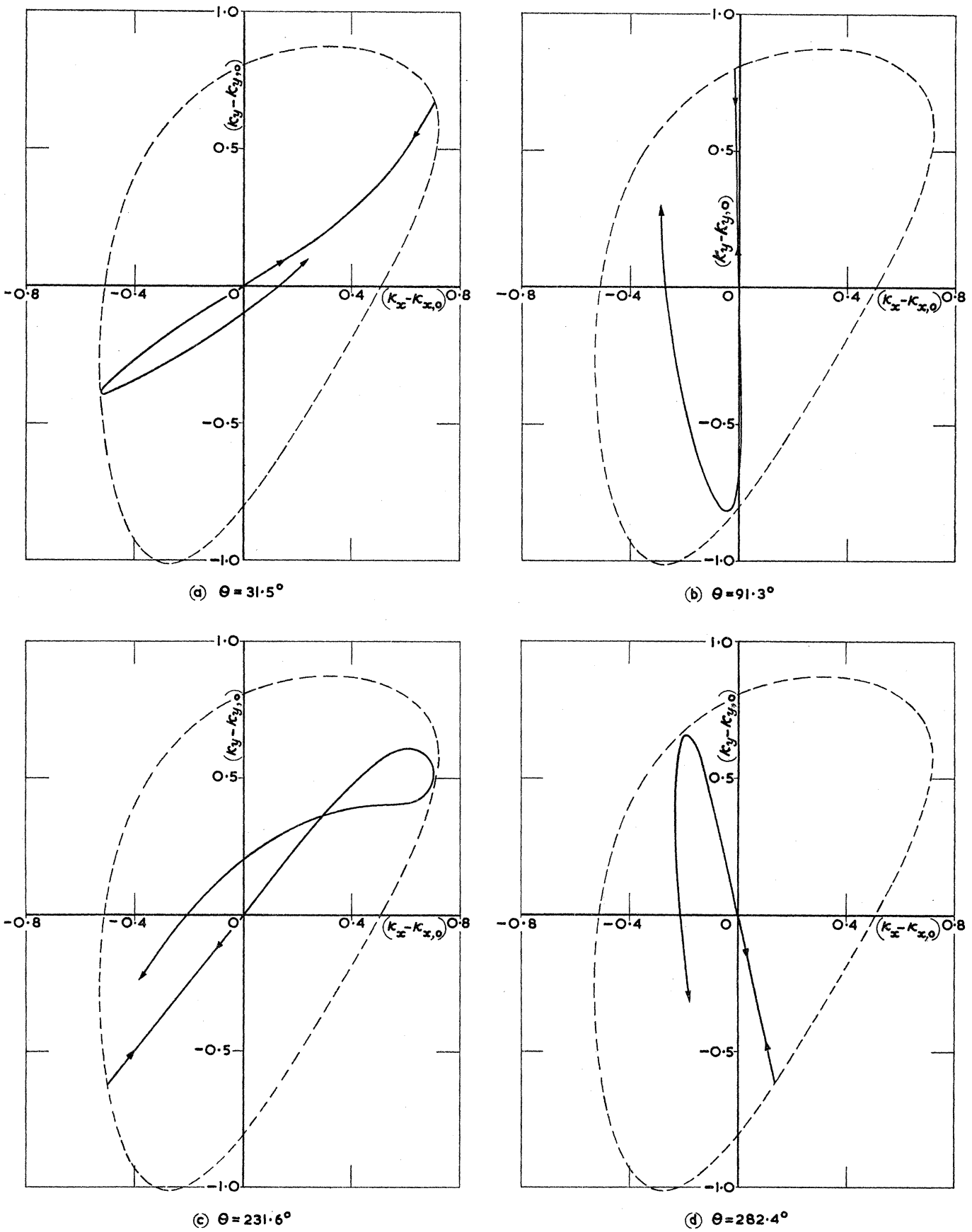

FIGURE 35. Vibrations returning to the equilibrium position after attaining state of rest.

PHILOSOPHICAL TRANSACTIONS OF THE ROYAL SOCIETY A MATHEMATICAL, PHYSICAL & ENGINEERING SCIENCES

at rest, they retrace these paths to the static equilibrium position. The subsequent motions, however, are far from repetitive as can be judged from the extent to which the next 'returns' miss the static equilibrium position. In figure 36 the plate curvatures follow paths which do not reach the bounding strain energy curve so that the plate is never at rest; the plate passes through the static equilibrium position after one (approximate) cycle, but the

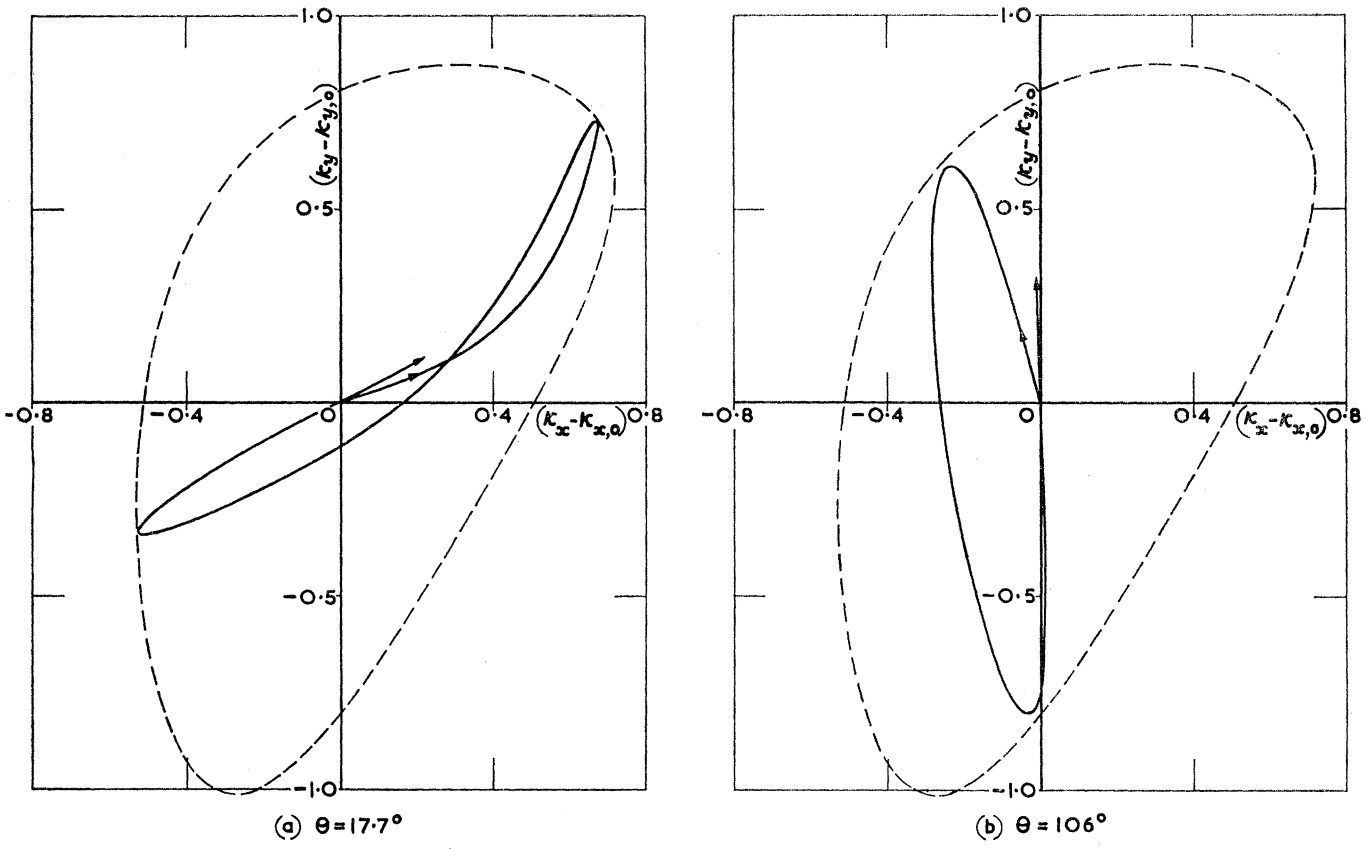

FIGURE 36. Vibrations returning to the equilibrium position after completion of approximate cycle.

velocities at the equilibrium position differ from their initial values so that the vibration is not repetitive. In figure 36*a* the angle θ changes from an initial value of 17·7° to 25·8°; in figure 36*b*, θ changes from 106° to 91·7°. Because of the reversibility of vibrations figure 36*a* is also appropriate—with arrowheads reversed—to an initial value of $\theta = 205{\cdot}8°$ (i.e. $180° + 25{\cdot}8°$); similarly figure 36*b* is appropriate to an initial value of $\theta = 271{\cdot}7°$.

The vibrations treated in this and the preceding section are associated with a given amount of energy. If progressively smaller amounts of energy are considered it is found that the vibrations typified by aa′ in figure 34 and the curves in figures 35*a*, *c* and 36*a* approach the small-deflexion bending mode, equation (22), for which $\theta = 46{\cdot}6°$. Similarly the other curves approach the small-deflexion dishing mode for which $\theta = 97{\cdot}7°$.

Stresses in a numerical example. The middle-surface and bending stresses have been determined from § 3·2·1 for a plate which corresponds to that considered in §§ 5·5·2 and 5·5·3; the plate is specified by

$$a = 30\,\text{in.}, \quad b = 20\,\text{in.}, \quad h_0 = \tfrac{3}{4}\,\text{in.}, \quad E = 10^7\,\text{Lb./in}^2 \quad (\nu = 0{\cdot}3),$$

and the curvatures in the stress-free state are such that

$$[w_0]_{x=\pm a,\, y=0} - [w_0]_{x=0,\, y=0} = -2{\cdot}51 \text{ in.},$$

and

$$[w_0]_{x=0,\, y=\pm b} - [w_0]_{x=0,\, y=0} = 2{\cdot}23 \text{ in.}$$

It follows from § 3·2·1 that *for all plates* of the type considered the maximum middle-surface stress occurs at the ends of the minor axis, whereas the maximum bending stress occurs at the centre. Furthermore, the middle-surface stresses and the bending stresses vary parabolically over the plate so that their sum also varies parabolically. The bending stresses are, of course, zero at the boundary of the plate and it follows that the maximum *combined* stress occurs either at the ends of the minor axis or at the centre.

In this numerical example the maximum combined stresses have been determined for configurations corresponding to points a, a′, b, b′ in figure 34. At the ends of the minor axis the greatest stress occurs in configuration b and is given by

$$\sigma_x = -28\,700 \text{ Lb./in}^2.$$

At the centre of the plate the greatest stress occurs in configuration a′ and is given by

$$\sigma_y = -21\,900 \text{ Lb./in}^2,$$

of which 98 % is due to the bending component.

5·5·4. *Bending vibrations of a plate exhibiting Brazier instability*

It is well known (Brazier 1927) that a long strip with transverse curvature may buckle under the action of an applied bending moment, due to the flattening of the cross section. The analysis for this Brazier instability is customarily restricted to an infinite strip, thus making the problem one-dimensional. Here we consider a finite (elliptical) plate acted on by distributed (inertia) loads—a two-dimensional version of the phenomenon—and we determine also the vibrational characteristics of such a plate.

To clarify the position we consider first the static behaviour of a plate with initial (positive) curvature $\kappa_{y,0}$ subjected to a distributed load proportional to the inertia loading in the κ_x component. It is convenient, but not essential, to envisage a small value for ζ so that the plate is not too dissimilar to a strip. With $\kappa_{x,0} = 0$ the governing equations may be deduced from equations (10) and (11):

$$(5\zeta^2+\nu)\,\kappa_x - (1+5\nu\zeta^2)\,(\kappa_{y,0}-\kappa_y) + \kappa_x\kappa_y(\kappa_x+5\zeta^2\kappa_y) = m, \tag{115}$$

$$(1+5\nu\zeta^{-2})\,\kappa_x - (5\zeta^{-2}+\nu)\,(\kappa_{y,0}-\kappa_y) + \kappa_x\kappa_y(5\zeta^{-2}\kappa_x+\kappa_y) = 0. \tag{116}$$

where m is a measure of the applied load.

The transverse curvature κ_y can be eliminated from these equations to yield the m, κ_x relation. It is found that for a given value of ζ there is a critical value of $\kappa_{y,0}$ above which $\mathrm{d}m/\mathrm{d}\kappa_x = 0$ for some positive value of κ_x, and another critical value above which $\mathrm{d}m/\mathrm{d}\kappa_x = 0$ for some negative value of κ_x. The fact that there are two critical values, rather than one, is because the section is not symmetrical about the plane of bending; when m is of the same sign as $\kappa_{y,0}$ the anticlastic curvature due to the Poisson's ratio effect tends to flatten the cross section, and this accounts for the positive peak value of m being smaller than the negative peak value.

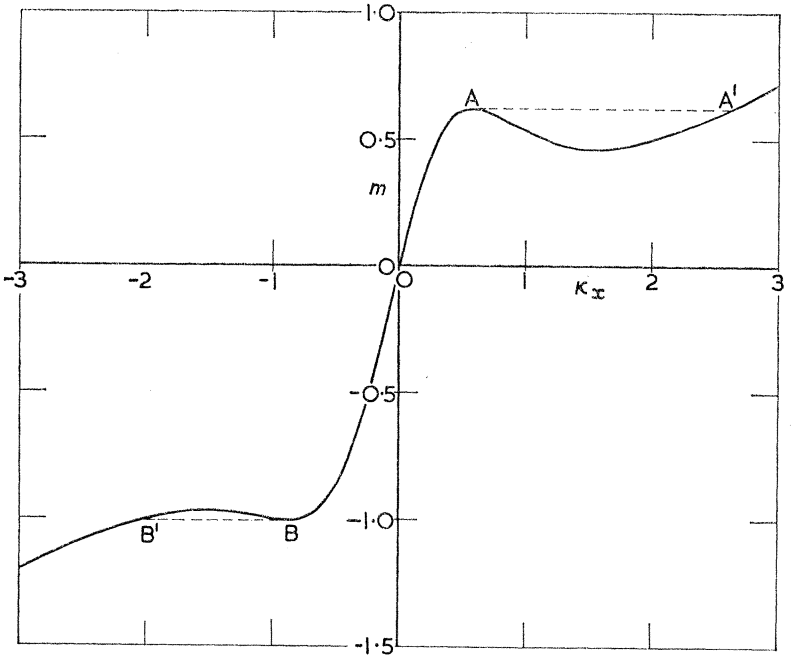

FIGURE 37. m, κ_x relation in plate exhibiting Brazier instability; $\zeta = \frac{1}{4}$, $\kappa_{y,0} = 2{\cdot}5$.

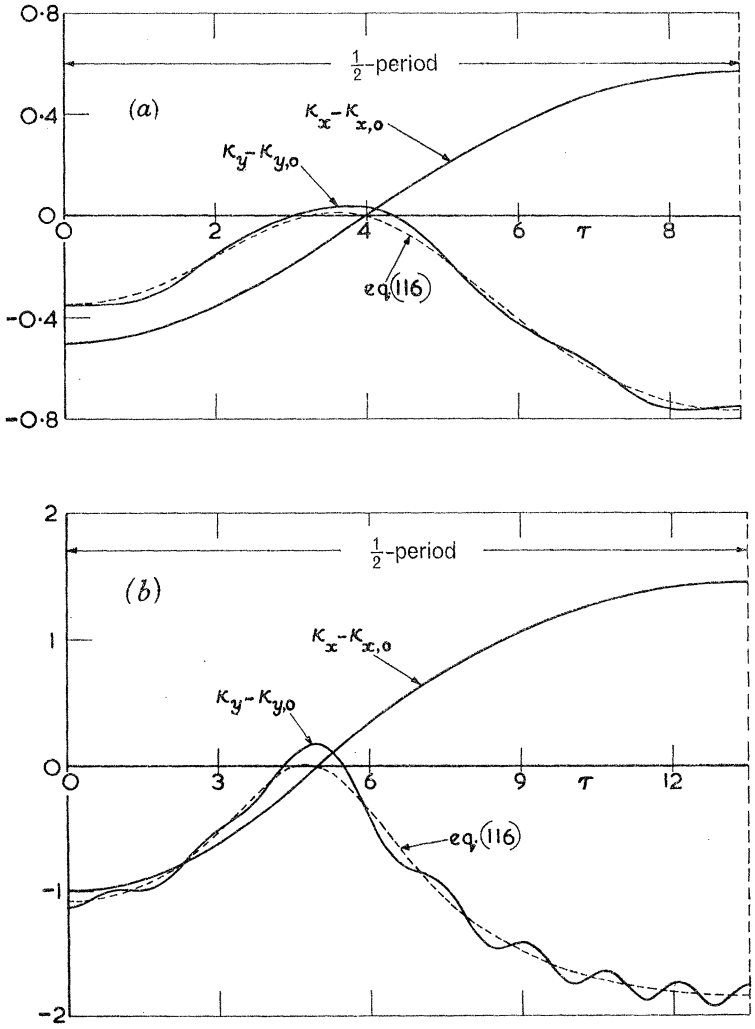

FIGURE 38. Modes of an elliptical plate exhibiting Brazier effect; $\zeta = \frac{1}{4}$, $\kappa_{x,0} = 0$, $\kappa_{y,0} = 2{\cdot}5$. (*a*) $\kappa_X = -0{\cdot}5$, $\kappa_Y = 2{\cdot}153$; (*b*) $\kappa_X = -1{\cdot}0$, $\kappa_Y = 1{\cdot}370$.

PHILOSOPHICAL TRANSACTIONS OF THE ROYAL SOCIETY A MATHEMATICAL, PHYSICAL & ENGINEERING SCIENCES

A typical example which exhibits Brazier instability with positive and negative values of κ_x occurs when $\zeta = \frac{1}{4}$, $\kappa_{y,0} = 2{\cdot}5$; the corresponding relation between m and κ_x is shown in figure 37. If the load is increased beyond points A, B the plate snaps through to points A', B'. In a vibration, however, the plate does not snap through, because the inertia load is itself reduced beyond points A, B. The behaviour is similar to a vibrating mass attached to a spring whose load-deflexion characteristics follow the m, κ_x curve; the analogy is not rigorously exact because it ignores the inertia effects associated with the transverse curvature κ_y. The actual behaviour is exemplified in figures 38*a* and *b* which show the modal vibrations of this plate following releases from given curvatures κ_X, namely $-0{\cdot}5$ and $-1{\cdot}0$. It is found that a mode occurs when κ_Y has a value close to that given by equation (116); in other words, the initial value of the transverse curvature is given approximately by static considerations. Also plotted in figure 38 are values of κ_y related to the current value of κ_x by equation (116). The closeness of this curve to the modal variation is a reflexion of the validity of the analogy considered previously.

Finally, we note that the differing time scales of figures 38*a* and *b* conceal a marked difference in frequency; when $\kappa_X = -0{\cdot}5$, $\Omega = 0{\cdot}353$, and when $\kappa_X = -1{\cdot}0$, $\Omega = 0{\cdot}233$, values which may be compared with 0·421 for the small-deflexion frequency.

We are grateful to Mr B. C. Merrifield for his help in the computation and preparation of the figures.

References

Brazier, L. G. 1927 *Proc. Roy. Soc.* A **116**, 104–114.
Chu, H-N & Herrmann, G. 1956 *J. Appl. Mech.* **23**, 532–540.
Fung, Y. C. & Wittrick, W. H. 1954 *J. Appl. Mech.* **21**, 351–358.
Fung, Y. C. & Wittrick, W. H. 1955 *Quart. J. Mech. Appl. Math.* **8**, 191–210.
Herrmann, G. 1956 *N.A.C.A. Tech. Note* 3578.
Mansfield, E. H. 1959 *Quart. J. Mech. Appl. Math.* **12**, 421–430.
Mansfield, E. H. 1962 *Quart. J. Mech. Appl. Math.* **15**, 167–192.
Mansfield, E. H. 1965 *Proc. Roy. Soc.* A **288**, 396–417.
Lord Rayleigh 1877 *The theory of sound*, vol. 1, 1944 edition. London: MacMillan and Co.
Rosenberg, R. M. 1964 *Proc. Camb. Phil. Soc.* **60**, 595–611.

PHILOSOPHICAL TRANSACTIONS OF THE ROYAL SOCIETY A MATHEMATICAL, PHYSICAL & ENGINEERING SCIENCES